Desalination 600 (2025) 118524

Contents lists available at ScienceDirect

Desalination

journal homepage: www.elsevier.com/locate/desal

Advanced computational strategies for lithium chemical and electrochemical adsorption: A comprehensive state-of-the-art review

Yanan Pan [a], Weiquan Zhan [b,*], Wencai Zhang [a,*]

[a] Department of Mining and Minerals Engineering, Virginia Polytechnic Institute and State University, Blacksburg, VA 24061, USA
[b] Instituto de Física, Universidad Autónoma de San Luis Potosí, Av. Manuel Nava 6, Zona Universitaria, San Luis Potosí 78290, Mexico

HIGHLIGHTS

- Computational advancements in lithium adsorption methods are reviewed.
- Simulations of lithium adsorption at macro and micro levels are presented.
- Principles for optimizing material design and predicting properties are explored.
- Kinetic and thermodynamic behaviors are analyzed to study phase transitions.
- Pros and cons of computational strategies are discussed with future directions.

GRAPHICAL ABSTRACT

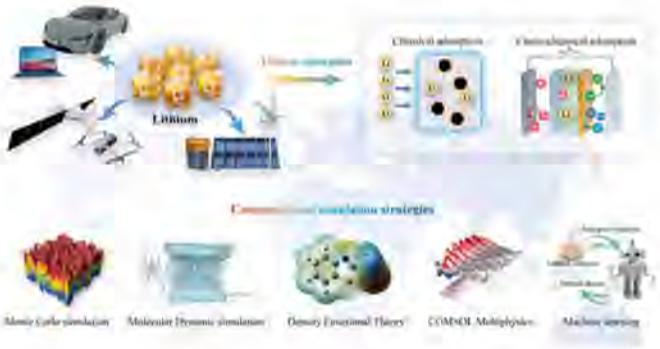

ARTICLE INFO

Keywords
Lithium adsorption
Computational simulations
Materials
Interfacial interaction

ABSTRACT

The extraction of lithium resources through chemical and electrochemical adsorption has become increasingly vital to meet the growing demands of new energy sources. In the adsorption process, computational strategies have been proven indispensable in elucidating the microscopic mechanisms and quantum properties underlying lithium adsorption. While experimental studies on lithium adsorption have advanced significantly, the underlying mechanisms are not yet fully understood. Herein, this review presents recent advancements in computational methods, including Molecular Dynamics (MD), Monte Carlo (MC) simulations, Density Functional Theory (DFT), COMSOL Multiphysics, and Machine Learning (ML), as applied to both chemical and electrochemical lithium adsorption and related materials. The review delves into the principles and methodologies of these approaches, showcasing their effectiveness in optimizing material design and predicting properties. Furthermore, the review highlights these computational strategies in analyzing kinetic and thermodynamic behaviors, studying phase transitions, and tracing flux migration trajectories. Finally, this review evaluates the strengths and limitations of different computational strategies and outlines future research directions. Comprehensively, this review not only provides an insightful understanding of simulation methods for lithium adsorption, but also inspires further upgrade of integrated computational strategies in this field.

* Corresponding authors.
E-mail addresses: zhan_weiquan@163.com (W. Zhan), wencaizhang@vt.edu (W. Zhang).

https://doi.org/10.1016/j.desal.2024.118524
Received 8 November 2024; Received in revised form 12 December 2024; Accepted 31 December 2024
Available online 3 January 2025

1. Introduction

Lithium, the lightest metallic element with the smallest atomic radius, high specific heat, high electrical conductivity, and low electrochemical equivalent (0.26 g/h), plays a critical role in energy conversion and environmental protection [1,2]. It is the core material for high-efficiency lithium-ion batteries, which are essential for electric vehicles and renewable energy storage. These applications help reduce carbon emissions and dependence on fossil fuels [3,4]. Statistically, in 2023, lithium-ion batteries accounted for 87 % of global lithium consumption, with demand continuing to rise as the push for electric vehicles accelerates. According to the United States Geological Survey (USGS), the need of global lithium production will increase by approximately 500 % to meet the projected energy storage demands by 2050 [5]. Consequently, there is a growing concern about lithium resources, making the recovery of lithium from natural sources an urgent task.

Global lithium resources are concentrated in six countries, as shown in Fig. 1(a). Bolivia and Argentina hold the largest reserves, accounting for 21.4 % and 20.4 % of the total global reserves, respectively [6]. Lithium resources primarily exist in two forms: brines and minerals (see Fig. 1(b)), with brines constituting 62.6 % of these resources, making them the predominant sources for lithium extraction and production [7]. The primary sources of brines for lithium extraction include Salt Lake brines (e.g., Atacama Salt Lake in Chile and Uyuni Salt Lake in Bolivia), geothermal brines (e.g., Salton Sea Geothermal Area in California, USA), brines from oil and gas field extraction, and seawater [8–10]. The widespread availability of these brines worldwide offers favorable conditions for the sustainable extraction and recycling of lithium resources. So far, various methods for lithium extraction have been developed, including chemical adsorption, ion exchange, solvent extraction, and electrochemical adsorption techniques, as schematically shown in Fig. 1(c). Among these methods, adsorption techniques including chemical and electrochemical adsorption stand out for their high selectivity, efficiency, and environmentally friendliness [11–13].

Lithium adsorption technology utilizes specific adsorbents or electrode materials to selectively capture Li^+ through chemical adsorption

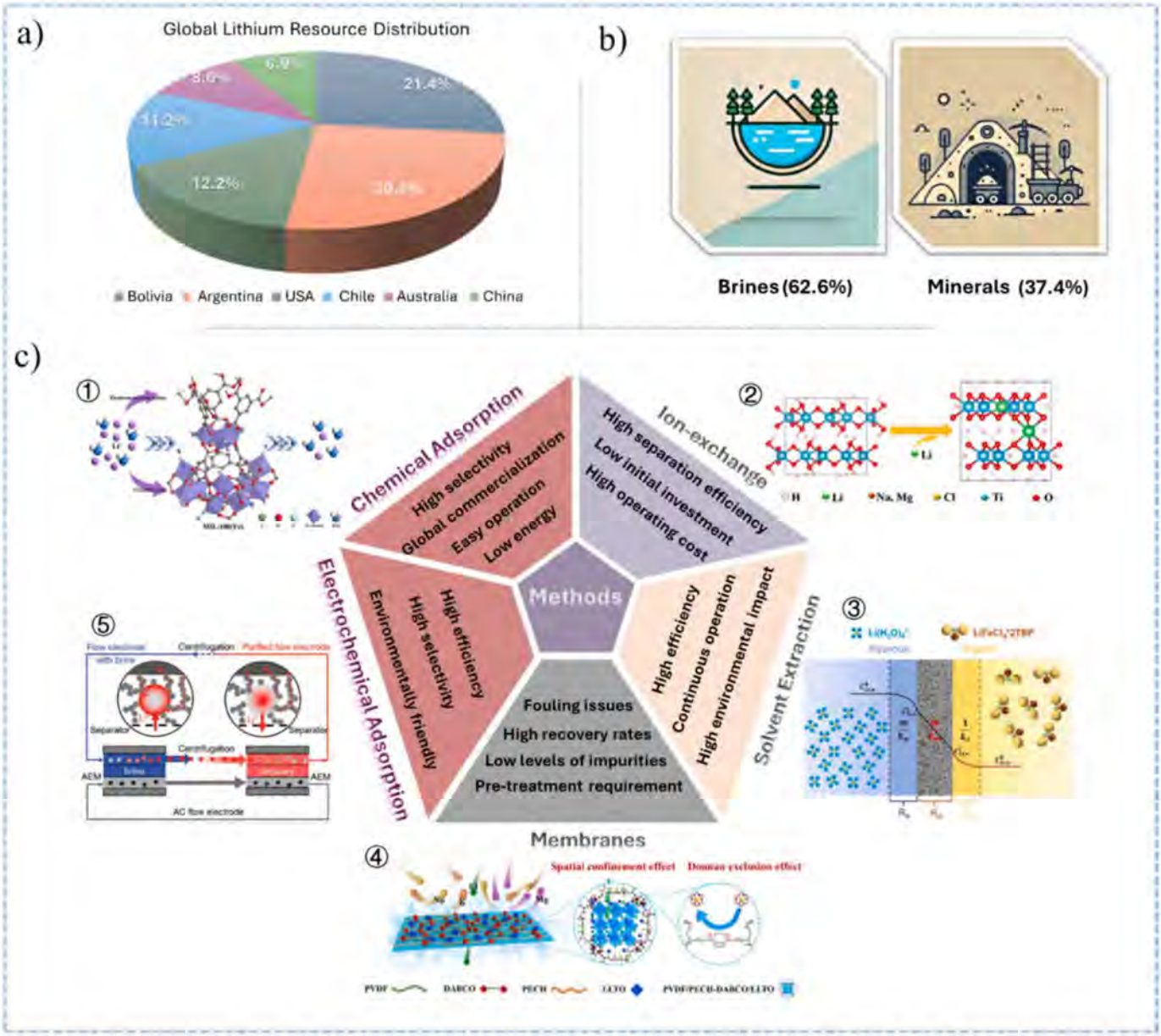

Fig. 1. (a) Global lithium resource distribution by countries; (b) Types and proportions of lithium resource; (c) Various lithium extraction methods and the schematic mechanisms for chemical adsorption [14], ion-exchange [15], solvent extraction [16], membranes [17], electrochemical adsorption methods [18], respectively.

or electrochemical adsorption. The key to these technologies lies in the selection of adsorbents and electrode materials [19]. The selectivity of the adsorbents for Li^+ determines the efficiency of the enrichment process, where Li^+ is separated from the brine and subsequently recovered through desorption. The mainly studied lithium adsorbents include manganese-based adsorbents (LMO-LISs), titanium-based adsorbents (LTO-LISs), aluminum-based adsorbents (LiAl-LDHs), ionic sieve-type adsorbents as well as functionalized polymer adsorbents [20–24]. After imparting high electrical conductivity to these materials, several related derivatives can be developed for the use in the electrochemical adsorption process. The application of an electric field promotes the accumulation of Li + on the material's surface, enhancing its adsorption efficiency.

In addition to material selection, the lithium adsorption process is also influenced by several complex factors, including brine pH, temperature, initial lithium concentration, and the presence of coexisting ions. The pH of the brine affects the stability and renewability of the adsorbent material [25]. Temperature influences ion migration rate, adsorption equilibrium, adsorption rate, and desorption energy [26]. Initial lithium concentration impacts the lithium adsorption isotherm and selectivity [27]. Coexisting ions affect the adsorbent's lithium adsorption capacity and selectivity [28]. These factors, either individually or in combination, influence the mechanism of lithium adsorption and the overall effectiveness of the process. Therefore, it is crucial to find reasonable experimental methods and strategies to help understand the detailed reaction routines and inner mechanisms in various complex lithium resource systems, ultimately leading to highly efficient lithium adsorption.

In a typical experimental study of lithium adsorption, various materials are firstly selected. During this stage, parameter optimization experiments are conducted to adjust the morphology, microstructure, and other characteristics of the adsorbent materials to achieve optimal lithium capture efficiency. Lithium adsorption capacity q_e(mg/g) and selectivity (α_{Li}) are considered as crucial reference indices [20,29]. Characterization experiments using techniques such as Transmission Electron Microscopy (TEM), X-ray Diffraction (XRD), and X-ray Photoelectron Spectroscopy (XPS) are performed to determine the microstructure of the materials [30]. Next, systematic lithium adsorption experiments are carried out, including studies on adsorption kinetics and thermodynamics, as well as the effects of co-existing species, temperature, and pH value [31]. In electrochemical adsorption studies, a comprehensive assessment of the material's performance involves several key tests. Conductivity measurements, cyclic voltammetry (CV), and electrochemical impedance spectroscopy (EIS) are essential techniques used to evaluate the material's electrical conductivity and cyclic stability. Together, these techniques provide a robust framework for characterizing and optimizing materials for enhanced electrochemical adsorption [32]. While these traditional approaches cover both the systematic evaluation of lithium adsorption performance and the fundamental characterization of materials, they still lack reliable visualization of the behavior and interaction mechanisms of Li^+ on the surface of materials and within their pores. Additionally, the material screening stage and the optimization of the lithium adsorption process can significantly reduce research efficiency and increase experimental costs. Therefore, employing advanced computational strategies to assist in exploring the lithium adsorption process, screening high-performance adsorbent materials, and optimizing experimental procedures will greatly improve both the scientific understanding and efficiency of lithium adsorption research.

Computational strategies refer to the use of computer-based methods and techniques for modeling, simulating, and analyzing complex systems and processes [33]. These strategies encompass a variety of advanced techniques that leverage computational power to gain insights into phenomena that are difficult to observe directly or experimentally. The main computational strategies include Statistical Mechanics Simulations, Density Functional Theory (DFT) Simulations, Numerical Simulations, Machine Learning (ML), and other methods such as Molecular Mechanics and Quantum Monte Carlo (QMC). Their fundamental principles, application scopes, and computational objectives are summarized in Table 1. Based on the information in the table, it can be concluded that computational strategies can play a crucial role in the field of lithium adsorption. These tools provide in-depth analysis of microscopic mechanisms and accurate simulation of macroscopic processes, aiding in the study of the dynamic behavior of Li^+ ions. Additionally, they can optimize materials and their electronic structures, elucidate lithium adsorption reaction mechanisms, and predict lithium adsorption processes in complex brine systems.

According to the Web of Science, there have been a total of 135 publications on the study of lithium adsorption from brine using computational tools from 2020 to the present. As shown in Fig. 2(a), there were fewer articles on this topic before 2015. However, the number of publications has gradually increased over time, indicating that the demand for lithium resources grows as society develops, more researchers are employing computational tools to study lithium adsorption processes and investigate their inner mechanisms to enhance lithium resource recovery. Fig. 2(b) illustrates the number of publications for different computational strategies applied to lithium adsorption studies. DFT and Statistical Mechanics, including MD and MC simulations, are the predominant research tools. Additionally, there has been a noticeable increase in publications involving ML and other simulation strategies in recent years.

Given the anticipated rise in lithium resource demand due to the advancements of the new energy industry, it is expected that research will increasingly focus on efficient adsorption and recovery of lithium from various complex brine systems. This will drive new demands for the rational and intensive use of computational strategies. Nevertheless, to date, there has been no comprehensive and detailed explanation of how different computational strategies contribute to the lithium adsorption process. Additionally, there is a lack of systematic clarification on how these computational strategies can assist in deeply studying microscopic mechanisms, as well as their contributions to material screening and process optimization.

This review offers a comprehensive analysis of the application of various computational simulation strategies in the lithium adsorption process, covering both traditional chemical adsorption and electrochemical adsorption. It spans a range of simulations, including MD simulations, DFT simulations, numerical simulations, ML, and the less commonly used QMC methods. The principles and methodologies of these simulations are systematically summarized, followed by an in-depth examination of their application in lithium adsorption research. Special emphasis is placed on MD and DFT simulations due to their extensive use in uncovering reaction mechanisms, analyzing phase transitions, and aiding in material design optimization. Additionally, the review delves into the role of strategies such as COMSOL, CFD, and ML in studying flux migration during the lithium adsorption process. Finally, the review summarizes the significant contributions of these simulation methods to lithium adsorption, highlighting the advantages and limitations of each approach, along with insights into potential future research directions in this field. This work significantly enhances the understanding of computational strategies in lithium adsorption, providing essential guidance for improving material design and process efficiency in lithium recovery. By leveraging advanced simulation techniques, it bridges theoretical frameworks and practical applications, contributing to the development of more efficient and sustainable lithium extraction technologies. Furthermore, the findings of this review have far-reaching implications for the advancement of resource extraction methodologies, supporting sustainable development goals and aiding the transition to a low-carbon energy future.

2. Statistical mechanics simulations

Statistical Mechanics Simulations focus on the statistical properties

Table 1
Brief introduction of different computational strategies.

Classification	Main type	Fundamental principle	Application scope	Computational objective
Statistical Mechanics	Molecular Dynamic (MD) Simulations	Numerical calculations [34].	Materials science, chemistry, biology, drug design, and physics [35].	Study the motion of molecules and atoms and their interactions.
	Monte Carlo (MC) Simulations	Random sampling and statistical analysis [34].	Financial engineering, physics, chemistry engineering, and computational biology [35].	Estimate the performance from statistical properties of large random samples.
Density Functional Theory (DFT)	–	Describe the ground state properties by means of electron densities [36].	Materials science, chemistry, physics and biology.	Predict and interpret the electronic structure, and energy states [37].
Numerical Simulations	COMSOL Multiphysics	Finite element analysis [38].	Multi-physics [39].	Accurately predict and optimize the behavior.
	Computational Fluid Dynamics (CFD)	Numerical methods based on the governing equations [40].	Aerospace, automotive engineering, and chemical engineering.	Analyze the flow behavior of gases and liquids [41].
	Network Simulations	Mathematical modeling and computer simulation.	Communication engineering, computer science, network security, transportation, and social sciences [42].	Optimize network design, improve transmission efficiency.
Machine Learning (ML)	–	Build and train algorithms [43].	Engineering areas.	Develop models that can learn and self-improve [44].
Other	Quantum Monte Carlo (QMC)	Random sampling and statistical methods.	Physics, chemistry and materials science [45].	Solve quantum mechanical problems.

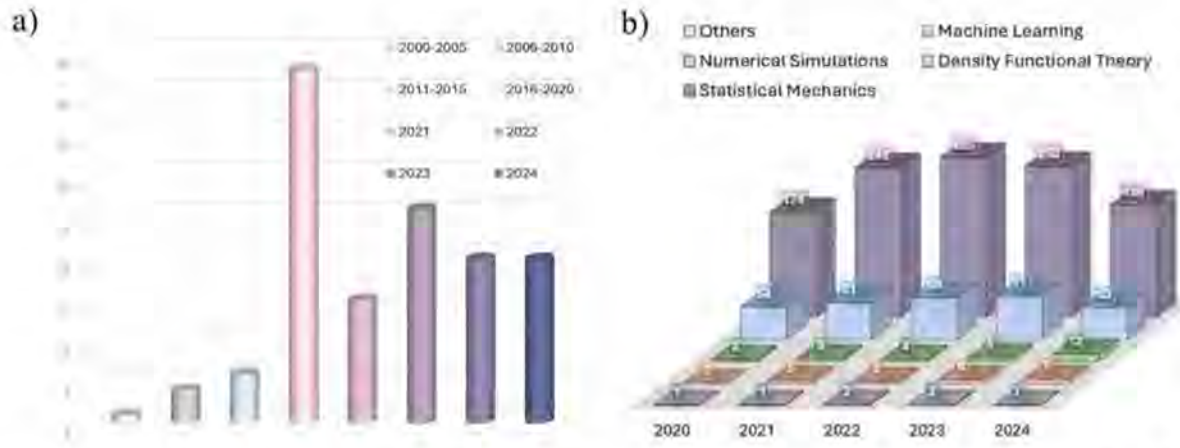

Fig. 2. (a) The number of publications obtained using the guidance word "lithium adsorption, brine, modeling, simulation, computational" in different publication year ranges from Web of Science, accessed on August 8st, 2024; (b) The number of publications obtained using the guidance word "lithium adsorption" under different classifications in year 2020, 2021, 2022, 2023, and 2024 from Web of Science, accessed on August 8st, 2024.

and macroscopic behaviors of lithium adsorption. These simulations can predict the dynamic behavior and thermodynamic properties of systems composed of many particles, typically targeting the large-scale behavior of systems in equilibrium. In the field of lithium adsorption research, MD and MC simulations are two mainstream methods that fall under the category of Statistical Mechanics Simulations. The following sections will systematically explain the principles of these two methods and their applications in the field of lithium adsorption.

2.1. Principle and methodology

2.1.1. MD simulations

2.1.1.1. Software PACKAGE. Several software programs are available for MD simulations, including Groningen Machine for Chemical Simulations (GROMACS), Large-scale Atomic/Molecular Massively Parallel Simulator (LAMMPS), Assisted Model Building with Energy Refinement (AMBER), and Nanoscale MD (NAMD), etc. Among these, GROMACS, LAMMPS, and AMBER are the most used by researchers in the field of lithium adsorption.

GROMACS is a highly efficient and widely utilized open-source software package, originally developed by the University of Groningen in the Netherlands, which is renowned for its exceptional computational speed, particularly in simulating large-scale molecular systems. GROMACS can support a wide range of force fields, making it adaptable to various types of molecular systems. Additionally, flexibility and extensibility contribute to its popularity in biomolecular, chemical, and materials science research [46]. Shen et al. used the GROMACS software package to simulate the immersion of MIL-101(Cr) into aqueous solutions containing different amounts of lithium chloride by means of molecular modeling, which helped to investigate the hydrogen adsorption properties of lithium-doped MIL-101(Cr) [47].

LAMMPS is an open-source software package designed for large-scale simulations of atomic, molecular, and particulate systems. Developed by Sandia National Laboratories under the U.S. Department of Energy (DOE), LAMMPS is particularly well-suited for simulating and analyzing complex material systems using parallel computing techniques. Its key features include robust parallel computing capabilities, support for a wide range of interacting force fields and potential functions, efficient performance, and highly flexible scripting options [48]. Thomas, Glosli, and their colleagues effectively utilized the LAMMPS script to investigate temperature-dependent lithium diffusion in phographene and Li^+ adsorption in aqueous media at charged electrodes [49,50].

AMBER is renowned for its comprehensive and accurate force fields, which precisely describe changes in potential energy surfaces within molecular systems, enabling reliable prediction and analysis of

molecular behavior. One of the key advantages of the AMBER package is its modularity, which is composed of several specialized programs, each designed to perform specific computational tasks. The software supports both explicit and implicit solvent modeling, allowing for flexible adaptation to a wide range of research needs [51]. This flexibility is particularly valuable for in-depth understanding of Li^+ behavior in aqueous solutions and its interactions with surrounding environments. AMBER's capabilities are especially prominent in the study of lithium batteries, electrolyte solutions, and related fields, where its robust features and accuracy are critical. Zhao et al. employed the Gromacs program suited with the General Amber Force Field to simulate the THDX system, which helped to explore the issues of excess additives in the electrolyte and crystallized Li_2CO_3 on the $TiNb_2O_7$ negative electrode [53]. Besides, Purtscher and his teammates also utilized this force field simulation to help explore the applicability of structural and energetic tuning of QM/MM linking bonds using laminar as an example [54]. In conclusion, there are several software options available for studying the lithium adsorption behavior in various complex systems. Each software program offers distinct advantages and is specialized for different aspects of research, making the selection of the most appropriate tool dependent on the specific research needs and objectives. Researchers should select the software that best aligns with their research system's complexity, available computational resources, and specific simulation goals to ensure both accuracy and efficiency in their studies.

2.1.1.2. Algorithm. In computer science, an algorithm is a precisely defined sequence of instructions or steps designed to accomplish a specific task or solve a problem. The selection of an appropriate algorithm depends on factors such as system requirements, computational resources, and the conditions under which simulations are conducted. In MD simulations, different algorithms are employed to meet diverse simulation needs, such as Verlet Algorithm, Ewald summation method, Propagator Algorithm, Langevin Dynamics, and Particle Mesh Ewald (PME). In lithium adsorption research, the Verlet Algorithm, Ewald summation method, and Propagator Algorithm are key computational techniques which have been prioritized to choose.

The Verlet Algorithm is widely regarded as one of the most used integration methods in MD simulations. Initially proposed by Loup Verlet in 1967, the algorithm's core principle is to predict the position of particles at the next time step using the positions from both the current and previous time steps, rather than directly depending on velocity information [52]. This approach enhances the algorithm's stability and accuracy, particularly when simulating particle motion over extended periods. As studied by Ding et al., the Verlet Algorithm was applied to integrate the equations of motion to investigate electron trapping and ion leaching at the Li-modified quartz-water interface [53]. The findings revealed that the interaction between localized electrons and Li^+ influenced the energy levels of excess electrons but also significantly affected the degree of structural distortion and hydrogen bonding at the interface.

The Ewald summation method, introduced by Paul Peter Ewald in 1921, is a numerical technique designed to efficiently handle long-range Coulomb interactions in charged systems. Directly computing the interactions between all charged particles in a system with long-range interactions is highly complex and computationally demanding. The Ewald summation method addresses this challenge by decomposing the Coulomb interaction into two components: a short-range part that converges quickly and can be calculated in real space, and a long-range part that is handled in reciprocal space using Fourier transforms [54]. This decomposition is guided by a convergence parameter, which balances the accuracy of the calculation with computational efficiency. Due to its ability to accurately and efficiently manage complex electrostatic interactions, this method has become an indispensable tool in MD simulations, including those involving lithium adsorption. Quezada et al. published a study in which they utilized the Ewald summation method to accurately compute long-range interactions between cations adsorbed on the surface of both neutral and charged spodumene [55]. Their work provided significant insights into the structural characteristics of the interface between lithium-rich spodumene and saltwater.

The Propagator Algorithm is fundamental in MD simulations, responsible for advancing the system's evolution over time. Its core function is to calculate the state of a particle system at subsequent time steps based on known initial conditions using numerical integration techniques [56]. Propagator Algorithm is an essential tool in simulations, as it determines the accuracy and stability of particle motion. In the field of lithium adsorption, Propagator Algorithm plays a critical role. It not only aids in understanding the trajectory of lithium ions on the surface of adsorbent materials but also effectively handles complex interfacial diffusion reactions. Additionally, it is invaluable for optimizing the properties of adsorbent materials and ensuring the system's energy conservation throughout the simulation. Xiao et al. investigated the kinetic of Li^+ intercalation into $LiFePO_4$ by means of analyzing the phase boundary propagation pattern, showing how the phase in Li_xFePO_4 evolves in the absence of experimental parameters [57]. To summarize, different algorithms targeting different complex systems can strongly assist the multiple applications of MD simulations in the field of Li^+ adsorption. Researchers can choose a reasonable algorithm according to the objective needs to improve the efficiency of scientific research.

2.1.1.3. Ensemble. In MD simulations, an ensemble is a mathematical concept used to describe the possible microstates of a multiparticle system under specific macroscopic conditions. Ensembles provide a statistical framework for studying the macroscopic properties of a system by considering all possible microstates and their associated probability distributions. Common ensembles include the Microcanonical Ensemble (NVE), Canonical Ensemble (NVT), Isothermal-Isobaric Ensemble (NPT), and Isobaric-Isenthalpic Ensemble (NPH). In the context of lithium adsorption studies, selecting the appropriate ensemble is crucial. The chosen ensemble determines the macroscopic conditions (e.g., temperature, pressure, energy) of the simulated system, directly influencing the accuracy and physical relevance of the Li^+ adsorption process.

NVE ensemble in statistical mechanics is used to describe all possible microstates of an isolated system with a fixed number of particles, volume, and total energy. Unlike other ensembles, an NVE system does not exchange matter or energy with its surroundings, making it an energy-conserving system [58]. This characteristic makes the NVE ensemble particularly suitable for simulating systems under isolated conditions. In the context of lithium adsorption research, the NVE ensemble is crucial for accurately simulating the system's energy conservation and for calculating the kinetic and thermodynamic properties that underlie the lithium adsorption process. It allows researchers to study the intrinsic behavior of the system without external influences, making it the optimal choice for investigating isolated systems. Nasr Esfahani et al. utilized an NVE ensemble, with velocities assigned according to the Maxwell-Boltzmann distribution at various temperatures ranging from 50 to 1000 K, to investigate the structural transitions in monolayer MoS_2 induced by lithium adsorption. This approach allowed them to explore how lithium adsorption affects the structural dynamics of MoS_2 under different thermal conditions, providing insights into the material's behavior across a wide temperature range [59].

NVT ensemble is used to characterize all possible microstates of a system under constant particle number, volume, and temperature. In this ensemble, the system exchanges energy with its surroundings to maintain a constant temperature, while the particle number and volume remain fixed [60]. This setup is typically employed to simulate closed systems at a constant temperature. In MD simulations, the NVT ensemble is frequently utilized to study the dynamics and thermodynamics of systems, particularly in processes such as lithium adsorption. For example, Park et al. utilized an isothermal NVT ensemble in their

simulations, applying thermostats to control the temperature while keeping the volume constant [61]. This approach allowed them to maintain room temperature conditions and successfully investigate the mechanisms of lithium adsorption and intercalation in bilayer TiC_3.

NPT ensemble describes a system under conditions of constant particle number, pressure, and temperature. In this ensemble, the system can exchange energy and volume with its surroundings, but the number of particles remains constant. It is commonly used in MD simulations to model the behavior of systems under realistic experimental conditions, particularly where temperature and pressure are held constant [62]. NPH ensemble, on the other hand, describes a system with a constant number of particles, pressure, and enthalpy. In this case, the system can exchange volume with its environment, but the total energy remains fixed. The NPH ensemble is crucial for understanding the kinetic behavior and energy distribution of materials under constant pressure conditions. By modeling enthalpy changes, researchers can more accurately predict how materials will respond to different pressure conditions. Through employing the NPT and NPH ensembles, researchers can accurately simulate the behavior of materials under various macroscopic conditions, leading to a deeper understanding of the intrinsic properties

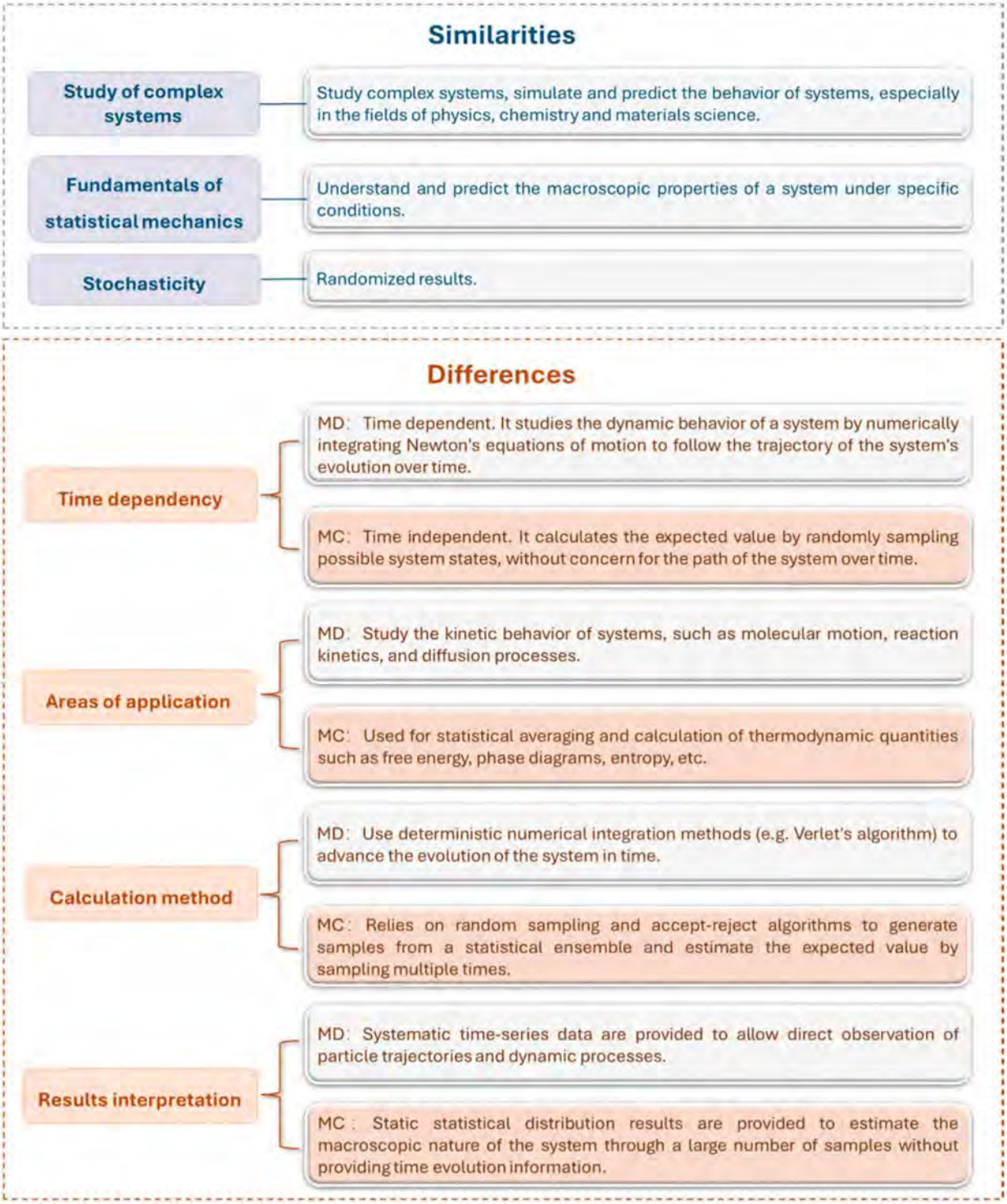

Fig. 3. The similarities and key differences between MC and MD simulations.

and reaction processes of these materials [63]. These ensembles are widely applicable and hold significant theoretical importance in fields such as materials science, chemical engineering, and physics research, particularly in studies related to lithium adsorption. For example, Li et al. and his team conducted NPT-assisted simulations to model the real-time intercalation process of Li^+ into graphite. Their findings revealed that as Li^+ accumulates, the graphite layers undergo expansion, leading to the formation of wrinkles and eventually resulting in inhomogeneous cracks [64,65]. Shumeyko et al. also investigated the Li^+ transport process into graphite, but utilized the NPH ensemble to specifically examine the effects of grain boundary structures [66]. Their study provided valuable insights into how these structural features influence the behavior of Li^+ as they move through the graphite matrix.

To sum up, in MD simulations, choosing the appropriate software, algorithms, and ensembles is essential for obtaining accurate and reliable results. Each component plays a critical role in modeling the system's behavior and ensuring the precision of the simulation, particularly in complex studies like lithium adsorption in different systems.

2.1.2. MC simulations

MC simulations, like MD simulations, are a widely used computational technique grounded in statistical mechanics. The similarities and key differences between MC and MD simulations are systematically outlined in Fig. 3. Briefly, although they are employed to study complex systems and rooted in the principles of statistical mechanics, they differ significantly in their methodologies and areas of application. MD simulations emphasize the time evolution of systems, making them ideal for studying dynamic behaviors and processes. Conversely, MC simulations focus on random sampling to compute expected values, primarily for statistical averaging and thermodynamic property calculations. Each method has its unique strengths, and the choice between them depends on the specific objectives of the study [67].

Furthermore, beyond the methodologies previously discussed in MD simulations, MC simulations incorporate unique features such as random sampling and acceptance-rejection algorithms, along with path integration methods for quantum systems [68–70]. These elements offer significant advantages in handling high-dimensional integrals, studying phase transitions, analyzing quantum effects, and performing statistical confidence analysis. These capabilities make MC simulations an excellent complement to MD simulations, catering to different types of scientific studies and providing robust tools for exploring complex systems. For example, Malik et al. investigated why $LiFePO_4$ can be charged and discharged rapidly despite having to undergo a first-order phase transition, figuring out the Li^+ intercalation mechanism in phospho-olivines through an acceptance-rejection algorithms scheme [71]. Besides, Dubecky et al. introduced basic notions of electronic structure Quantum MC based on random walks in real space as well as its advances and adaptations to systems with noncovalent interactions, clarifying its potential and significance in simulating noncovalent interactions between different substances in complex systems [72]. In conclusion, choosing different algorithms in MC simulation is crucial as it directly influences the efficiency, accuracy, and convergence speed of the simulation, allowing researchers to tailor the approach to the specific nature and complexity of the problem being studied.

2.2. Applications in lithium adsorption

The application of Statistical Mechanics Simulations, especially MD and MC simulations, offers powerful tools for uncovering microscopic mechanisms of lithium adsorption. These techniques are invaluable for predicting material properties, investigating kinetic behaviors, analyzing thermodynamic properties, and optimizing structural designs. By guiding experimental validation and driving scientific progress, MD and MC simulations play a crucial role in advancing research in this field. This section systematically discusses the role of Statistical Mechanics Simulations in uncovering the mechanisms of lithium adsorption, their applications in structure optimization and design, and their contribution to experimental validation and guidance.

2.2.1. Mechanisms revelation

Statistical Mechanics Simulations offer valuable insights into the microscopic mechanisms governing Li^+ intercalation and de-intercalation at the atomic and molecular levels. These simulations enable detailed observation of Li^+ adsorption processes on various material surfaces, such as titanium dioxide, Li/Al-LDH, and carbon-based materials. In their study of lithium adsorption on layered H_2TiO_3, Marthi et al. utilized MD simulations alongside systematic characterization analysis to challenge the previously accepted mechanism, which suggested that lithium adsorption occurs via Li^+-H^+ ion exchange without breaking chemical bonds. As illustrated in Fig. 4(a), the -OH groups on the surface of H_2TiO_3 are disrupted during the lithium adsorption process. H_2TiO_3 contains both isolated -OH groups and hydrogen-bonded -OH groups. Among these, the isolated -OH groups within the HTi_2 layer are more actively involved in lithium adsorption process compared to the hydrogen-bonded -OH groups [73]. Li/Al-LDH, a widely used material for the adsorptive extraction of lithium from brine, has greatly benefited from MD simulations. Chen and her team developed a one-step interlayer restoration strategy, leveraging MD simulations to swiftly replace intercalated SO_4^{2-} with preferentially adsorbed Cl^-, addressing issues that impair cycling performance [74]. As shown in Fig. 4(b), the simulation results indicate that SO_4^{2-} anions are progressively displaced from the Li/Al-LDH interlayer to the bulk phase as Cl^- concentration increases. This suggests that a high Cl^- concentration facilitates anion exchange, effectively removing intercalated SO_4^{2-} and restoring the interlayer structure to its original Cl^--intercalated form. This approach offers a promising solution for lithium extraction in sulfate-rich Salt Lake brines. Carbon-based materials, such as carbon nanotubes, also benefit from this strategy. Song et al. conducted a detailed investigation into the intercalation and diffusion behaviors of Li^+ in carbon nanotube bundles using ab initio MD simulations [75]. As illustrated in Fig. 4(c), Li^+ rapidly penetrates the spaces between adjacent carbon nanotubes. At low Li^+ ion densities, these ions tend to congregate near the ends of the nanotubes. Additionally, Li^+ can traverse the carbon nanotubes, moving from one end to the other, and can remain lodged between neighboring nanotubes. This behavior reveals a novel pathway for Li^+ deposition and storage, helping following researchers broaden their scientific horizons.

Additionally, Statistical Mechanics Simulations are instrumental in studying interfacial reactions, shedding light on the reaction mechanisms of Li^+ at the electrode/electrolyte interface, thereby enhancing our understanding of electrochemical reactions at the solid-liquid boundary. Jorn et al. simulated the ion desolvation phase, focusing on the entry and exit of Li^+ in two solid electrolyte interphase models composed of lithium ethylene dicarbonate and Li_2CO_3, attached to an ethylene carbonate electrolyte [76]. By correlating the free energy changes with the solvation structure, they discovered that the insertion path of Li^+ follows a two-step mechanism, requiring the overcoming of two energy barriers: adsorption and absorption (see Fig. 4(d)). Besides, Aggarwal et al. explored the driving forces behind the adsorption of Li^+ onto $Li_{0.5}CoO_2$ electrodes in electrolytes based on $LiClO_4$, $LiPF_6$, and LiTFSI in an EC/EMC (3:7) mixture, using enhanced sampling MD simulations [77]. As illustrated in Fig. 4(e), two key energetic features-the driving force for adsorption and the thermodynamic barrier to desorption-were identified. These features, analyzed through free energy curves, reveal the molecular origins within various $Li_{0.5}CoO_2$ electrolyte systems.

2.2.2. Dynamic behavior studies and thermodynamic properties

Statistical Mechanics Simulations also play a crucial role in studying the dynamic behavior and thermodynamic properties of lithium adsorption processes. These simulations allow for the detailed analysis of how Li^+ interacts with various materials at the atomic level, providing

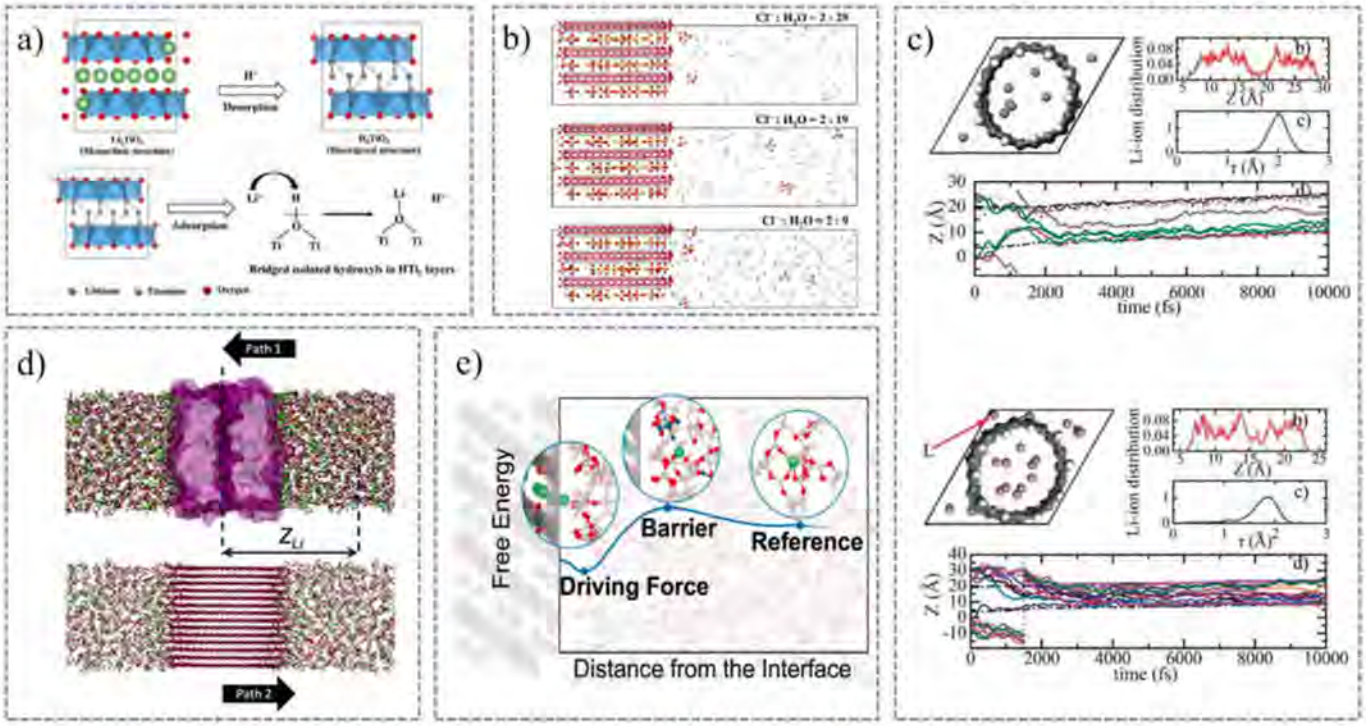

Fig. 4. (a) Graphical abstract for Li^+ adsorption mechanism on layered H_2TiO_3 [73]; (b) System snapshots of MD simulations for interlayer anion exchange of SO_4^{2-} intercalated Li/Al-LDH in different $MgCl_2$ concentration bulk phases with a run time for 8 ns [74]; (c) Behavior of the eight/sixteen Li^+ ions intercalating and diffusing inside or between the carbon nanotubes [75]; (d) Snapshots of the simulation cells [76]; and (e) Graphical abstract for the insertion mechanism path of Li^+ [77].

insights into the kinetics of adsorption, diffusion pathways, and the stability of adsorbed states. For example, to investigate the deactivation mechanism of Li/Al-LDH, Chen et al. employed MD simulations to model the intercalation reaction of Li^+ into gibbsite in the experimental regeneration solution [78]. As shown in Fig. 5(a), the Li^+ intercalation into gibbsite increased after 100 ps of reaction, correlating with a higher initial Li^+ concentration in the bulk phase regeneration solution. Additionally, as the system temperature increased, the amount of Li^+ intercalation also rose by 0.4 mg/g after 1100 ps of reaction. This demonstrates the significant impact of initial Li^+ concentration and temperature on the regeneration of deactivated Li/Al-LDH. In addition, Park et al. also studied the lithium adsorption and intercalation in bilayer TiC_3 using NVT-MD simulations and simulated the interaction between the electrode material $LiTiC_3$ and the electrolyte tetraethylene glycol dimethyl ether (TEGDME) molecules at a temperature of 800 K. As illustrated in Fig. 5(b), 800 K was selected as the temperature for the chemical reaction to occur due to the exothermic reaction at the electrode-electrolyte interface, which generates a heat flow, causing the temperature to rise instantaneously [61]. Besides, at 50 fs, the highest temperature peak enhanced the chemical reaction between the electrode and electrolyte, leading to electrolyte decomposition. As the simulation progressed, heat began to react between the lithium ions and electrolyte molecules, transferring energy to the TEGDME molecules. Olou'ou Guifo et al. also conducted a study on the lithiation of amorphous silicon using MD simulations to explore the behavior of an amorphous Si@Li interface model at various temperatures [79]. Fig. 5 (c) illustrates the final structure of the a-Si@bcc-Li system after geometric relaxation followed by 1 ns of equilibration at different temperatures. The initial geometric relaxation led to a decrease in potential energy by -0.6 J/m^{-2}, attributed to the formation of adhesive lithium-silicon bonds. Simulations in this study were crucial for understanding the diffusion behavior of lithium ions, providing valuable insights into the material's performance under different conditions. In addition to the aforementioned studies, MD simulations can also be employed to model changes in material structure over time. Zheng and his team utilized this approach to investigate the dynamics of nanoporous polyethylene membranes for Li^+ transport [80]. As illustrated in Fig. 5(d), during the stretching simulations, the pore volumes in the P8 and P10 models increased rapidly after $t = 0.8$ ns and $t = 4.0$ ns, respectively, indicating significant growth in pore size. In contrast, the P12 model exhibited a slower increase in pore volume, resulting in smaller pore sizes when stretched to 8 nm. Furthermore, a film consisting of 16 polyethylene chains was found to be extremely dense with nearly no pores, hence those results are not presented.

By calculating thermodynamic quantities such as free energy, entropy, and enthalpy, Statistical Mechanics Simulations can also help predict the feasibility and efficiency of lithium adsorption under different conditions. This information is vital for optimizing material design and improving the performance of lithium-ion batteries and other related technologies. In the current work, Aggarwal et al. used MD simulations to explore the free energy associated with Li^+ solvation environments in the presence of $TFSI^-$ or ClO_4^- anions [77]. The results, shown in Fig. 5(e), reveal distinct behaviors of these electrolytes within the thermodynamic barrier region (3–5 Å from the electrode). For $LiClO_4$, a continuum of nearly isoenergetic Li^+ solvation configurations are observed, while for LiTFSI, only one dominant solvation configuration is present. Another study that examined the thermodynamics of Li-intercalated graphite using vibrational and configurational contributions, aided by MD simulations, further confirmed the significant contribution [81]. As shown in Fig. 5(f), for the range $0.5 < x < 1$, the entropy change (ΔS) of -0.16 meV·K^{-1}·Li^{-1} is attributed to the vibrational contribution. This entropy reduction can be ascribed to the restricted motion of Li^+ in Li_xC_6. This thermodynamic analysis provides critical insights into the behavior and stability of Li-intercalated graphite, enhancing the understanding of its potential applications in energy storage systems.

In conclusion, Statistical Mechanics Simulations are invaluable for research on lithium adsorption/desorption. They offer a detailed

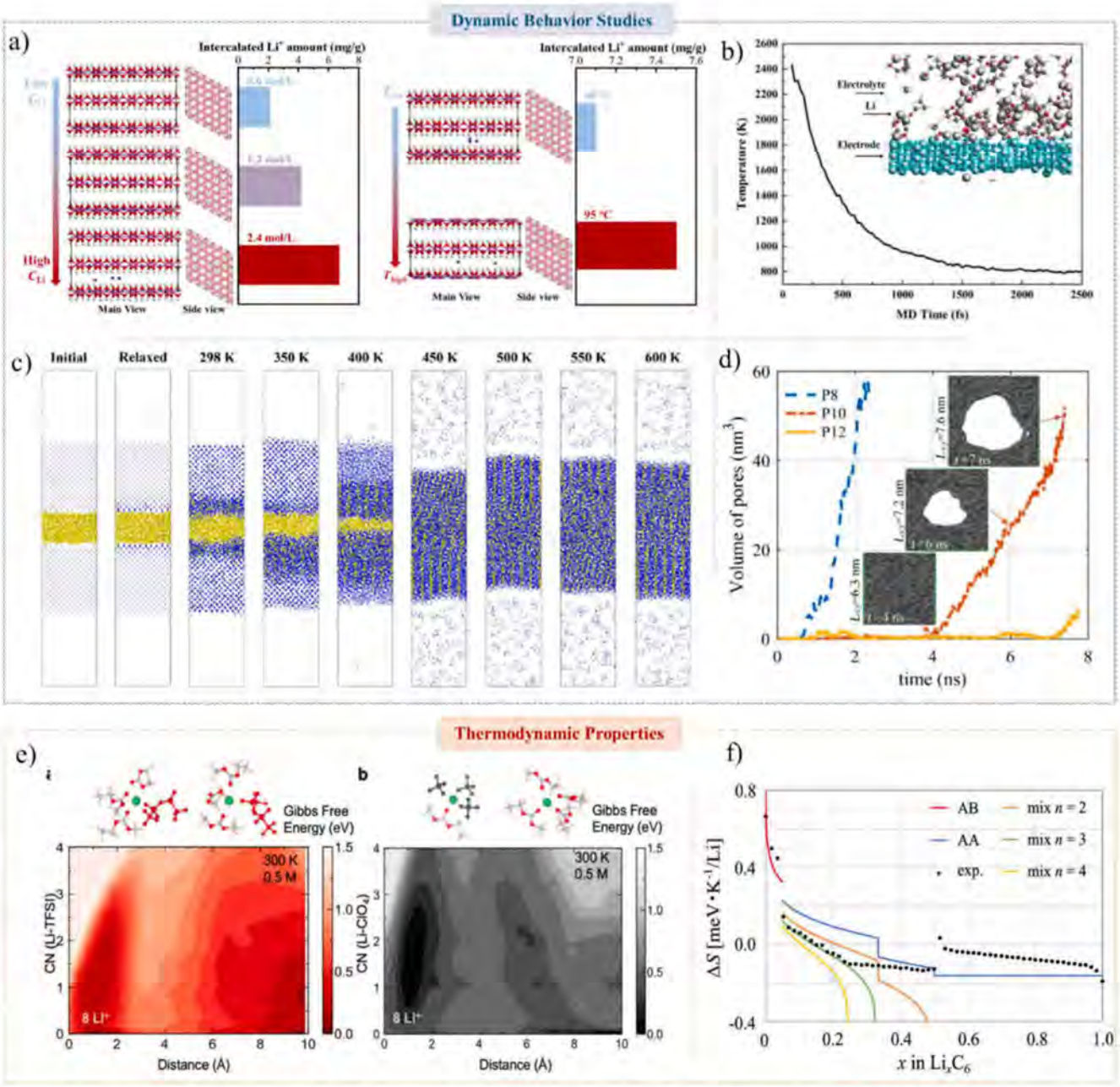

Fig. 5. (a) Simulation results of Li^+ intercalation into gibbsite under different conditions [78]; (b) Simulation snapshot at 0.25 fs and temperature contribution as a function of MD time [61]; (c) Concentration profiles of Si and Li atoms interdiffusing at various temperatures [79]; (d) Evolutions of pore volumes during the tensile simulation process [80]; (e) Free energy changes as a function of solvation environment of Li^+ ions [77]; (f) Entropy change (ΔS) of Li_xC_6 as a function of lithium concentration (Red, blue, orange, green, and yellow lines show the entropy changes of the configurational parts) [81].

understanding of the kinetic behavior and thermodynamic properties of the system. By simulating molecular interactions over time, researchers can uncover the transport of Li^+ and predict how different variables influence adsorption efficiency. This capability not only enhances our comprehension of the underlying processes but also informs the optimization of materials and conditions for more efficient lithium recovery.

2.2.3. *Structure optimization and design*

Statistical Mechanics Simulations play a crucial role in optimizing and designing materials for lithium adsorption studies. These simulations provide a detailed understanding of the molecular or atomic-level interactions, allowing researchers to predict the behaviors of lithium within different material structures. By accurately modeling the adsorption process, Statistical Mechanics Simulations can help identify the most efficient materials, optimize their performance, and guide the development of new materials with enhanced adsorption capabilities. For example, Sun et al. utilized MD simulations with the Materials Studio software to investigate the diffusion behavior of counterions within polyelectrolyte materials [82]. As shown in Fig. 6(a), the polyelectrolyte molecules maintained electrical neutrality. The figure also presents two models of the molecular configuration of the polyelectrolyte chain, corresponding to different numbers of Mg^{2+} ions in the system. The results demonstrate that as the concentration of Mg^{2+} ions in the aqueous solution increases, a greater number of Mg^{2+} ions preferentially bind to the sulfonate groups. This finding provides a theoretical foundation for the screening and performance prediction of lithium-selective materials.

In helping research on electrode materials, Tritsaris et al. conducted

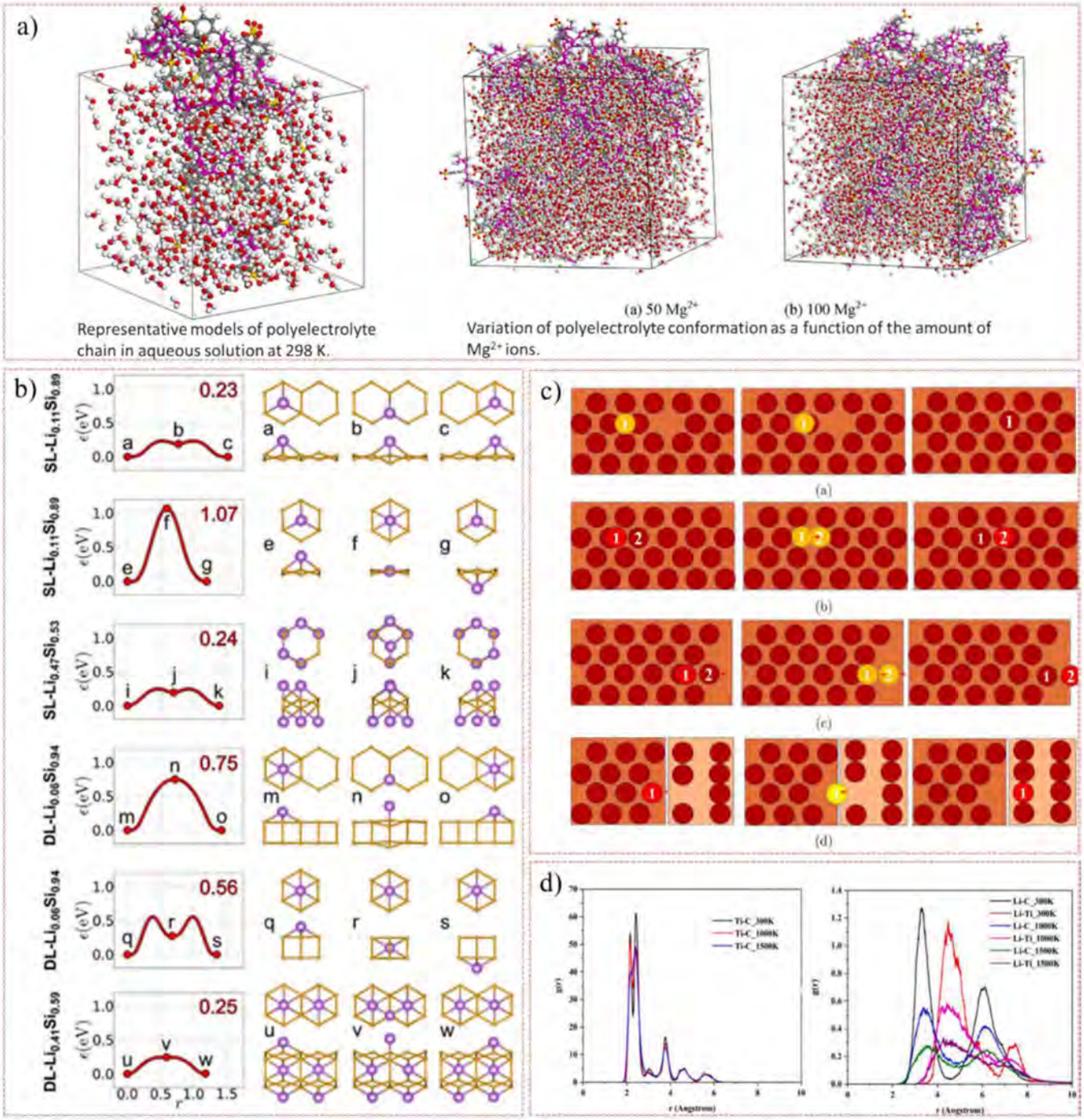

Fig. 6. (a) MD model of polyelectrolyte chain in aqueous solution at 298 K and its varization as a function of the amount of Mg^{2+} ions (Purple, red, yellow, white, dark green, and light green parts represent the backbone chain of the polyelectrolyte molecules, O atoms, S atoms, H atoms, Mg 2p ions, and Cl ions, respectively) [82]; (b) Pathways for the diffusion of atomic Li^+ on single-layer (SL) and double-layer (DL) silicene, Li_xSi_{1-x}, at low ($x = 0.11$) and high ($x > 0.40$) Li contents [83]; (c) Top view of four possible diffusion mechanisms [84]; (d) Radial distribution function g(r) of Ti—C and Li—C and Li—Ti at different temperatures [61].

a simulation study on the adsorption and diffusion of Li^+ on layered silicon [83]. According to the results shown in Fig. 6(b), they found that the energy barriers for Li^+ diffusion pathways are smaller than or comparable to those in bulk silicon and silicon nanowires (<0.6 eV). The study revealed that the number of silicon layers did not significantly affect the energetics of lithium adsorption. Therefore, if more precise control over the energetics of lithium adsorption is desired, other strategies must be employed, such as doping or exploring finite size effects in silicane nanoribbons. Through this research, they successfully evaluated whether two-dimensional silicon in the form of silicane layers is suitable for Li^+ storage and provided useful guidance for optimizing layered silicane material. Fig. 6(c) also presents the results of this study, which employed kinetic MC methods and the Embedded Atom Method to investigate the electrodeposition of metallic lithium on the surface of lithium anodes in lithium-ion batteries LIBs [84]. As depicted in the figure, the diffusion of adsorbates during the electrodeposition process can be quite complex, differing significantly from the diffusion of adsorbed atoms on metal surfaces grown from vapor. To describe the complex adsorption and diffusion behavior on the deposit surface, the model used by the study suggests four potential diffusion mechanisms:

hopping, bulk atom exchange, step edge atom exchange, and grain boundary. Understanding these diffusion mechanisms more deeply can aid in optimizing the operating conditions of lithium-ion batteries and enhancing the chemical structure of the adsorbate materials on the anode surface. In addition, Park et al. conducted a study on lithium adsorption and intercalation in bilayer TiC_3, utilizing simulations and radial distribution function (RDF) to understand the relationship between lithium and the TiC_3 bilayer material [61]. As shown in Fig. 6(d), at 300 K, the primary peaks of the Li—C and Li—Ti g(r) are located at 3.30 Å and 4.51 Å, respectively. The RDF peaks are sharper at 300 K but gradually broaden and decrease in intensity at higher temperatures, indicating weaker atomic interactions due to increased atomic kinetic energy. At 1500 K, the second peak of the Li—Ti interaction begins to disappear, suggesting that lithium loses its interaction with titanium, while the interaction between Li and C remains intact. This simulation provided crucial insights that helped deepen the understanding of the interaction dynamics in the TiC_3 bilayer, contributing significantly to the following modification of TiC_3 material.

In summary, Statistical Mechanics Simulations are essential in optimizing and designing lithium-selective adsorption materials and electrode materials by offering deep insights into atomic and molecular interactions. Researchers can strategically select simulation strategies and methodologies tailored to the specific material requirements and anticipated lithium adsorption effects, using experimental results to further enhance the achievement of targeted outcomes.

2.2.4. *Experimental validation and guidance*

Statistical Mechanics Simulations are vital for experimental validation in the field of lithium adsorption. By accurately predicting the interactions between lithium ions and adsorbents, researchers can validate their experimental results against simulation outcomes, ensuring that the observed behaviors align with expected outcomes. This process not only strengthens the credibility of the research but also pinpoints potential areas for improvement in the adsorption process before committing to costly and time-consuming experiments.

Han et al. investigated the modulation of the microenvironment in adsorption processes to enhance the efficiency of lithium extraction under natural pH conditions [85]. They pointed out that a shift in the zeta potential of the adsorbent surface from negative to positive could be achieved by incorporating quaternary ammonium groups via selective electrostatic interactions. As illustrated in Fig. 7(a), this modification significantly improved lithium adsorption selectivity, reduced the consumption of bases, and facilitated the separation of Li^+ from Mg^{2+}. To elucidate the underlying mechanism, MD simulations were conducted using the COMPASSII atomic force field, which incorporates original force field parameters for various elements. The simulation results, depicted in Fig. 7(a), revealed a pronounced gradient in the distribution of H^+ within systems exhibiting a positive electric field. In contrast, systems lacking a positive electric field showed a uniform and stable distribution of H^+ throughout the diffusion process. These findings suggest that a positive electric field enhances the migration of H^+ away from the adsorbent, thereby minimizing competitive adsorption. The simulation results strongly support the effectiveness of microenvironmental modulation in adsorption techniques and provide a mechanistic understanding of the adjustments employed in this study. In addition, Ge et al. explored the influence of the 15C crown ether moiety (2-hydroxymethyl-15-crown-5, abbreviated as 15C) on Li^+ ion pathways in graphene oxide membranes using MD simulations performed with the LAMMPS [86]. As depicted in Fig. 7(b), an optimal concentration of 15C enhances the water permeability of the membranes. However, excessive amounts of 15C lead to channel blockage, impeding water molecule transport. Furthermore, the selective recognition of Li^+ by 15C promotes Li^+ transport within the channel. In order to validate the conclusion, the simulations revealed that an excessive concentration of 15C occupies crucial separation space within the channel, leading to increased interactions between water molecules and the membrane. This strong adsorption of water molecules decreases membrane permeability. This study corroborates experimental observations with simulations and provides new insights into Li^+ transport and adsorption in membrane materials.

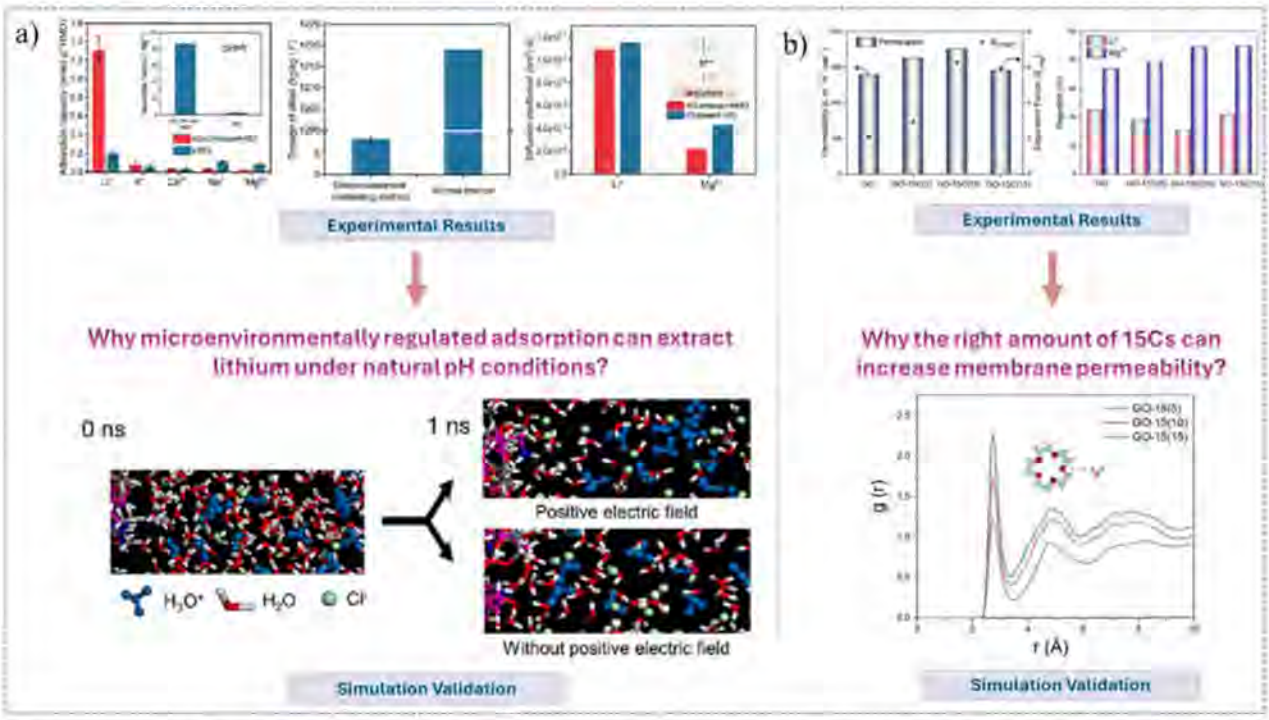

Fig. 7. (a) The selectivity of the adsorbent to different ions, the alkali dosage of different methods, the diffusivity coefficient of Li^+ ions and Mg^{2+} ions in different systems, and the migration state of hydrogen ions in different systems [85]; (b) The permeability and Li^+/Mg^{2+}separation factor of different GO-15C nanochannels, the rejections to Li^+ and Mg^{2+} of different GO-15C nanochannels, and the RDFs of water (H atom) and 15C (O atom) in different GO- 15C nanochannels [86].

In conclusion, Statistical Mechanics Simulations significantly contribute to research in lithium adsorption by providing a robust framework for predicting and optimizing the interaction dynamics between Li^+ ions and adsorbent materials. These simulations enable researchers to meticulously analyze and forecast the efficiency of adsorption processes under various conditions, thereby facilitating the design of more effective and selective adsorbents. By minimizing the need for extensive experimental testing, these tools not only save time and resources but also enhance the precision of the research outcomes, leading to more innovative and practical solutions in the field of lithium extraction technologies.

3. DFT simulations

Besides Statistical Mechanics simulations, DFT specializes in electronic structure calculations, offering insights into the ground state energy and electronic interactions within materials, making it ideal for investigating the microelectronic mechanisms of lithium adsorption. DFT calculations are essential for providing a deeper understanding of the electronic properties and energy changes associated with lithium adsorption, which are crucial for elucidating the lithium adsorption mechanism and optimizing material properties. This section presents the software, methodologies, and key application cases of DFT in lithium adsorption studies.

3.1. Commonly used software

DFT is a quantum mechanical method used to investigate the electronic structure of many-body systems, particularly atoms, molecules, and solids. DFT is based on the Hohenberg-Kohn theorems, which states that the ground state properties of a system are uniquely determined by its electron density rather than its wavefunction. By solving the Kohn-Sham equations, DFT allows the calculation of electronic properties with relatively low computational cost, making it widely used in chemistry, physics, and materials science. Currently, various software packages are employed by researchers to study lithium adsorption/intercalation in complex systems. These include Vienna Ab-initio Simulation Package (VASP), Quantum ESPRESSO, Cambridge Serial

Software	Characteristics	Applications	*Ref.*
VASP	Efficient and accurate first-principles calculations based on plane-wave basis sets and pseudopotentials.	Electronic structure and dynamics simulations of solids, surfaces and nanostructures.	29, 87-96
Quantum ESPRESSO	Open-source nature and flexibility, supporting a wide range of first-principles computational methods.	Electronic structure, phonon and MD of solid materials, with good parallel computing performance.	97-101
CASTEP	A first-principles computational software based on plane-wave and pseudopotential methods, with special expertise in electronic structure, energy bands.	Solid-state physics, chemistry, materials science, nanotechnology and other fields.	102-106
Gaussian	Powerful quantum chemical computational capabilities to accurately calculate molecular structures, reaction energy barriers, and spectral properties.	Organic chemistry, drug design, and materials science, it is capable of accurately calculating molecular structures, reaction energy barriers, and spectral properties.	90, 103, 107, 108
ORCA	A flexible and powerful quantum chemistry software with excellent parallel computing capabilities.	Organic, inorganic and biochemistry for molecular structure prediction, reaction mechanism study, spectral simulation.	109-111
DMol³	A quantum chemistry software with a numerical basis group approach.	Materials science, catalysis research, surface science, and molecular chemistry.	106, 112-114

Fig. 8. Commonly used softwares of DFT simulations in the research field of lithium adsorption and their characteristics and application areas [87,96–101,107,108,110,111].

Total Energy Package (CASTEP), Gaussian, Open-Source Release of Chemical Applications (ORCA), and Density Functional Theory Molecular Orbital Package (DMol [3]). The main characteristics and applications of these tools are summarized in Fig. 8 [29,87–114]. Statistical analysis indicates that different software can cater to distinct simulation needs in lithium adsorption research. Among these, VASP and CASTEP are the most widely used. Besides, selecting the appropriate DFT simulation software is essential for researchers, as each software offers unique strengths in computational efficiency, accuracy, and the ability to handle specific systems (e.g., molecules, solids, surfaces) and scalability of functions. Making the right choice ensures accurate and reliable results while significantly enhancing the efficiency of the research process.

3.2. Principle and methodology

In DFT simulations, the choice of algorithms and basis sets is critical. The algorithm determines computational efficiency and accuracy, directly influencing the reliability of the results, while the basis set represents the electronic wave function, with its quality and suitability being essential to accurately describing the electronic structure. Selecting appropriate algorithms and basis sets enhances computational efficiency and accuracy, meeting the research requirements of various systems.

The main classifications, characteristics, and application areas of different algorithms for DFT in the field of lithium adsorption are summarized in Table 2. As shown, several algorithms, including Kohn-Sham DFT, Hybrid Functionals, Transition State Search, Dispersion Correction, PAW (Projected Augmented Wave) Method, and Hybrid Exchange-Correlation Functional, are widely used. Specifically, Kohn-Sham DFT encompasses GGA (Generalized Gradient Approximation), PBE (Perdew-Burke-Ernzerhof Functional), and LDA (Local Density Approximation). Transition State Search includes methods like LST (Linear Synchronous Transit), QST (Quadratic Synchronous Transit), and Cl-NEB (Climbing Image Nudged Elastic Band). In the field of lithium adsorption, Kohn-Sham DFT is the most commonly used foundational algorithm, simplifying complex many-electron problems into independent electrons moving in an effective potential field, thus balancing computational accuracy and efficiency across various materials and chemical systems. Additionally, the Transition State Search algorithm is frequently employed to identify transition states along reaction pathways, aiding in the study of reaction mechanisms and energy barriers. It is often combined with Kohn-Sham DFT to precisely predict reaction paths and activation energies. The distinct characteristics of these algorithms enable them to play significant roles in different areas of research. Besides, different basis sets are also detailed in Table 2, including Plane-Wave Basis Sets, DNP (Double Numeric Polarization), def2-TZVP, and OTFG/Ultrasoft Pseudopotential. Among these, CASTEP is particularly notable for its use of plane-wave functions as the basis set to represent electronic wave functions, making it the most frequently used basis set in lithium adsorption-related literature. This preference highlights CASTEP's efficiency and accuracy in handling complex periodic systems. Other basis sets, such as DNP and def2-TZVP, offer advantages in specific applications, providing researchers with a range of

Table 2
Commonly used principles and methodologies of DFT simulations in the research field of lithium adsorption.

Methodologies	Classifications	Sub-classifications	Characteristics	Application areas	Ref.
Algorithms	Kohn-Sham DFT	GGA PBE LDA	Consider gradients in electron density.	Fundamental electronic structure calculations in solid state physics and materials science.	[17,29,88,89,92–95,102–106,112–116] [17,29,88–93,95,102–105,112,114–117] [118,119]
	Hybrid Functionals	B3LYP	Combine the exchange-correlation generalization with a portion of the exact Hartree-Fock exchange energies.	Molecular structure, reaction energy barriers, spectroscopic properties.	[113,120]
	Transition State Search	LST QST Cl-NEB	Pinpoint transition states in chemical reaction paths, which are the highest energy points at which reactants are transformed into products.	Kinetics of reactions, calculating reaction energy barriers, and predicting reaction rates	[116,121,122] [116,121,122] [17,91–93]
	Dispersion Correction	DFT-D	Improve the accuracy of calculations by introducing additional correction terms to compensate for the lack of description of van der Waals forces.	Molecular docking, adsorption energy calculations and interaction energy analysis.	[91,105,120]
	PAW Method	–	Retain the high accuracy of all-electron calculations while reducing the computational resource requirements.	Electronic structural calculation.	[17,88–91,95]
	Hybrid Exchange-Correlation Functional	B3LYP	Combine DFT exchange-correlation energies with a fraction of the exact Hartree-Fock exchange energies.	Intermolecular interactions, excited states, and in energy gap calculations.	[17,94,103–105,113]
Basis Sets	Plane-Wave Basis Sets	CASTEP	Representation of the electronic wave function using the plane wave function as a basis group.	Periodic crystal structure, energy band structure, etc.	[17,88,90,92,93,102,105,115,116]
	DNP	–	Using two different numerical functions to represent each atomic orbital.	Structure optimization, reaction mechanism studies, etc.	[112–114]
	def2-TZVP	–	The introduction of polarization functions allows for a better description of bond angles.	Molecular structure optimization, reaction mechanism studies, etc.	[103,123]
	OTFG/Ultrasoft Pseudopotential	–	Suitable for systems containing heavy elements or transition metals.	Substructure, energy band structure, and mechanical properties.	[105,116]
Variants	CDFT	–	Impose constraints on electron density or charge distribution in DFT calculations.	Electron transfer, local charge distribution, etc.	[124,125]
	DFT + U	–	Introduce the Hubbard U correction term in traditional DFT.	Strongly correlated materials.	[93,121]
	DFPT	–	Linear response of a system to small perturbations via direct computation.	Lattice dynamics, dielectric and elastic properties.	[106,126]

tools to optimize computational precision and performance in various contexts.

Several DFT variants, including CDFT (Constrained Density Functional Theory), Density Functional Theory plus Hubbard U (DFT + U), and DFPT (Density Functional Perturbation Theory), have also been employed in lithium adsorption studies. CDFT is particularly advantageous for applying specific constraints on electron density or charge distribution, enabling the exploration of complex electronic environments and charge transfer processes within lithium adsorption systems. DFT + U addresses strong electron correlations, making it well-suited for systems containing transition metals or materials with localized d or f electrons, which are prevalent in lithium-ion batteries. Meanwhile, DFPT is used to analyze the system's response to perturbations, such as phonon interactions or external fields, offering critical insights into the dynamic properties and stability of lithium-adsorbed materials. These DFT variants enhance the versatility of standard DFT, providing improved accuracy and specialized tools for investigating the complex mechanisms underlying lithium adsorption.

3.3. Applications in lithium adsorption

DFT simulations play a crucial role in the field of lithium adsorption by providing detailed insights into the electronic structure and interactions between Li^+ and adsorbent materials. Through DFT

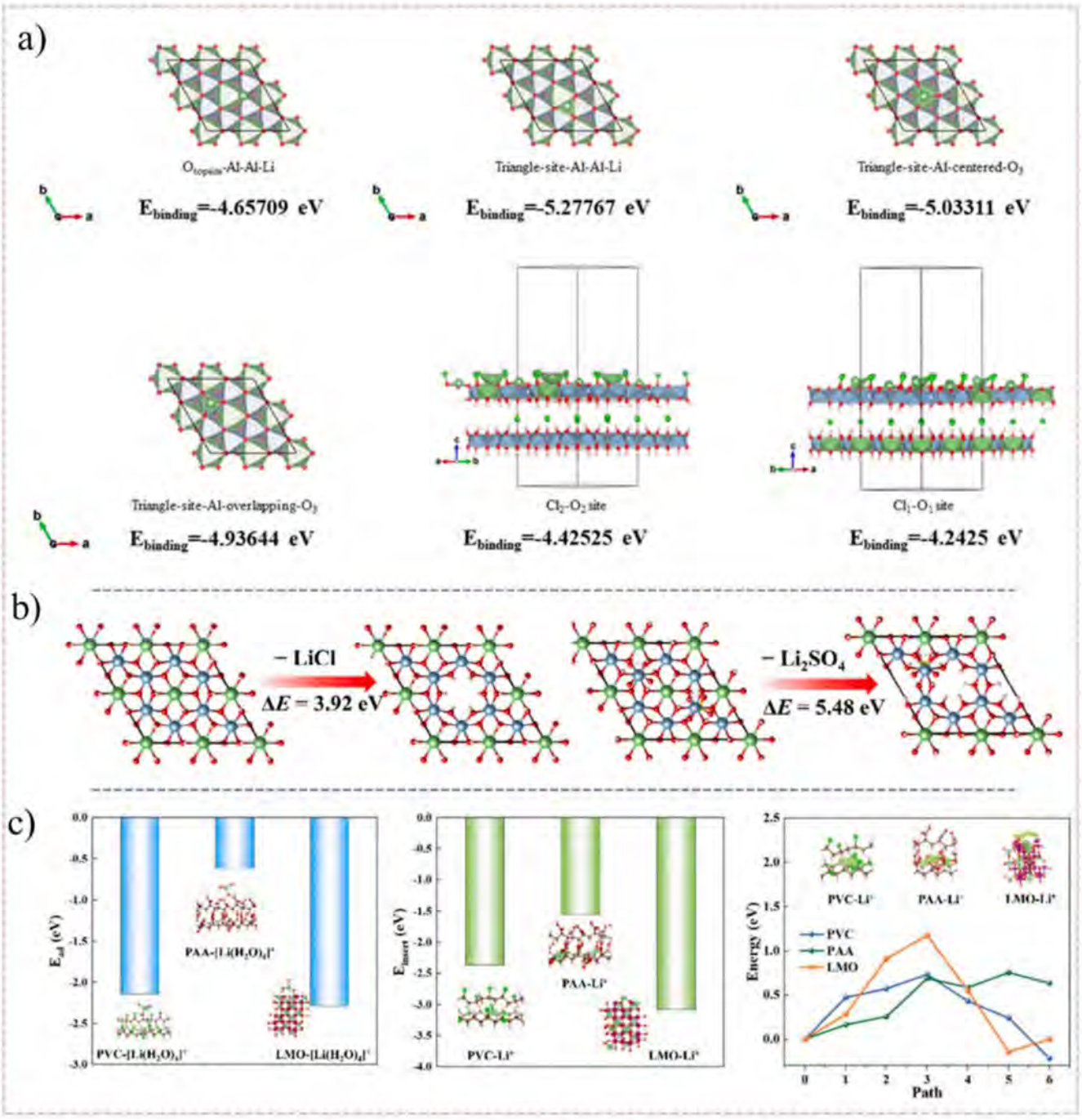

Fig. 9. (a) Calculation of adsorption energies at different sites [127]; (b) Optimized structure of the systems and deintercalation of Cl^- and SO_4^{2-} from Li/Al-LDHs [128]; (c) The adsorption energy of $[Li(H_2O)_4^+]$ on PVC, PAA, and LMO surfaces, the energy of the Li^+ insertion reaction on PVC, PAA, and LMO, and the diffusion energy barrier of Li^+ within PVC, PAA, and LMO [91].

calculations, researchers can identify optimal adsorption sites, predict binding energies, and understand the fundamental mechanisms of lithium adsorption at the atomic level. This theoretical approach significantly contributes to the design and optimization of advanced materials, enhancing their efficiency and performance in lithium capture and storage applications. This section will systematically explore the advantages of DFT simulations in lithium adsorption research, highlighting their effectiveness in uncovering microscopic mechanisms, predicting material properties, analyzing thermodynamic behaviors, and characterizing interfaces.

3.3.1. Revealing microscopic mechanisms

3.3.1.1. Adsorption site identification. DFT simulations can accurately identify adsorption sites for Li^+ on material surfaces, providing a comprehensive analysis of electronic distributions and offering precise calculations of adsorption energies. This detailed information is crucial for understanding how Li^+ interacts with different materials, enabling the design and optimization of more efficient adsorbents for lithium capture. For example, in the experiments on the adsorption of Li^+ on novel high-performance electrospun PAN/Kaolin nanofibers, Ding et al. calculated the adsorption energies of Li^+ on PAN/Kaolin, as well as the structural energy differences for the Al, O, Li, Cl, and H compounds using GGA-PBE functions [127]. As depicted in Fig. 9(a), adsorption energies were identified at six sites within the layered PAN/Kaolin structure, with higher values observed for the Al—O and Al—Al structures. These findings contribute to a deeper understanding of the mechanism behind Li^+ intercalation in this material. Besides, in the study on why aluminum-based lithium adsorbents are ineffective in extracting Li^+ from sulfate-type brines, Chen et al. performed DFT calculations using VASP and PAW methods [128]. The results, as shown in Fig. 9(b), revealed that the energy required to desorb Li^+-SO_4^{2-} ion pairs from an aluminum-based adsorbent is 1.56 eV higher than that needed to desorb Li^+-Cl^-. These findings provide valuable insights for understanding the mechanism and improving the practical application of this adsorbent in sulfate-type Salt Lake brines. In addition, Zhao et al. explored a highly selective granulation adsorbent for gas field brines and calculated the adsorption energy (E_{ad}) and energy difference (E_{dif}) of Li^+ on the PVC/PAA binder matrix and the LMO adsorbent [91]. As shown in Fig. 9(c), the E_{ad} of PAA, acting as a co-binder with $[Li(H_2O)_4^+]$ and Li^+, is smaller than that of pure PVC (where E_{ad} follows the order LMO > PVC > PAA). This indicates that introducing PAA reduces lithium adsorption on the binder, allowing more Li^+ to adsorb onto the LMO surface and access the lithium adsorption sites within the LMO. All these studies utilized DFT to identify Li^+ adsorption sites and calculate adsorption energies, demonstrating the crucial role of DFT simulations in advancing our understanding of lithium adsorption mechanisms.

3.3.1.2. Interface reaction analysis. DFT simulations are instrumental in studying the reaction mechanisms of Li^+ ions at the electrode/electrolyte interface, providing insights into reaction pathways and energy barriers during electrochemical adsorption. Liu et al. were the first to prepare polyimide-based carbon microspheres (PCMs) organized by ultra-long nanowires through a solvent polarity-induced interfacial self-assembly strategy, subsequently applying them in electrochemical experiments [129]. As illustrated in Fig. 10(a), DFT simulations revealed the competition among Li^+ ions binding with different O atoms, with the binding energies ranked as follows: (C=O) at 2.83 eV < (COOH) at 3.09 eV < (C-OH) at 3.55 eV. This suggests that the interaction between Li and C=O is the most energetically favorable, further indicating that specific adsorption sites and closed channels in PCMs play a key role in the selective permeation behavior of Li^+ ions. Furthermore, Xiong et al. utilized first-principles techniques to investigate the properties of $LiFePO_4$ cathode materials prior to synthesis [130]. To elucidate the influence of chemical bonds, they calculated the electron density difference (EDD) and bond order. Fig. 10(b) offers a clear understanding of

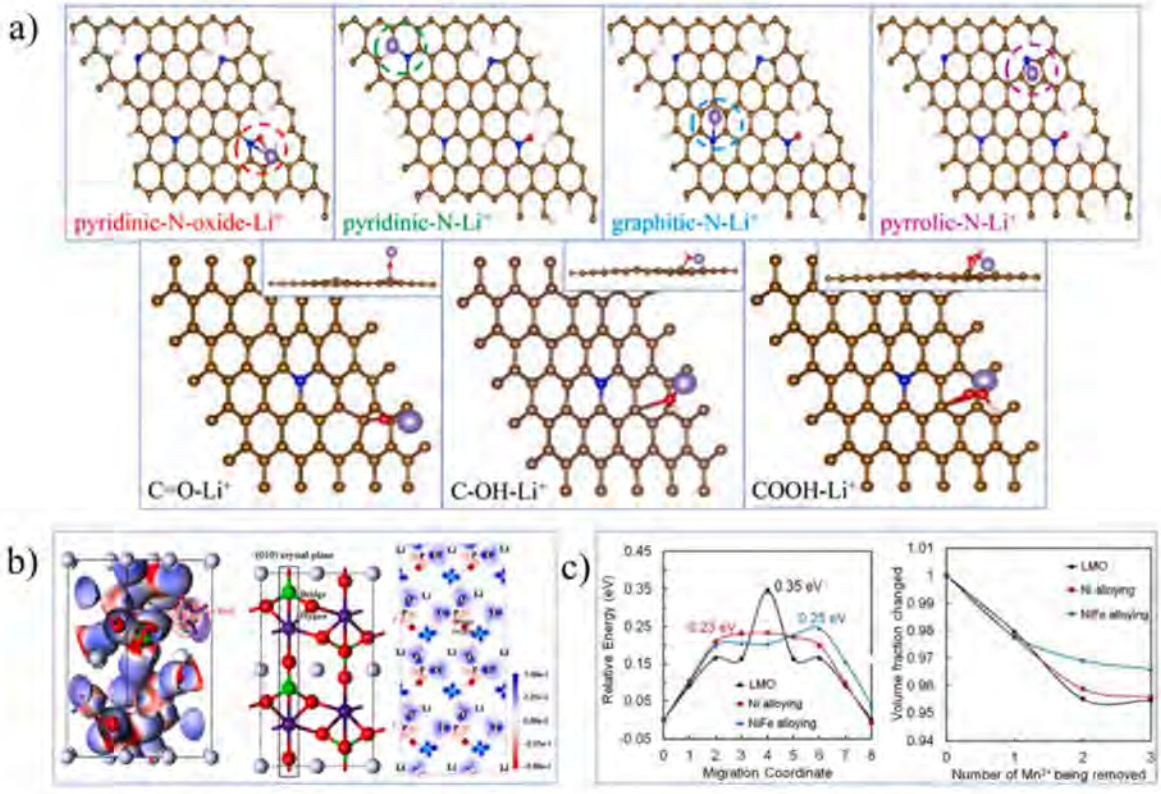

Fig. 10. (a) The binding energies of different N and O atoms to Li^+ [129]; (b) EDD diagram of $LiFePO_4$, including 3D view, 2D view of (010) crystal plane [130]; (c) Li^+ intercalation relative energy and volume fraction change of Mn^{3+} dissolution under different structural materials [93].

the relationship between structure and properties during the dynamic process, providing valuable theoretical support for subsequent experimental synthesis. Besides, Luo et al. conducted interfacial alloying modifications to enhance the electrochemical extraction of lithium [93]. As shown in Fig. 10(c), the energy barriers for Li^+ diffusion in Ni-alloyed LMO and NiFe-alloyed LMO are 0.23 eV and 0.25 eV, respectively, which are lower than that of pure LMO (0.35 eV). This indicates that the formation of the $LiNiCoMn_2O_4$ structure at the interface effectively reduces the energy barrier for Li^+ intercalation. These calculations helped researchers understand the fact that the alloying structure significantly reduces the energy barrier for Li^+ insertion and mitigates the Jahn-Teller effect, further demonstrating the inner mechanism of the interface reaction.

3.3.1.3. Analysis of interacted atomic orbitals. DFT simulations are also a powerful tool for analyzing charge transfer, charge density differences, and density of states. In their study of electrochemical lithium adsorption by k-MnO_2/graphene composites, Zhang et al. used DFT calculations alongside electrochemical adsorption experiments to investigate the electronic conductivity of the composites [121]. The electron density difference plot in Fig. 11(a) illustrates that electrons are transferred from Mn atoms to O atoms, forming stable covalent bonds, while lithium remains in a pure ionic state, which is advantageous for electrochemical adsorption. In contrast, Na and Mg undergo electron transfer with the material, leading to a higher diffusion energy barrier. This analysis reveals the underlying electron transfer and bonding mechanisms within the material, providing insights into the behavior of different ions in k-MnO_2/graphene composites, particularly regarding their electronic states and diffusion properties. Coterillo et al. conducted DFT simulations to study the selective extraction of lithium from desalination concentrates, focusing on the electron densities of interactions between Li and β-diketone, organophosphate esters, and their combinations [109]. As depicted in Fig. 11(c), the electron density is concentrated around the atomic nuclei, connecting atoms within the molecule, while it zeroes out in the bonding region, supporting the hypothesis of electrostatic (ionic) interactions. Additionally, the electron density isosurfaces of the Li^+-TOPO and Li $(H_2O)_4^+$ systems show a clear separation of the cations from the electron cloud of the adsorbed material. These calculations provide valuable insights into the connection mode and bonding mechanisms between atoms within the molecule, offering essential theoretical guidance for optimizing intermolecular interactions. In addition, during the research on polyacrylic acid (PAA)-modified layered double hydroxides (LDHs), Pan et al. employed DFT simulations to analyze the changes in the density of electronic states per unit energy level before and after modification [29]. As shown in Fig. 11 (b), the density of electronic states at the Fermi energy level for the 2.5 % PAA@LDH material significantly increased compared to the unmodified material. This increase in electronic state density directly correlates with enhanced electrical conductivity in the 2.5 % PAA@LDH material. The improved electron density is linked to better electrical conductivity, which, in turn, enhances the interaction between Li^+ and the region of increased electron density and increases the affinity of the material for Li^+.

3.3.1.4. Research of electrical conductivity. DFT simulations provide valuable insights into the electron migration mechanism and its relationship with conductivity by accurately calculating a material's electronic structure and density of states. These simulations are also instrumental in predicting the electrical conductivity of new materials and analyzing the effects of temperature, pressure, and other environmental factors. This enables researchers to gain a deeper understanding of the conductive properties of various materials. For instance, Zhang

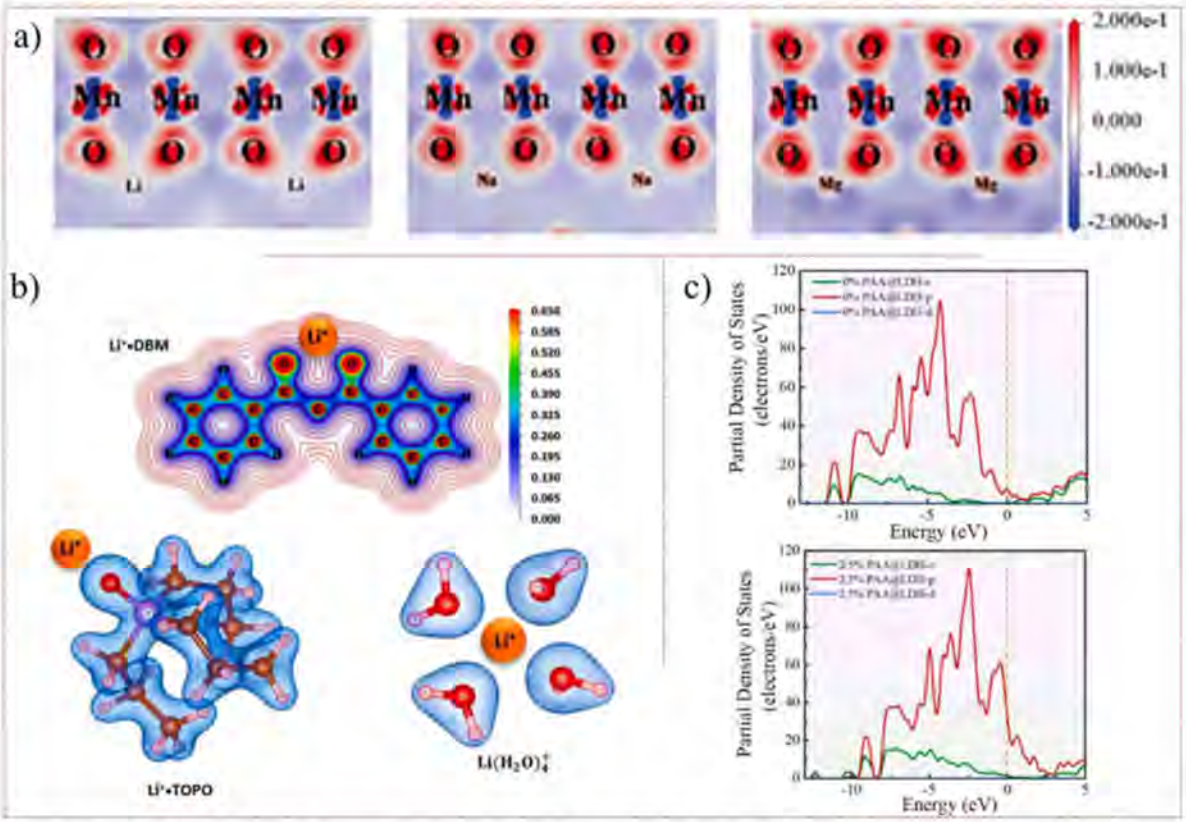

Fig. 11. (a) Electron density difference maps along the (101) crystal plane of $LiMn_2O_4$, $NaMn_2O_4$, and $MgMn_2O_4$ [121]; (b) Graphical representations of the normalized electronic density of lithium complexes with an β-diketone and an organophosphate, as well as its hydration-shell [109]; (c) Partial density of states for 0%PAA@LDH and 2.5%PAA@LDH [29].

et al. utilized DFT simulations to study the energy band structure and density of states (DOS) in a biochar-enhanced three-dimensional conductive network thick electrode, designed for efficient extraction from high Mg/Li ratio Salt Lake brines [90]. As shown in Fig. 12(a), the properties of LFP and its composite (LFP/WB) were calculated and compared, revealing that the initial band gap of LFP is 3.545 eV, while the conduction bands of the composite intersect with the band gap, indicating enhanced electronic conductivity. Additionally, there is a significant increase in the electrons at the Fermi level in LFP/WB, further enhancing conductivity. This increased conductivity facilitates faster electron movement within the composites, promoting more efficient charge transfer in electrochemical reactions and reducing both ohmic and charge transfer impedance. Furthermore, as depicted in Fig. 12(b), Surthi et al. utilized DFT analysis to gain deeper insights into the charge-discharge mechanism and lithium-ion diffusion in lithium titanate (LTO) anodes doped with Al, Ca, and Cu [131]. The study involved a comprehensive examination of the charge density and distribution (CDD) isosurface along various crystallographic directions, as well as an analysis of the lithium-ion diffusion pathways within the doped LTO structure. The CDD analysis revealed that doping with Al, Ca, and Cu significantly enhances electron conduction during the charging process. This enhancement is particularly crucial as it directly contributes to the improved electrochemical performance of the batteries, including increased discharge capacity, higher cycling rates, and

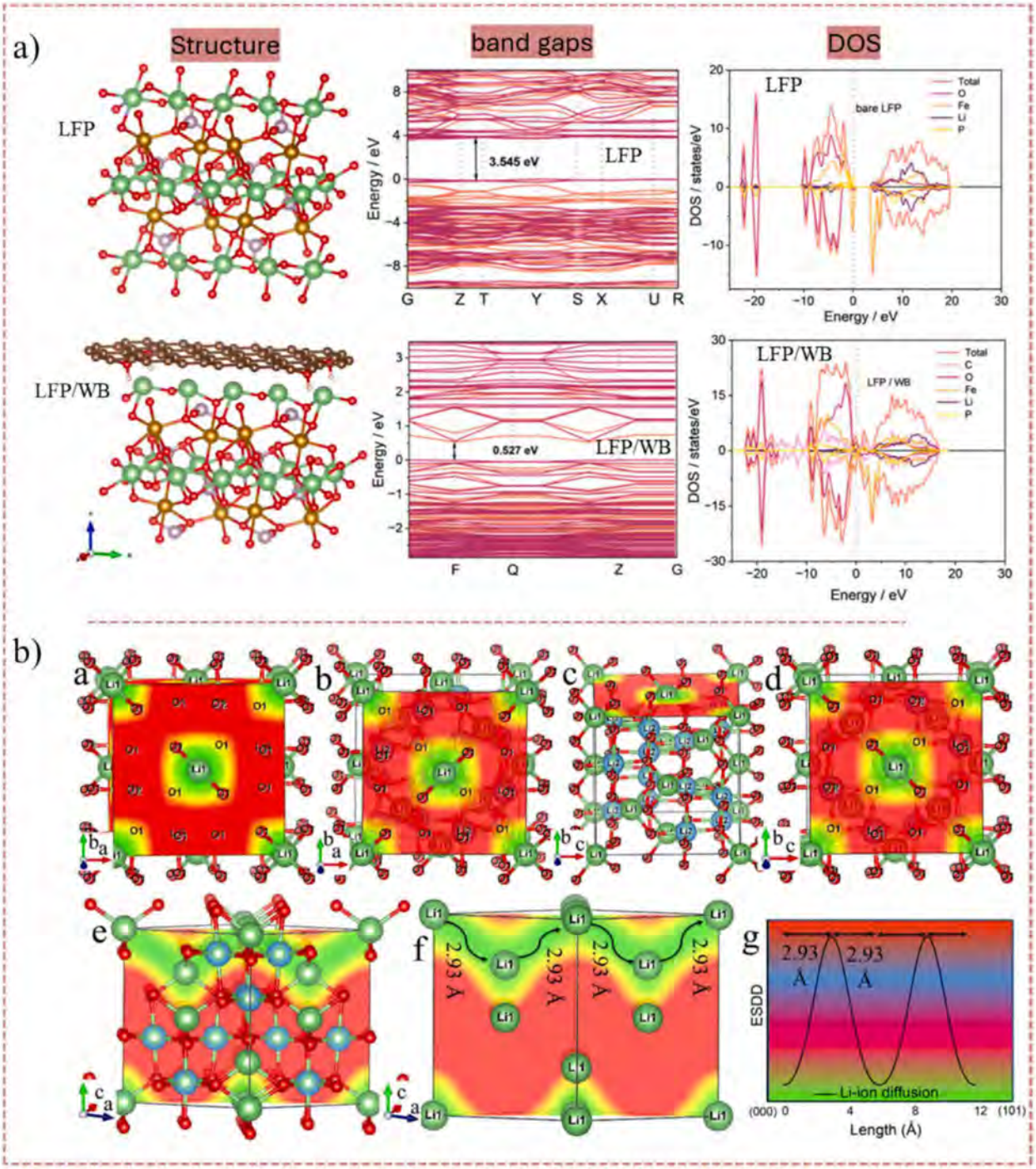

Fig. 12. (a) Structure, band gaps, and DOS of LFP and LFP/WB [90]; (b) The CDD of LTO: a-d 3D volumetric isosurface view together with the a and b-axes; e-g Li-ion diffusion isosurface, line profile of Li-ion diffusion along the ac-plane [131].

enhanced gravimetric energy and power density. The dopants facilitate more efficient charge transfer and reduce resistive losses, thereby boosting the overall efficiency and performance of the lithium-ion batteries. These results are in strong agreement with the electronic properties calculated, further validating the effectiveness of the dopants in optimizing the anode's performance.

3.3.2. *Predicting material properties*

Doping technology is extensively utilized in the modification of lithium adsorbents and electrochemical adsorption materials by introducing specific elements or compounds. This technique can significantly enhance material performance, including improvements in adsorption capacity, electrical conductivity, and chemical stability. These enhancements ultimately boost the efficiency and longevity of materials used in lithium extraction and electrochemical applications. DFT simulations play a crucial role in analyzing and predicting the performance of upgraded materials, offering essential theoretical support for material design and optimization. Through precise calculations of electronic structures, energy states, and reaction pathways, DFT simulations not only predict how materials will perform under various conditions but also guide experimental efforts, leading to enhanced overall performance and broader application potential.

Qian et al. sought to enhance the lithium adsorption capacity of $Li_{1.5}Mn_{1.6}O_4$ (LMO) through trace doping with fluorine (F) and sulfur (S) [132]. As illustrated in Fig. 13(a), the authors began by using DFT simulations combined with first-principles calculations to fundamentally understand the mechanism of F and S incorporation into the LMO surface. They discovered that O atoms located at the 32e sites in the bulk and on the (100) surface were replaced by F or S atoms. Furthermore, they compared the ability of F and S to substitute O, revealing that F atoms are more likely to replace O at the 32e sites in the bulk (5.89 eV) than on the surface (27.06 eV). Additionally, they calculated the DOS for both undoped LMO and the (100) surface structure of anion-doped LMO at the 32e sites. The results clearly showed that the valence band is primarily composed of Mn(d) and O(p) states, indicating a strong interaction between O and Mn in the MnO_6 octahedron. Interestingly, the band gap of LMO remained largely unchanged, suggesting that the electronic conductivity was not significantly improved by the anion doping. Finally, the charge densities of undoped and anion-doped LMO were calculated. The analysis revealed that anion-doped LMO exhibited a significant increase in charge density near the doped sites, leading to a higher lithium adsorption capacity compared to undoped LMO at a given doping concentration. This finding highlights the material's enhanced performance in lithium adsorption due to anion doping under

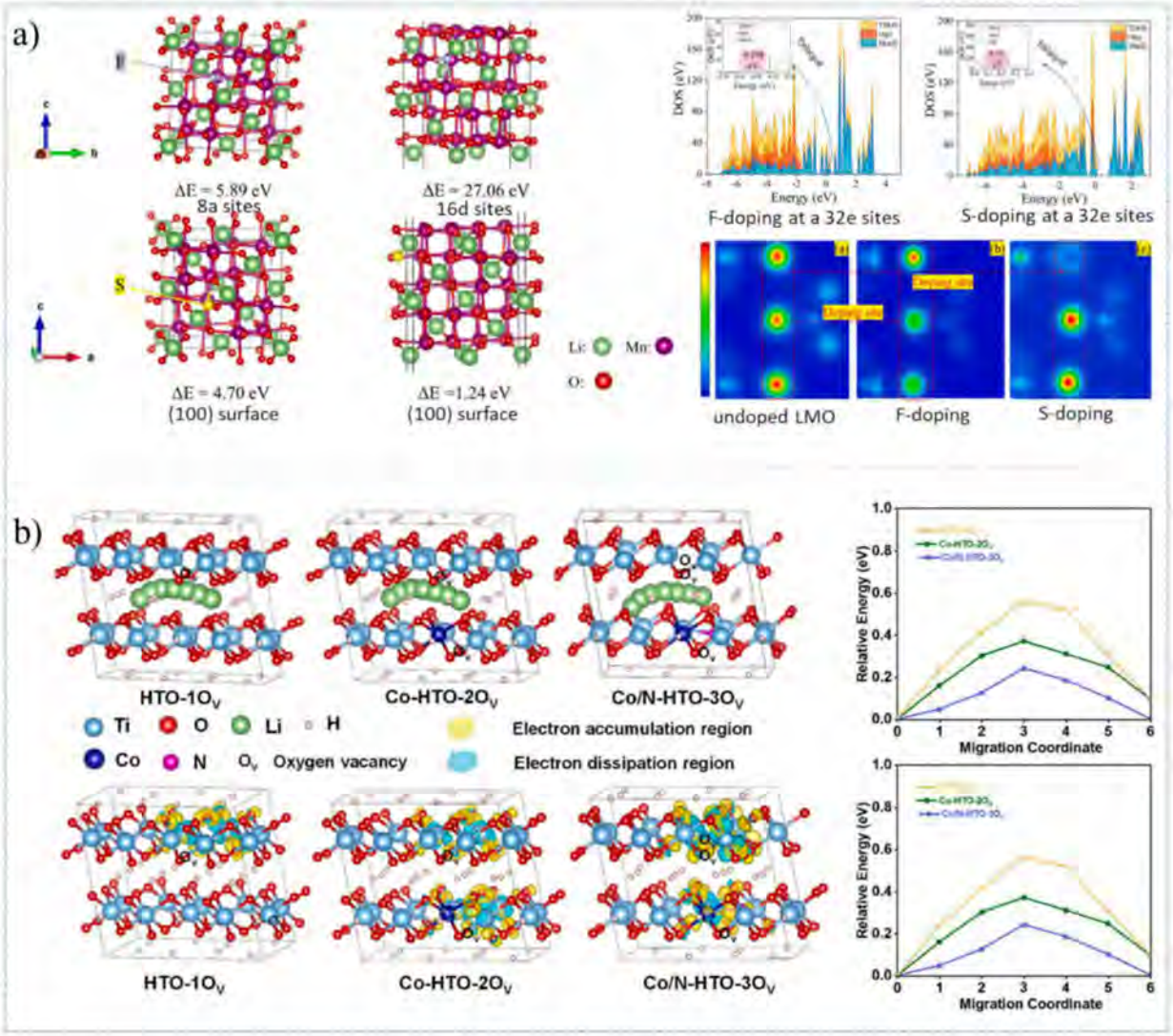

Fig. 13. (a) Optimized structures with substitution of O by F or S anions, DOS and PDOS for the (100) surface of LMO, and the charge density maps [132]; (b) Diffusion schematic of Li^+, calculation results of differential charge density, diffusion migration energy barriers of Li^+, and comparison of migration energy barriers [133].

the assistance of DFT simulations.

What's more, cobalt (*Co*) and nitrogen (N) doped titanium-based adsorbents (H_2TiO_3, HTO) were also investigated by Zhang et.al [133]. The diffusion processes of Li^+ in various doped material models are illustrated in Fig. 13(b), demonstrating that the increased electron density near oxygen vacancies generates a higher potential within the system. This electron accumulation and depletion creates an internal electric field that drives Li^+ migration. Among the models studied, the Co/N-HTO-3O_V model exhibited the lowest Li^+ migration barrier, followed by the Co-doped model with a moderately higher diffusion barrier, while the HTO-1O_V model presented the highest diffusion barrier. Furthermore, calculations of oxygen vacancy formation energy reveal that the introduction of *Co* and N facilitates the creation of oxygen vacancies. In summary, DFT theoretical calculations indicate that heteroatom doping with Co and N alters the crystal structure of the material, promotes the formation of oxygen vacancies, accelerates the solid-phase diffusion of Li^+, and thereby enhances the adsorption performance of HTO-LIS.

3.3.3. *Analyzing phase transition and thermodynamic stability study*

DFT simulations are integral to advancing our understanding of thermodynamic properties in the field of lithium adsorption, with particular emphasis on phase transitions and thermodynamic stability. By providing detailed insights into the energy distribution, phase transition behaviors, and stability of materials across various states, DFT simulations offer a comprehensive theoretical framework that underpins the performance mechanisms of lithium adsorption materials. These simulations not only help to elucidate how materials behave under different conditions but also guide the design and optimization of new materials with enhanced properties.

In their recent work, Wu et al. conducted a systematic investigation into the lithiation-induced phase transition behavior of two-dimensional fluorine-containing MXenes using first-principles density-functional calculations [134]. The crystal structures of the relaxed XY-$M_2CF_2Li_2$ configurations, as shown in Fig. 14, can be categorized into five distinct types based on the coordination number of the F atoms. Specifically:

- In the FH and HF configurations, F atoms are 6-coordinated within octahedral gaps.
- In the TF and TH configurations, F atoms are 6-coordinated at the center of hexagonal prisms.
- In the FF and HH configurations, F atoms are 4-coordinated within tetrahedral gaps.
- In the FT and HT configurations, F atoms and Li atoms form a graphene-like honeycomb structure where F atoms are 4-coordinated.

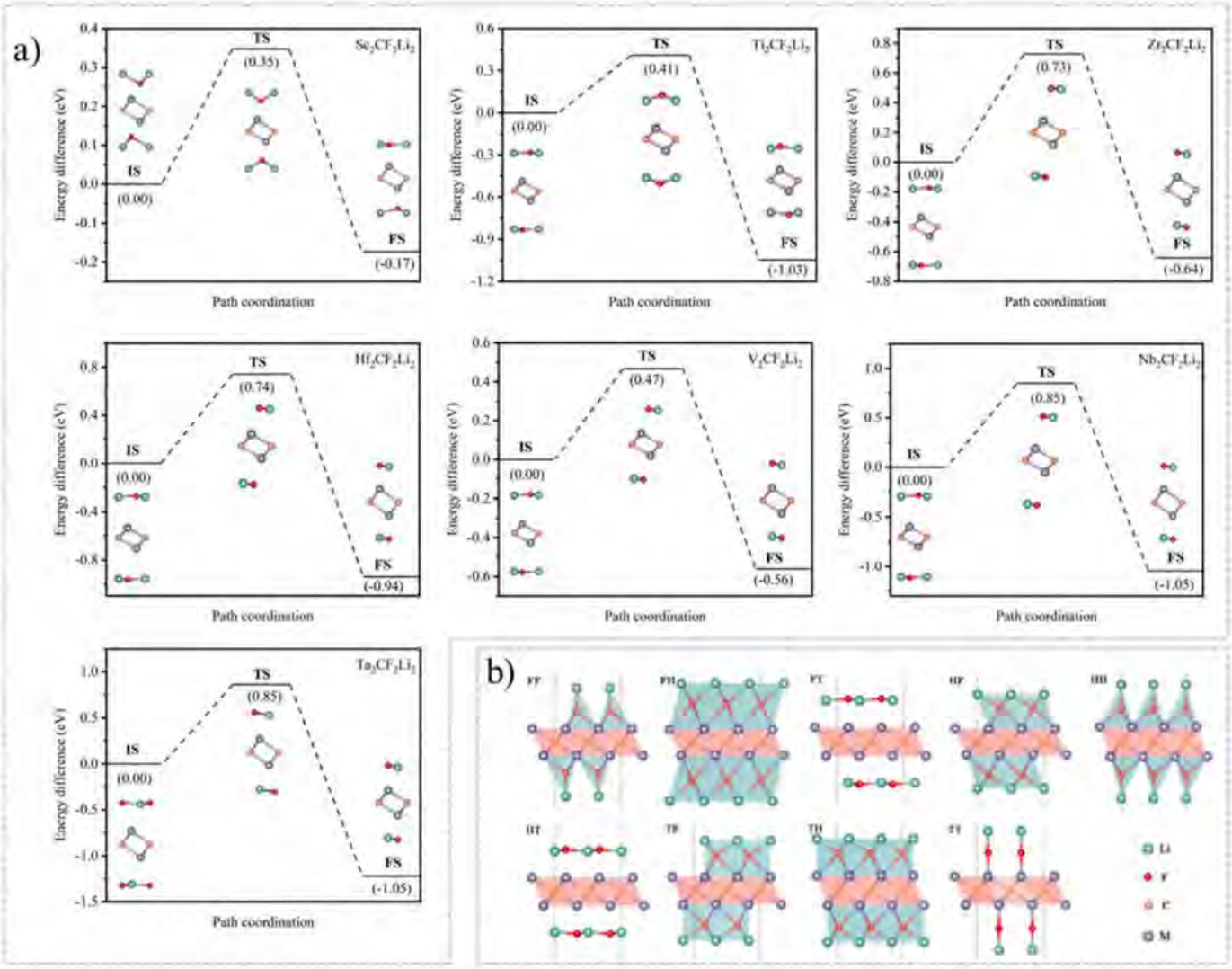

Fig. 14. (a) Energy profiles of $M_2CF_2Li_2$ and the corresponding barriers of structural transition of $M_2CF_2Li_2$; (b) The crystal structures of the relaxed XY-$M_2CF_2Li_2$ configurations [134].

- In the TT configuration, F atoms are 2-coordinated between Li and M atoms.

Based on the above configurations, the energy barriers associated with these structural transitions were also calculated using the CI-NEB method within VASP. The energy curves and corresponding energy barriers for the seven $M_2CF_2Li_2$ species were analyzed, revealing that these barriers increase progressively as the position of the M element shifts within the periodic table. Sc_2CF_2 and $Ta_2CF_2Li_2$ exhibit the lowest and highest energy barriers, respectively. Notably, all energy barriers are below 1 eV, suggesting that phase transitions can occur under ambient conditions. In conclusion, during lithium adsorption, the fluorine atoms in the nine MXenes studied migrate from the FCC site (or the HCP site in the case of Ta_2CF_2) to the TOP site.

Erraji et al. employed the FP-LAPW method, implemented within the WIEN2k code and based on DFT, to investigate the thermodynamic stability of the $LiTi_2O_4$ cathode material for Li-ion batteries [135]. Their research focused on determining various thermodynamic properties, including volume (V) and bulk modulus (B), under different temperature and pressure conditions. The study revealed that V increases with rising temperature at constant pressure and decreases with increasing pressure at constant temperature. In contrast, the bulk modulus B showed an inverse relationship, decreasing with increasing temperature at constant pressure and increasing with rising pressure at constant temperature. In conclusion, this study reveals the variation rules of V and B of the materials under different operating conditions, which is an important guidance for optimizing the design of battery materials and enhancing their stability and efficiency. By gaining a deeper understanding of these thermodynamic properties, the study provides a key reference for the development of more efficient and stable cathode materials for lithium-ion batteries.

3.3.4. *Studying interface reaction kinetics*

DFT simulations are instrumental in lithium electrochemical adsorption studies, offering atomic-level insights into the interfacial reaction kinetics of electrode materials. By accurately predicting reaction pathways, energy barriers, and charge transfer mechanisms at interfaces, these simulations guide the design and optimization of

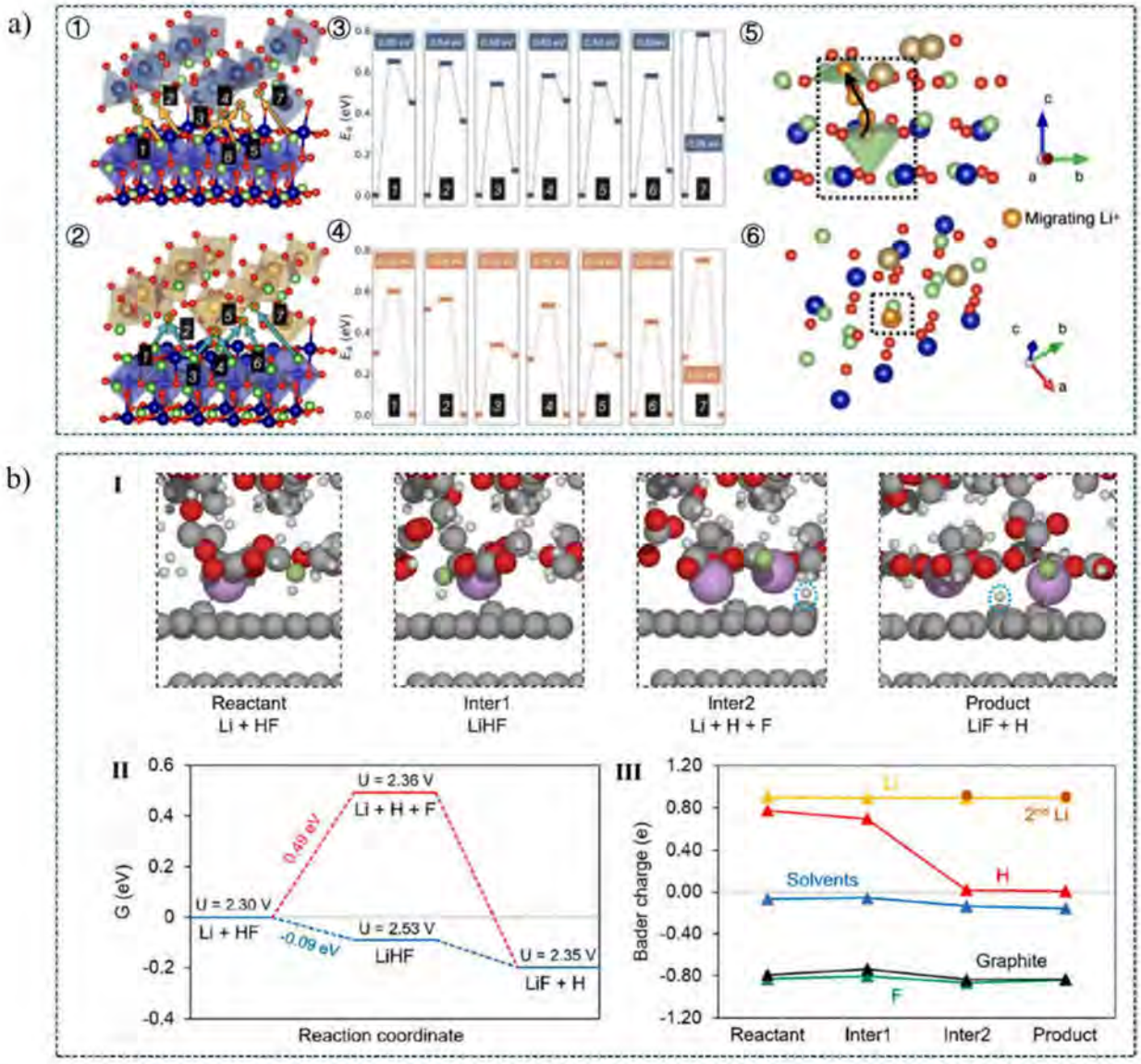

Fig. 15. (a) ① and ② Interface migration pathways for LiNbO *interf* and LiTaO *interf*, respectively. Arrows in ① and ② show each interface migration pathway corresponding to parts ③ and ④, respectively. The energy at initial, transitional, and final states are shown as horizontal bars ③ and ④. Numbers in dark blue and yellow show Ea for each migration pathway. Numbers shaded black indicate the pathway index as shown in ① and ② [137]; (b) (I) Key structures of LiF formation on graphite with defects, (II) Gibbs free energy diagram of LiF formation, and (III) charge analysis results of key structures during LiF formation [138].

electrode materials, ultimately improving the performance and efficiency of lithium-ion batteries.

Halldin Stenlid et al. investigated the coupled ion-electron charge transfer kinetics at the battery electrode-electrolyte interface using first-principles methods, combining CDFT with the Boltzmann-weighted CIET formula [136]. They developed a Boltzmann-averaged first-principles workflow that leverages constant potential and constrained density flooding theory to estimate atomic-scale factors influencing these kinetics. The study also compared experimental trends for $LixCoO_2$ ($0.5 \leq x \leq 1.0$) electrodes in various organic electrolytes containing $LiPF_6$ and $LiClO_4$ salts, identifying the Li^+ transport energy and Li^+ adsorption energy as key factors enhancing the kinetics of $LiClO_4$ based electrolytes over those with $LiPF_6$.

In addition, Zhou and colleagues also conducted an in-depth investigation into the diffusion characteristics of Li^+ ions at and near the LiNb(*Ta*)O interfaces, as well as within the bulk material, using DFT combined with the NEB method [137]. As illustrated in the Fig. 15, seven distinct diffusion pathways, labeled from "1" to "7," were explored for both the LiNbO and LiTaO interfaces, with a particular focus on single-vacancy migration mechanisms. To mitigate the potential impact of voids on the activation energy (Ea), the maximum migration distance was constrained to 5 Å. Among all the pathways examined, the "7" pathway exhibited the highest Ea across both interfaces. This elevated activation energy is attributed to the relatively longer migration distances observed for LiNbO and LiTaO, measuring 4.26 Å and 4.93 Å, respectively. This comprehensive analysis provides valuable insights into the ion diffusion behavior at these interfaces, which is critical for optimizing the performance of related materials in practical applications.

What's more, Qin et al. employed the DFT-D3 method to investigate LiF formation at graphite-electrolyte interfaces [138]. Their study, as depicted in the figure, highlights that during the formation of LiF at the interfacial region, Li—C bonds are present at defect sites throughout the reaction process. The free energy diagram indicates that LiF formation via the LiHF complex is more energetically favorable compared to an alternative intermediate pathway. To maintain a constant potential, an additional Li atom is introduced into the intermediate and product states, with the extra electron being transferred to the graphite surface and subsequently balanced by adsorbed hydrogen. The adsorbed hydrogen acquires slightly less charge (0.67 e) than that observed on perfect graphite (0.79 e), a difference attributed to the distinct localized electronic states within the LiHF complexes. This analysis provides a detailed understanding of the atomic-level mechanisms governing LiF formation at these critical interfaces. To summarize, DFT simulations lay a solid theoretical foundation for the in-depth understanding and effective regulation of electrode interfacial reactions.

In conclusion, DFT simulations have significantly contributed to the study of lithium adsorption by accurately characterizing atomic and electronic structures, thereby revealing energy changes, reaction pathways, and interfacial dynamics during the adsorption process. This deepens scientists' understanding of lithium adsorption behavior and electrode material reaction mechanisms, offering essential theoretical guidance for designing more efficient battery materials and enhancing overall battery performance.

4. Numerical simulations

Despite the lithium adsorption in micro-level could be explored using the above methods, multiphase fluid flows governed by capillary, wettability, adhesion, and so on due to macro-scale factors. In order to better reveal the mechanism of lithium adsorption in the solution environment, numerical simulations are powerful methods for investigating migration trajectories and flux transfer while reducing the influence of multiple factors [139]. Currently, prevalent numerical simulations for studying lithium adsorption under multi-physics field include COMSOL Multiphysics, CFD, and Network Simulations.

4.1. Principle and methodology

4.1.1. COMSOL Multiphysics

In the reaction process, the geometrical model is first discretized into elements through the mesh generator in COMSOL Multiphysics [140]. Subsequently, the governing partial differential equations (PDEs) are transformed into weak form equations, which are then discretized using the finite element method (FEM). After that, the PDEs problem is transferred into an ordinary differential equations (ODEs) problem. With time-discretization using backward difference (BDF), the implicit ODEs are transferred into algebraic equation which could be solved by Newton interaction method [141]. All the calculation processes could be conducted in the solver of COMSOL Multiphysics where offers a platform for solving PDEs.

Lithium adsorption simulation coupling problem in the solutions usually happens in electrochemical adsorption process where diffusion, convection, and electromigration are considered as parameters in the model [142]. In the electrochemical adsorption model, a three-stage current distribution module is adopted to figure out the migration of electrolyte species. The physical model and form could be adjusted and designed by the real reaction devices, for instance, in Zhang et al.'s work [143], they analyzed the steady-state condition of the fluid flow, time-dependent convection and diffusion in a dissolved substance in the flow channel. The fluid taken as Newtonian incompressible fluids are modeled by the continuity and Navier-Stokes equations:

$$\nabla \bullet u = 0 \tag{1}$$

$$\rho(\nabla \bullet \mu)u = -\nabla p + \mu\nabla^2 u \tag{2}$$

where u, ρ, p, and μ is the flow rate ($m{\cdot}s^{-1}$), density ($kg{\cdot}m^{-3}$), pressure (Pa), and kinematic viscosity (Pa·s) of the fluid, respectively; ∇^2 means the Laplace operator.

Accordingly, the Reynolds number (R_e) for microfluidic characteristics about channel geometry is calculated in the following equations:

$$R_e = \frac{\rho u L}{\mu} \tag{3}$$

$$L = \frac{4A}{P_{wet}} \tag{4}$$

where L is hydraulic diameter of the channel; A represents the channel cross-sectional area; P_{wet} means the wetted perimeter.

Lithium ions transfer is controlled by the diffusion-convection equation:

$$(u \bullet \nabla)c - D\nabla^2 c = R \tag{5}$$

where c is the concentration; D means the diffusion efficient; R represents the reaction rate.

4.1.2. Computational fluid dynamics

CFD is performed on the lithium adsorption process to optimize the conditional parameters, thus to simplify plenty of experimental works and quickly find the way for the optimal process flow [144]. The advantage of this method is allowing visual description of how the entire process happens by equipment during lithium adsorption. Based on the real sample, a continuous multi-column adsorption model could be established involves the columns, as well as pumps, values, headers, etc. connected to the columns [145]. In the system, every individual model has its own inlet, outlet ports including flow variables to communicate with each other. Based on some assumptions like uniform size of sorbent particles, constant temperature, uniform distribution of lithium concentration, and advection flow, the adsorption process is given. Diffusion and boundary conditions inside adsorbents particles could be given as the equations:

$$\frac{\partial q}{\partial t}=\frac{D_s}{r^2}\bullet\frac{\partial}{\partial r}\bullet\left(r^2\frac{\partial q}{\partial r}\right) \tag{6}$$

$$t=0, 0\le r\le r_p, q=0, C_p=0 \tag{7}$$

$$t=0, t>0, \frac{\partial C_p}{\partial r}=0 \tag{8}$$

$$r=r_p, t>0, \rho_p D_s\frac{\partial C_p}{\partial r}=k_f\left(C-C_{p,\ r=r_p}\right) \tag{9}$$

where C_p is lithium concentration in adsorbent, mg/L; k_f means the diffusion constant, cm/s; r represents radial coordinate within adsorbent particles, cm; D_s is the diffusion constant on the surface of particles, cm^2/s; r_p means the radius of adsorbent particles, cm.

Currently, major mass transfer kinetic processes are widely described by three models, external diffusion, internal diffusion, and adsorption to active sites from the perspective of mass transfer steps. The three models usually combine kinetics and isotherm and consider rate-limiting step [146]. Here, external mass transfer as a dimensionless diffusion process is driven by concentration difference of liquid film, and being defined by the following equation:

$$\frac{dq(t)}{dt}=K_{ext}(C(t)-C_e(t)) \tag{10}$$

where K_{ext} is the parameter, $L\cdot g^{-1}\cdot min^{-1}$; C_e is the equilibrium concentration of target ions, g/L.

The Freundlich model is used to depict the adsorption behavior of target ions on electrode, being described as the equation below:

$$\frac{dq(t)}{dt}=K_{ext}\left(C_0-\frac{mq(t)}{V}-\frac{q(t)^n}{K_F^n}\right) \tag{11}$$

Internal diffusion of target ions on the pore of electrode is described by internal mass transfer model expressed by linear driving force model as following equation:

$$\frac{dq(t)}{dt}=-K_{int}(q(t)-q_e(t)) \tag{12}$$

where K_{int} is the coefficient, min^{-1}; q_e is the equilibrium concentration of target ions.

4.1.3. Network simulations

The network simulations basically model the physicochemical process through a graphical representation similar to a circuit diagram [147]. It has the advantages of obtaining dynamic behaviors without dealing with the governing differential equations, being well matched in understanding the electrical properties of the system, permitting the impose of electric potential electric current at any conditions [148]; dealing with steady-state and transient responses, and allowing any transport process through spatial regions [149]. There are some assumptions during the simulation process, such as ionic transport in one-dimensional and perpendicular to the material/solution interface [150]. After that, the migration behaviors are determined by the laws of mass conversion or continuity equations:

$$\frac{\partial J_1'(x,t)}{\partial x}=-\frac{\partial c_1'(x,t)}{\partial t} \tag{13}$$

$$\frac{\partial J_2'(x,t)}{\partial x}=-\frac{\partial c_2'(x,t)}{\partial t}-\frac{\partial c_{2S}'(x,t)}{\partial t} \tag{14}$$

The Nernst-Planck flux for dilute solutions:

$$J_i'(x,t)=-D_{ip}'\left[\frac{\partial c_i'(x,t)}{\partial x}+z_i c_i'(x,t)\frac{E}{RT}\frac{\partial \varnothing'(x,t)}{\partial t}\right], i=1,2 \tag{15}$$

And the Poisson equation:

$$\frac{\partial D'(x,t)}{\partial x}=F\left[z_1 c_1'(x,t)+z_2 c_2'(x,t)+z_2 c_{2S}'(x,t)\right]=\rho'(x,t) \tag{16}$$

where,

$$D'(x,t)=-\varepsilon'\frac{\partial \varnothing'(x,t)}{\partial x} \tag{17}$$

$J_i'(x,t)$, D_{ip}', $c_1'(x,t)$, and z_i respectively display the ionic flux, diffusion coefficient, molar concentration, and charge number ($z_1=1$ *and* $z_2=2$) of ion *i*.

In the network model, the process is divided into many small physical regions of interest till spatial variations of each compartment are negligible, N volume elements or compartments of width $\delta_k(k=1,\ldots,N)$ with a unit cross-sectional area. The Langmuir kinetics could be calculated as [151]:

$$f_a'=k_{ad}'\left[C_M' k' c_2'(x,t)-\left(1+k' c_2'(x,t)c_{2S}'(x,t)\right)\right] \tag{18}$$

where k_{ad}' is rate constant for adsorption/desorption process, and C_M', k' respectively represent maximum concentration and adsorption constant.

4.2. Applications in lithium adsorption

According to the above-mentioned model and calculations, the results obtained for lithium adsorption process could be classified as mass transfer and flux transfer [150]. Commonly, under the concentration-driven force, ions would migrate from high concentration region to low concentration region because of the concentration gradients, which realized the separation and adsorption [152]. Velocity field distribution map and turbulence kinetic energy map are applied to reveal the solution velocity field and ion concentration field.

4.2.1. Flux migration trajectories

Analyzing the hydrodynamic behaviors of lithium adsorption in electrochemical or column devices is very important for optimizing operative parameters. Most nanofiltration processes work best under laminar flow conditions because these conditions help manage flow through the membrane and make it easier to assess concentration polarization. For examples, Wiley et al. developed a comprehensive CFD model to study polarization, which demanded finely detailed wall meshes and advanced numerical methods to accurately capture the effects of fouling and high polarization [153].

The simulation for lithium adsorption in nanofiltration was conducted under both laminar and turbulent flow conditions. Khan et al. have introduced an innovative CFD technology called continuous spatial distribution diafiltration [154]. This innovation significantly improved solvent efficiency and output, and it has also set up a versatile framework for small-scale automated flow experiments. In addition, as given in Fig. 16(a), an automated spacer design method using the response surface method along with a multi-objective genetic algorithm was proposed, which resulted in an 8 % reduction in flux attenuation and a 57.9 % increase in the minimum wall shear force, significantly reducing membrane fouling [155].

To address the decreased permeability issues and optimize the lithium adsorption, researchers have focused on designing hydrodynamic conditions on membrane surfaces. This includes adjustments to geometry, the use of pulses and gas sparging, as well as incorporating spacers and Dean vortices [156]. Liu et al. predicted the mass transfer of magnesium and lithium ions in Salt Lake solutions through porous media, combining the extended Nernst-Planck equation, Donnan effect, ion diffusion, electromigration, and convection within membranes pores [157]. They found that when solution closed to narrow space, as shown in Fig. 16(c), the kinetic energy of liquid molecules would be very high. In the presence of shear flow, the closer the membrane surface, the slower the lithium solution flow velocity. Karode et al. conducted a

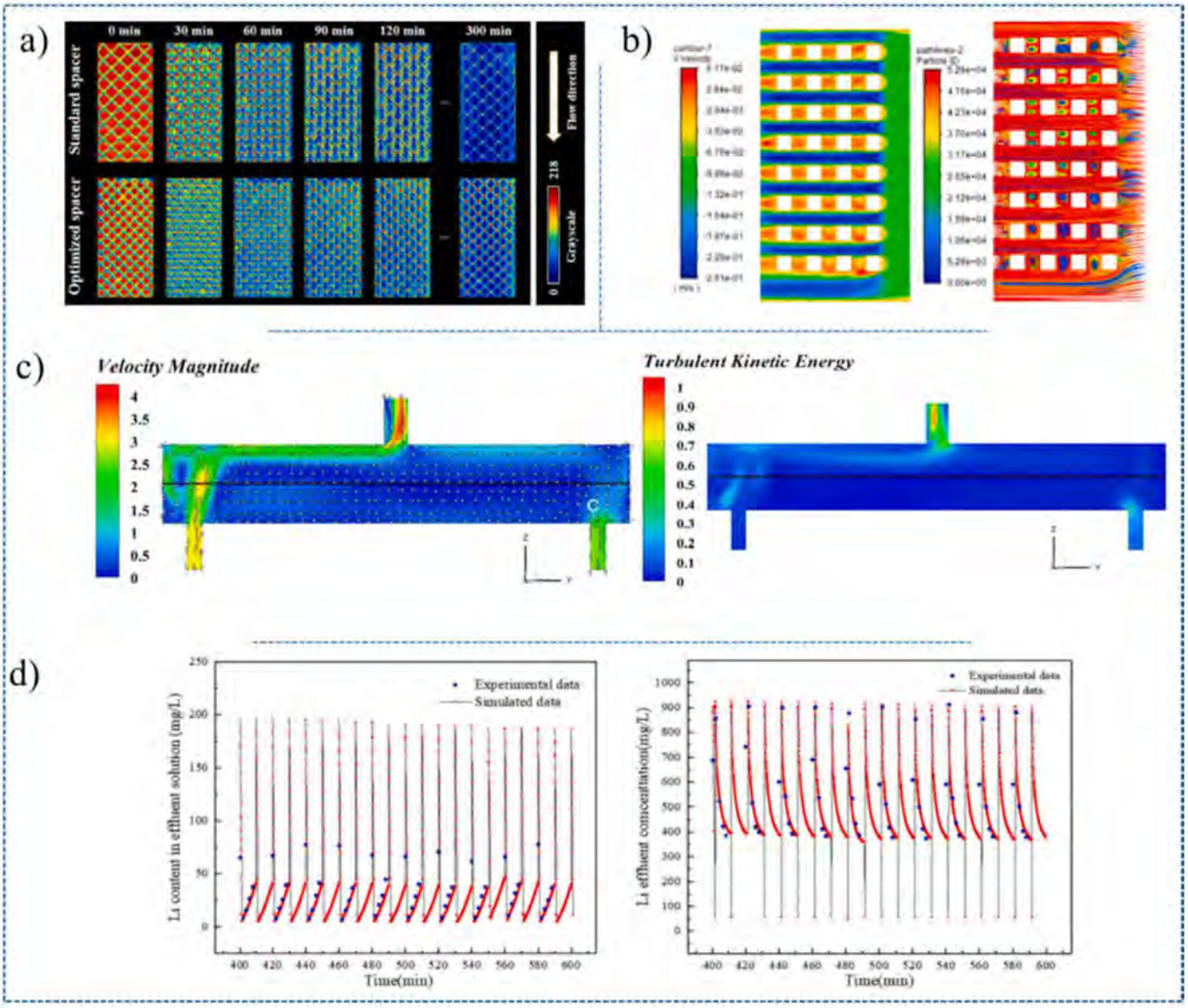

Fig. 16. (a) The grayscale of humic acid fouling on the membrane surface was analyzed using both optimized and standard spacer-filler membranes [155]; (b) CFD simulation of 3D printing packing [159]; (c) Absolute value of membrane velocity and turbulent kinetic energy [157]; (d) Experimental and simulation data of lithium concentration at the exit of one zone [145].

study on flow pressure drops in membranes with porous walls and found that the experimental pressure drops closely matched the predicted values, with an error range of 2–10 %. This confirmed the accuracy of the CFD numerical model [158].

In capacitive deionization for lithium electrochemical adsorption, Jeon et al. investigated the stagnant zones by CFD, and flow channel minimized the dead zones or flow overlapping to enhance separation efficiency [160]. As the flow rate increased, the stagnant regions at the two corners were reduced in the effect of flow rate on stagnant zone in square capacity deionization [161]. The stagnant regions of the low flow rate were bigger than those of the high flow rate. The increasing flow rate could effectively reduce the stagnant zone [162].

Numerical simulation could be not only applied in lithium adsorption for simple devices, but also complex models. Li et al. simulated and optimized operating parameters and efficiency of multi-column with lithium recovery set as performance evaluation [145]. It was observed in Fig. 16(d) that the trend of lithium concentration in the effluent from the adsorption zone was nearly identical after each switch, which closely matched the experimental curves. This indicates that the model used in the numerical simulation effectively represents the multi-column continuous lithium adsorption process. In a multi-column continuous lithium adsorption process, the lithium recovery rate in the adsorption zone should be maximized to minimize lithium loss during the adsorption process. Yu et al. constructed 3D printed packing in the fixed bed, and studied the adsorption process by CFD [159]. As illustrated in Fig. 16(b), the staggered structure in the 3D printed packing was beneficial for solution diffusion and led to an increased adsorption rate. Besides, the various packings exhibit good selectivity for different ions, including K^+, Na^+, and Mg^{2+}. The feasibility of continuous separation of Mg^{2+} and Li^+ ions by free flow ion concentration polarization has been demonstrated through numerical simulations [163]. This method enabled enrichment perpendicular to the flow direction of the analyte and can reduce the maximum Mg^{2+}/Li^+ ratio by approximately 85 % under the electroneutrality limit.

4.2.2. Flux transfer near electrodes

Electrodes play a crucial role in the lithium electrochemical adsorption process. Joo et al. studied the concentration lithium ions over

time and space with λ-MnO_2/$LiMn_2O_4$ electrodes, and the spatiotemporal concentration distribution were divided into three regions [164]. As shown in Fig. 17. In the electrochemical system, the spacer mesh would affect the velocity profile, resulting in various concentration distribution. The dominant convective mass transfer perpendicular to the electrode is controlled by the pressure-driven flow toward the flow direction. Introducing a spacer mesh reducing the concentration polarization, so a flat concentration distribution was obtained compared to the concentration distribution in a plane separator channel.

In previous studies, lithium concentration decreased as one approaches the electrode surface was investigated [165]. This decrease occurred because lithium was inserted into the electrode material during the discharge process. While diffusion and convection work to replenish the lithium on the electrode surface, a balance was eventually reached between the replenishment and depletion rates, resulting in the formation of a depletion zone. In electrochemical lithium adsorption systems, improved lithium extraction performances can be achieved by using flow-through reactors that maintain higher lithium ions concentrations at the electrode surface. The gas flush operation significantly reduced the consumption of ultrapure water during electrochemical lithium adsorption. Multiple gas flush operations use less water and are more time efficient.

Zhang et al. studied the mass transfer of lithium adsorption in micro-level channel spiral-microstructure electrochemical reaction using COMSOL Multiphysics [143]. In unstructured channel in Fig. 18 (a-b), only laminar flow was observed, while there appeared spiral vortex streamlines in the spiral structures [166]. The flow rate significantly increased near the electrodes in the spiral-microstructure. Without spiral structure, the velocity near the electrode would approach zero due to the non-slip boundary condition [167]. However, the spiral design in the flow channel allows for vortex formation even at low flow rates, with their intensity increasing as the flow rate rises. Besides, the various flow behaviors affecting lithium distribution were investigated, and they found that the forced vortex in the spiral-microstructure electrochemical reaction induced strong convection, which significantly enhanced mass transfer. This reduced the lithium concentration gradients near the anode and promoted lithium desorption from the anode surface into the bulk recovery solution. The forced vortex in the spiral-microstructure electrochemical reaction efficiently transferred lithium from the bulk brine to the cathode area, replenished the locally consumed lithium, and ultimately accelerated the lithium adsorption process.

Inside the electrodes with porous structure, Li et al. investigated the static flow field [168]. As shown in Fig. 18(c-d), the velocity magnitude along with the electrode direction shown in the contour about gas

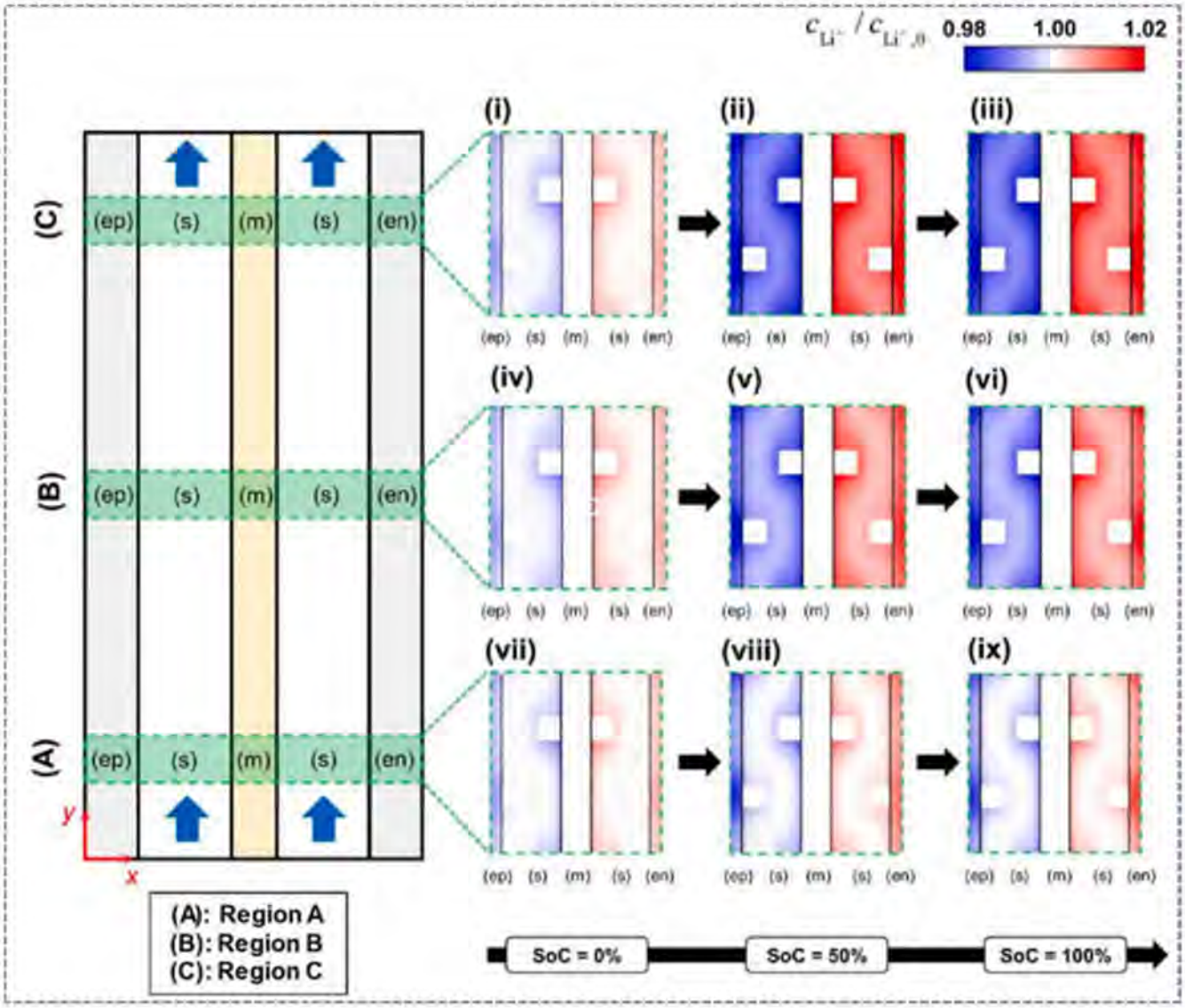

Fig. 17. Concentration distribution of lithium ions in three reprehensive regions (A: initial; B: central; C: terminal) at three distinct time points [164].

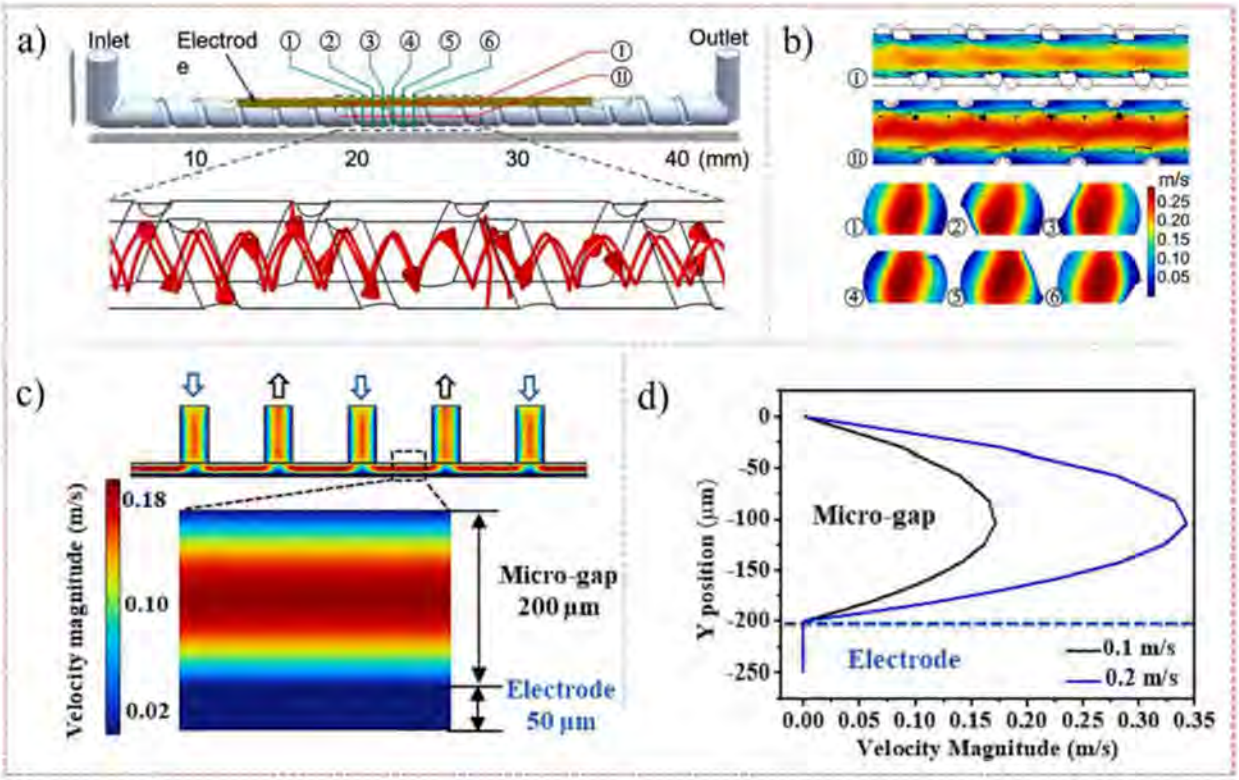

Fig. 18. (a) 3D model of the anode channel in spiral-microstructure electrochemical reaction, including a zoomed-in view of the 3D streamlines of the spiral vortex [143]; (b) Cross-sectional 2D flow-speed profiles at the positions marked in (a) [143]; (c) Contour plot of gas velocity magnitude in the micro-gap and electrode with an inlet velocity of 0.1 m/s [168]; (d) Gas velocity magnitude in the micro-gap and electrode along the y-axis for inlet velocities of 0.1 m/s and 0.2 m/s [168].

velocity in micro-gap and the electrode, and the velocity magnitude remained almost zero which is much lower than in the micro pores. The main reason for decreased fluid velocity was the loss of fluid momentum owing to the drag force affected by the obstacles in solid, which verified that the transfer in electrode was dominated by diffusion rather than convection. After lithium recovery, Jiang et al. confirmed the effect of reaction time and applied voltage on capacity deionization ability using spinel lithium manganese oxide materials, which was consistent with the experimental results [169].

5. Machine learning

Machine learning (ML), particularly in feature representation, has become the foundation for most modern applications and is classified into three types: supervised, unsupervised, and reinforcement leaching [61]. Supervised machine learning involves training on data with explicit categorical labels, where the goal is to map features to these categories. In contrast, unsupervised machine learning deals with data that lacks explicit categorical labels [170]. It extracts features through algorithmic models and relies on these algorithms to determine relationships within the data. Reinforcement leaching focuses on optimizing a model's performance by learning from interactions with the environment to maximize rewards or benefits. Reinforcement learning focuses on optimizing a model's performance by learning from interactions with the environment to maximize rewards or benefits [171]. With the advancement of ML algorithms, significant process has been achieved in their integration with materials science and ions adsorption. ML methods enable the rapid and accurate prediction of materials properties and structures, fostering innovation in the design and lithium adsorption of high-performances [172]. By employing appropriate ML algorithms to optimize the design and discovery of materials, new materials and structures can be systematically identified, thereby reducing resource waste and environmental pollution from unnecessary experiments [173]. This approach can provide significant social value.

ML models have been increasingly applied to evaluate material performance, including predicting material properties and assessing their application performance. For instance, nanomaterials exhibit unique effects due to their nanoscale size, such as interfacial effects, small-size effects, quantum-size effects, and macroscopic quantum tunneling effects [174]. There characteristics often differ significantly from their bulk counterparts and can vary with size, providing opportunities for targets optimization. A notable application is the work of Lee et al. [175],. who employed artificial neural networks to design the shapes of crystalline nanoporous materials in energy space. They conducted extensive molecular simulations to identify performance limits and demonstrated the high accuracy of these predictive methods. Their findings not only validated the potential of artificial neural networks in predicting material performance but also introduced innovative approaches to the study of nanomaterials.

5.1. Principle and methodology

Data are fundamental to all performance predictions. The acquisition, generation, and preprocessing of data are critical for ML models. A substantial amount data is essential for efficiently applying ML models, and the quality of the data directly impacts the models' generalization ability [176]. Currently, researchers could obtain data in the two primary ways, one is to collect data from literatures or existing databases, and the second is to generate their own datasets through high-throughput experiments or simulations. They typically use appropriate methods to design features and manage the size and distribution of the dataset to be generated. This approach is a well-established method for data preparation and ensures that the dataset is both representative and useful for modeling purposes [177]. This design has led to the development of several databases, including AFLLOW, Materials Project, MATDAT, MatWeb, MatMatch, MakeltForm, and MatNavi. These

databases offer a wide range of material information, such as mechanical properties, constituent units, and electronic characteristics, providing valuable data to support the prediction of material properties and structures [178].

For lithium insertion into bulk materials, one method involves estimating the energetics as a charge-transfer process between different energy levels, while typically neglecting other interactions, particularly complex electrostatic ones [179]. In contrast, lithium adsorption on surfaces, including 2D materials, is considered a chemisorption process, where the Li 2 s orbital hybridizes with the surface valence levels. The energy change in this process depends on the degree of filling of the antibonding orbital. This understanding aligns well with experimental observations and provides useful qualitative trends [180]. The most used models include random forest, support vector regression, artificial neural networks, gradient boosting methods, Gaussian process regression, and K-nearest neighbors.

5.1.1. Random Forest

Random Forest is a powerful ML algorithm from the ensemble learning category, renowned for its ability to address complex problems with high accuracy by combining multiple decision trees [181]. This approach not only enhances model diversity but also significantly reduces the risks of overfitting and variance, which are common issues with single decision trees. Random Forest operates by constructing numerous decision trees during training, each built on a different bootstrap sample of the dataset, where samples are drawn with replacement. Additionally, Random Forest introduces further variability and reduces correlation among trees by selecting a random subset of features for splitting at each node within a tree.

5.1.2. Support vector regression

Support Vector Regression is an adaptation of the Support Vector Machine framework designed specifically for regression tasks [182]. Unlike Support Vector Machine, which is focused on classifying data by finding an optimal separating hyperplane, Support Vector Machine aims to fit a hyperplane that approximates the underlying trend in the data. Support Vector Regression is especially effective for scenarios where understanding the underlying trend or pattern in the data is more important than classification. Its versatility with kernel functions makes it a robust tool for addressing diverse regression challenges.

5.1.3. Emotional neural network

Emotional Neural Network represents an innovative integration of artificial intelligence with human-like emotional processing, aiming to endow neural networks with the ability to understand and incorporate emotions into their decision-making processes [183]. Although this concept is not yet widely recognized in the complex interplay between cognition and emotion seen in humans. The theoretical basis for Emotional Neural Network is the belief that emotions significantly impact human learning, reasoning, and problem-solving, suggesting that artificial intelligence could similarly benefit from emotional awareness to enhance adaptability, context sensitivity, and interaction capabilities.

5.1.4. Gaussian process regression

Gaussian Process regression is a probabilistic, non-parametric technique designed for regression analysis [184]. It is adept at capturing intricate, nonlinear relationships in data and provides a measure of uncertainty for its predictions. Gaussian Process regression works by establishing a distribution over a set of potential functions and adjusting this distribution based on the observed data. This method enables both nuanced predictions and the quantification of confidence intervals, making it highly adaptable and precise.

5.1.5. K-nearest neighbors

K-nearest Neighbors is an uncomplicated, non-parametric supervised learning method suited for classification and regression tasks [185]. In K-nearest Neighbors, the prediction for a given data point is derived from the k closest points in the feature space. For classification, the result is determined by the most frequent class among these neighbors, whereas, for regression, it is calculated as the mean of the values from these nearest points. The method's straightforward approach and ease of implementation make it a popular choice for a range of predictive tasks.

5.2. Applications in lithium adsorption

Modeling brine mining using 2D materials is a complex task that encompasses various factors, including the properties of 2D materials, the composition of the brine solution, and the operating conditions of the brine mining process. ML algorithms can be trained on data from experimental studies to predict the performances of brine mining processes [186]. These models can then be used to optimize the design and operation of brine mining processes and to troubleshoot issues that may arise. The recent integration of ML and artificial intelligence principles in materials science has enabled advanced structural predictions for extracting resources from brine using 2D materials [187].

A high-throughput screening framework that integrates first-principles calculations, graph convolutional networks, and physics-based learning has been employed to evaluate lithium adsorption on 2D metallic materials. As given in Fig. 19(a), they proposed that the adsorption energy is partitioned into three components: ionization potential, the work function of 2D metals, and coupling energy [188]. Dou et al. demonstrated that combining these ML descriptions effectively predicted the adsorption energy of alkali metals on 2D transition metal dichalcogenide substrates using a straightforward regression approach [189]. By extending their density functional theory calculations to additional alkali atoms and transition metal dichalcogenide substrates, they observed that the predicted energies exhibited a clear linear correlation with the DFT-calculated energies, highlighting the efficiency of the proposed descriptions (see Fig. 19(c-d)). Chaney et al. employed a supervised ML model using cluster wise linear regression to predict the adsorption energies of lithium ions on 2D transition metal dichalcogenide, with the aim of gaining further physical insights and preparing for investigations into both regular and Janus transition metal dichalcogenide materials [190]. A representation with a few key descriptors was developed in Fig. 19(b), considering the intrinsic dipole moment, the electronic structure of both regular and Janus 2D layers, the adsorption site, and the concentration dependence of adatom doping.

Abba et al. introduced the Emotional Neural Network and Random Forest models using various dependency selection approaches to predict the adsorption energy for lithium adsorption on 15-crown-5 and 18-crown-6 embedded 2D materials [191]. The Emotional Neural Network and Random Forest models are advanced ML well-suited for modeling adsorption energies due to their capacity to handle nonlinearity and complex patterns. Abdulazeez et al. utilized ML to enhance the predictive accuracy for 2D materials [192]. Based on their predictions, ion transmission channels were created by integrating 9-crown-3 and 12-crown-4 molecules with graphene, hexagonal boron nitride, and silicene nanosheets.

Beyond the 2D materials, ML has also been applied to lithium extraction in other contexts. Kireeva et al. employed ML to optimize the structure of phosphoryl-containing ligands for selective lithium extraction from brine [193]. They proposed di-podandic ligands based on phosphoryl-containing organic ligands for lithium and sodium cations in a 4:1 THF: $CHCl_3$ solution, demonstrating high selectivity for lithium adsorption.

6. Others

In addition to the commonly used simulation methods mentioned above, some new approaches have also been introduced and applied to lithium adsorption. Compared with density functional theory, Quantum Monte Carlo (QMC) could more accurately handle electronic correlation

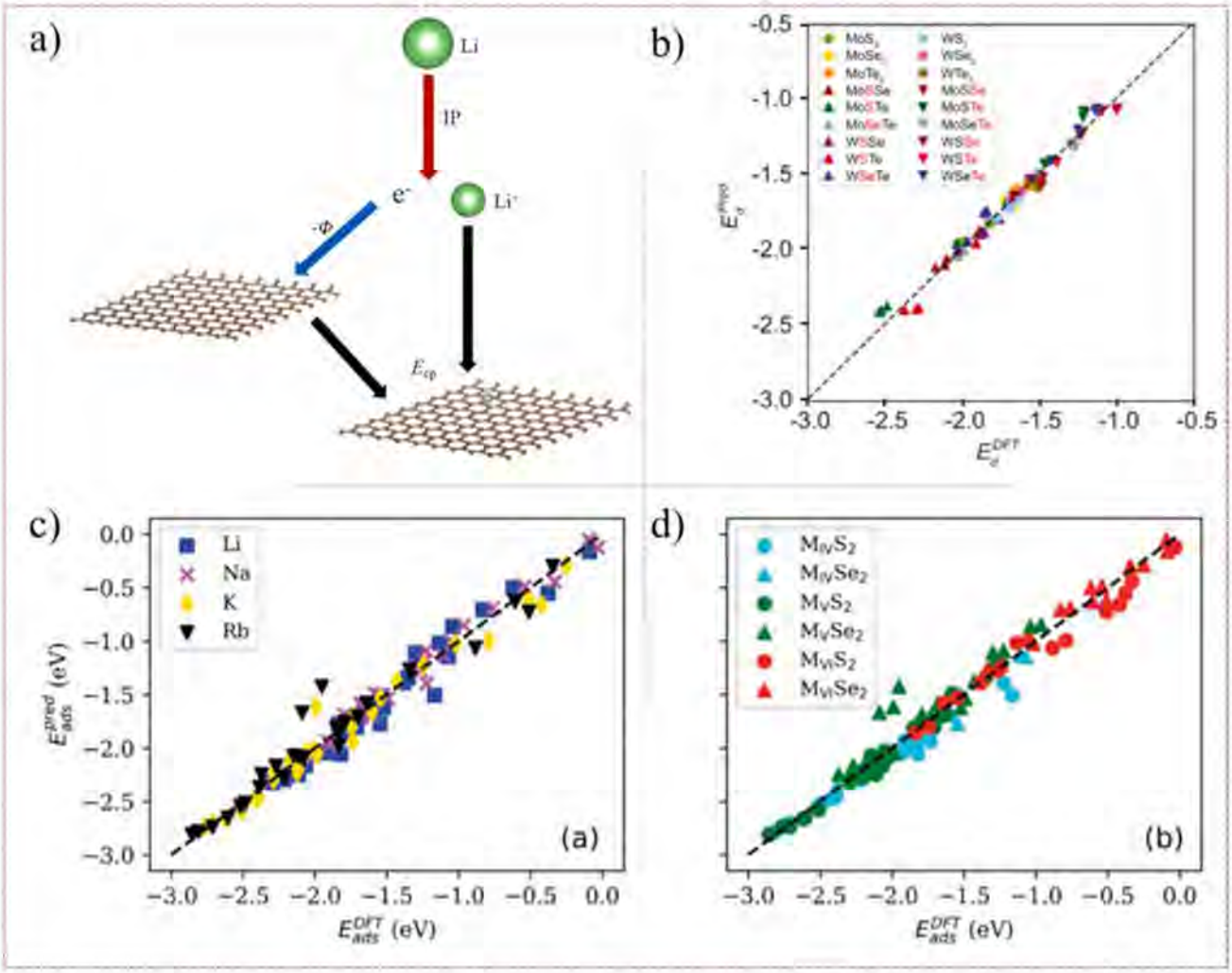

Fig. 19. (a) Illustration of the proposed three-step lithium adsorption mechanism, Φ represents the work function, IP denotes the ionization potential of lithium, and Ecp refers to the coupling energy between lithium and the negatively charged substrate [188]; (b) Predictions of adsorption energies from CLR (Epredd) versus original DFT values (EDFTd) [190]; (c-d) the same data using different labels [189].

energy [194]. Additionally, QMC is an effective tool for addressing electron-related energies in molecules and solids. It excels at handling electro-related effects, providing valuable insights into the structural and electronic properties of clusters. Gao et al. demonstrated that the QMC method was successfully applied to small $Li_nCl^{(0,1+)}$ (n = 1–7) cluster, suggesting that QMC maybe a viable tool for investigating the electronic properties of lithium adsorption materials [195]. Ganesh et al. conducted highly accurate diffusion QMC studies on the adsorption and diffusion of atomic lithium in AA-stacked graphite and compared the results with van der Waals-inclusive density functional theory calculations [196]. The lattice constants for pure AA-stacked graphite predicted by QMC were found to be in excellent agreement with experimental values. Prayogo et al. employed diffusion Monte Carlo to assess the adsorption characteristics of a hydrogen molecule on a (5,5) armchair silicon-carbide nanotube [197]. Within the density functional theory framework, various exchange-correlation functionals, including those recently developed for treating dispersion or van der Waals interactions, were benchmarked. It was found that van der Waals-corrected density functional theory methods are in good agreement with diffusion Monte Carlo results, whereas local functionals significantly overestimate or underestimate binding.

7. Summary and prospects

In this discussion, we explored several computational strategies applied to lithium adsorption research, focusing on their principles, methodologies, and specific applications. Among these, Statistical Mechanics Simulations are particularly noteworthy for their ability to predict dynamic behavior and thermodynamic properties, typically addressing the large-scale equilibrium behavior of systems. MD and MC simulations, two widely used statistical mechanics approaches in lithium adsorption research, have distinct strengths and limitations. MD simulations are particularly advantageous for (1) providing detailed insights into atomic-level interactions between Li^+ ions and adsorbent materials, such as bonding, interaction energies, and interfacial structures; (2) visualizing diffusion behaviors and migration pathways, which are critical for understanding dynamic processes; and (3) analyzing surface phenomena during lithium adsorption, including surface reconstruction, defect evolution, and the role of active sites. These capabilities make MD simulations a valuable tool for investigating the fundamental mechanisms of lithium adsorption. MC simulations, on the other hand, offer advantages in terms of (1) lower computational resource requirements, making them well-suited for simulating larger systems; (2) effectively analyzing the distribution, occupancy probabilities, and macroscopic properties of lithium ions on the adsorbent surface; (3) studying long-term processes, such as adsorption-desorption

equilibria and changes in surface coverage; and (4) efficiently calculating adsorption energy distributions, providing insights into the contributions of different adsorption sites to the overall performance of the material.

Despite these advantages, both methods have limitations when used independently. MD simulations face challenges such as (1) requiring substantial computational resources and being limited by their time scale, which restricts their ability to capture long-term phenomena like extended Li^+ ion diffusion, slow surface interactions, and structural changes; (2) failing to reach true adsorption equilibrium due to short simulation durations, reducing the accuracy of adsorption kinetics and equilibrium property predictions; and (3) heavily relying on the accuracy of force field models, where inaccuracies in parameterization can lead to significant deviations from real-world behavior. MC simulations also have limitations, including (1) a focus on equilibrium properties, without capturing dynamic information, making them unsuitable for studying time-dependent processes; (2) reliance on the quality and extent of random sampling, which can limit their reliability for complex system geometries, porous materials, or dynamic surface changes; and (3) lack of detailed insights into atomic-level interactions and interfacial microstructures.

Among the limitations of MC simulations, the lack of dynamic information is particularly critical, as it significantly impacts the understanding of lithium adsorption kinetics. First, MC simulations cannot directly provide insights into the adsorption or diffusion rates of Li^+ ions, making it difficult to quantify the time dependence of the adsorption process and thereby limiting the understanding of kinetically controlled mechanisms. Second, due to the absence of a time dimension, MC simulations are unable to capture the migration paths of Li^+ ions as they move from the solution to the adsorbent surface or into the pores, restricting the exploration of detailed kinetic processes. Furthermore, MC simulations fail to observe transient phenomena that may occur during adsorption, such as changes in ion distribution during the initial phase of rapid adsorption. These short-term kinetic behaviors are essential for understanding adsorption dynamics but remain inaccessible through MC simulations. In complex systems, kinetic processes can also influence the final equilibrium distribution, such as the dynamic formation of surface-active sites or the redistribution of solute molecules. However, MC simulations, lacking time resolution, are unable to address these coupled kinetic-equilibrium effects. These limitations underscore the importance of integrating methods like MD simulations to complement the equilibrium-focused nature of MC simulations, enabling a more comprehensive understanding of lithium adsorption processes. The choice of simulation method should align with specific research objectives, considering the strengths and weaknesses of each approach. In many cases, combining MD and MC simulations can provide complementary advantages, offering a more comprehensive understanding of lithium adsorption processes by addressing both equilibrium and dynamic aspects.

DFT simulations were systematically examined as well, covering not only widely used software tools such as VASP and CASTEP but also methodologies like GGA, PEE, and DFT—D. The applications of DFT in lithium adsorption research were highlighted, particularly its role in revealing microscopic mechanisms, predicting material properties, analyzing phase transitions and thermodynamic properties, and investigating interfacial reaction dynamics. DFT simulations offer significant advantages, including the ability to quantitatively analyze lithium adsorption energies, assess diffusion barriers, and provide high-precision predictions with relatively efficient computation. However, these benefits come with certain limitations. They are computationally intensive, heavily dependent on the choice of exchange-correlation functionals and are subject to approximations that may limit accuracy. Additionally, DFT is not well-suited for simulating dynamic processes such as Li^+ diffusion. Given these strengths and limitations, it is advisable for researchers to select appropriate methods based on their specific research objectives. Often, a combination of DFT with other simulation techniques, such as MD or MC simulations, can provide a more comprehensive understanding of lithium adsorption processes.

The principles and methodologies of numerical simulations, including COMSOL Multiphysics, CFD, and network simulations, were discussed in detail, focusing on their common modeling parameters, governing equations, and specific characteristics. Their applications in studying flux migration trajectories and flux transfer near electrodes were also highlighted. COMSOL Multiphysics offers significant advantages in Multiphysics coupling and is highly flexible, making it suitable not only for Li^+ adsorption but also for comprehensive performance analysis of lithium batteries. However, its high computational resource demands and steep technical learning curve present challenges. CFD simulations excel in providing detailed analyses of Li^+ flow behavior within adsorption materials and related heat transfer processes. Despite their strengths, the complexity of the models and the extended computation times required are notable drawbacks. Network simulations, on the other hand, are effective in analyzing transport phenomena within systems using discrete models, offering insights into the microscopic transport mechanisms within lithium batteries. However, their inability to capture certain detailed phenomena in continuous media limits their accuracy. Therefore, when selecting numerical simulation methods, researchers should consider the specific research objectives and system characteristics, potentially combining these approaches to achieve the best research outcomes.

Finally, ML was categorized into three types, with methodologies such as Random Forest and Support Vector Regression systematically outlined. While its application in lithium adsorption is still relatively limited, we discussed its potential in optimizing experimental design and predicting material properties. ML offers significant advantages, such as the ability to build databases for predicting adsorption energies, diffusion coefficients, and other material properties with high efficiency. It holds great promise in discovering new adsorption and electrode materials. However, the generalization capability of ML models is often limited, and they are heavily dependent on large, high-quality datasets. Therefore, researchers must carefully manage data quality and consider integrating traditional physical and chemical methods to address the limitations in interpretability and generalization. By effectively combining ML with experimental and theoretical simulations, we can enhance the tools available for lithium adsorption research.

Future research on applying these computational strategies to lithium adsorption should focus on:

1) Develop Multiscale Modeling Approaches: Create methods that effectively capture Li^+ adsorption phenomena across different scales by integrating quantum mechanical techniques with mesoscale and macroscale simulations.

2) Increase Computational Efficiency: Enhance computational efficiency to support real-time or near-real-time simulations and predictions, which are crucial for studying dynamic processes such as Li^+ diffusion and interfacial reactions.

3) Strengthen Simulation-Experiment Collaboration: Foster closer collaboration between computational simulations and experimental validation to ensure that theoretical predictions align with actual behavior, thereby enhancing the reliability and applicability of computational research.

4) Improve Machine Learning Models: Boost the generalization capability and interpretability of machine learning models by incorporating domain-specific knowledge, refining feature engineering, and developing hybrid models that combine data-driven methods with traditional physical modeling.

Declaration of competing interest

The authors declare that they have no known competing financial interests or personal relationships that could have appeared to influence the work reported in this paper.

Data availability

The authors do not have permission to share data.

References

[1] Y. Hu, H. Su, Z. Zhu, T. Qi, Q. Pang, Environmentally benign techniques of lithium extraction from salt lakes: a review, Environ. Chem. Lett. 22 (1) (2024) 105–120, https://doi.org/10.1007/s10311-023-01669-0.

[2] C. Han, Q. Zheng, J. Jin, J. Zhang, W.-Q. Cao, K. Xiang, M. Zhang, M.-S. Cao, Multidimensional hollow SiO_2/C nanofibers modified by magnetic nanocrystals for electromagnetic energy conversion and lithium battery storage, Nano Res. 17 (8) (2024) 7301–7314, https://doi.org/10.1007/s12274-024-6746-7.

[3] D. Chandrasekharam, M.F. Şener, Y.K. Recepoğlu, T. Isık, M.M. Demir, A. Baba, Lithium: An energy transition element, its role in the future energy demand and carbon emissions mitigation strategy, Geothermics 119 (2024) 102959, https://doi.org/10.1016/j.geothermics.2024.102959.

[4] F.N. Zargar, R. Mohnot, F. Hamouda, N. Arfaoui, Risk dynamics in energy transition: evaluating downside risks and interconnectedness in fossil fuel and renewable energy markets, Res. Policy 92 (2024) 105032, https://doi.org/10.1016/j.resourpol.2024.105032.

[5] J. Farahbakhsh, F. Arshadi, Z. Mofidi, M. Mohseni-Dargah, C. Kök, M. Assefi, A. Soozanipour, M. Zargar, M. Asadnia, Y. Boroumand, et al., Direct lithium extraction: a new paradigm for lithium production and resource utilization, Desalination 575 (2024) 117249, https://doi.org/10.1016/j.desal.2023.117249.

[6] Y. Hu, H. Su, Z. Zhu, T. Qi, Q. Pang, Environmentally benign techniques of lithium extraction from salt lakes: a review, Environ. Chem. Lett. 22 (1) (2023) 105–120, https://doi.org/10.1007/s10311-023-01669-0.

[7] T. Ding, M. Zheng, S. Peng, Y. Lin, X. Zhang, M. Li, Lithium extraction from salt lakes with different hydrochemical types in the Tibet Plateau, Geosci. Front. 14 (1) (2023) 101485, https://doi.org/10.1016/j.gsf.2022.101485.

[8] S. Murodjon, X. Yu, M. Li, J. Duo, T. Deng, Lithium recovery from brines including seawater, salt lake brine, underground water and geothermal water, Thermodynamics and Energy Engineering (2020) 90371.

[9] C. Wang, M. Zheng, X. Zhang, Q. Wu, X. Liu, J. Ren, S. Chen, Geothermal-type lithium resources in Southern Xizang, China, Acta Geologica Sinica-English Edition 95 (3) (2021) 860–872.

[10] D. Bloch, Pre-salt energy genesis, brine streams replenishing oil, gas salt diapirs in "salt mirror petro-leum formations"–40 years in retrospect, and ancient Qanat Kare mineral salt leaching technology, Petro Chem Indus Intern 6 (2) (2023) 25–31.

[11] B. Disu, R. Rafati, A.S. Haddad, J.A.M. Roca, M.I.I. Clar, S.S.E. Bakhtiari, Review of recent advances in lithium extraction from subsurface brines, Geoenergy Science and Engineering 241 (2024) 213189.

[12] L. Guo, Y. Yao, J. Xu, E.H. Ang, G. Xu, J. Liao, A. Sotto, J. Shen, Strategies for lithium extraction from salt lakes by nanofiltration and selective-electrodialysis and analysis of differences between the two methods, Desalination 586 (2024) 117749.

[13] Q. Dong, H. Gang, J. Xu, Z. Li, Z. Wang, The technologies of electrochemical extraction lithium process from lithium-containing solutions, J. Exp. Theor. Anal. 2 (4) (2024) 91–102.

[14] C. Huangfu, S. Yu, B. Tong, A. Yang, J. Lyu, X. Guo, Efficient lithium extraction from aqueous solutions by MIL-100(Fe): a study on adsorption kinetics, thermodynamics and mechanism, Sep. Purif. Technol. 322 (2023) 124365, https://doi.org/10.1016/j.seppur.2023.124365.

[15] J. Zhang, Z. Cheng, X. Qin, X. Gao, R. Yun, X. Xiang, Bifunctional modification enhances lithium extraction from brine using a titanium-based ion sieve membrane electrode, ACS Appl. Mater. Interfaces 15 (24) (2023) 29586–29596, https://doi.org/10.1021/acsami.3c04682.

[16] W. Li, B. Bai, R. He, J. Song, T. He, Lithium solvent extraction by a novel multiframe flat membrane contactor module, Sep. Purif. Technol. 328 (2024) 125061, https://doi.org/10.1016/j.seppur.2023.125061.

[17] L.-P. Guo, Z.-Y. Guo, J. Wang, P.-P. Zhang, Z.-H. Huang, Z.-Y. Ji, Flexible lithium selective composite membrane for direct lithium extraction from high Na/Li ratio brine, J. Membr. Sci. 703 (2024) 122843.

[18] Q. Zhu, X. Yu, Y. Liu, Y. Wang, P. Yang, K. Liu, Electrochemical lithium extraction with continuous flow electrodes, Desalination 574 (2024) 117250, https://doi.org/10.1016/j.desal.2023.117250.

[19] J. Xu, X. Wei, J. Han, W. Qin, Synthesis and optimisation mechanism of functionalised adsorption materials for lithium-ion extraction: a review, Sep. Purif. Technol. 339 (2024) 126237.

[20] J. Zhong, S. Lin, J. Yu, Effects of excessive lithium deintercalation on Li(+) adsorption performance and structural stability of lithium/aluminum layered double hydroxides, J. Colloid Interface Sci. 572 (2020) 107–113, https://doi.org/10.1016/j.jcis.2020.03.081.

[21] X. Xu, Y. Chen, P. Wan, K. Gasem, K. Wang, T. He, H. Adidharma, M. Fan, Extraction of lithium with functionalized lithium ion-sieves, Prog. Mater. Sci. 84 (2016) 276–313, https://doi.org/10.1016/j.pmatsci.2016.09.004.

[22] J. Zhong, S. Lin, J. Yu, Li^+ adsorption performance and mechanism using lithium/aluminum layered double hydroxides in low grade brines, Desalination 505 (2021) 114983, https://doi.org/10.1016/j.desal.2021.114983.

[23] K.A. Tarasov, V.P. Isupov, L.E. Chupakhina, D. O'Hare, A time resolved, in-situ X-ray diffraction study of the de-intercalation of anions and lithium cations from $[LiAl_2(OH)_6]nX{\cdot}qH_2O$ ($X = Cl^-$, Br^-, NO_3^-, SO_4^{2-}), J. Mater. Chem. 14 (9) (2004) 1443–1447, https://doi.org/10.1039/B314473A.

[24] H. Su, Z. Li, J. Zhang, W. Liu, Z. Zhu, L. Wang, T. Qi, Combining selective extraction and easy stripping of lithium using a ternary synergistic solvent extraction system through regulation of Fe^{3+} coordination, ACS Sustain. Chem. Eng. 8 (4) (2020) 1971–1979, https://doi.org/10.1021/acssuschemeng.9b06432.

[25] J. Zhong, S. Lin, J. Yu, Li^+ adsorption performance and mechanism using lithium/aluminum layered double hydroxides in low grade brines, Desalination 505 (2021) 114983, https://doi.org/10.1016/j.desal.2021.114983.

[26] V. Schenker, P. Bayer, C. Oberschelp, S. Pfister, Is lithium from geothermal brines the sustainable solution for Li-ion batteries? Renew. Sust. Energ. Rev. 199 (2024) 114456 https://doi.org/10.1016/j.rser.2024.114456.

[27] X. Liu, X. Chen, L. He, Z. Zhao, Study on extraction of lithium from salt lake brine by membrane electrolysis, Desalination 376 (2015) 35–40.

[28] P.-Y. Ji, Z.-Y. Ji, Q.-B. Chen, J. Liu, Y.-Y. Zhao, S.-Z. Wang, F. Li, J.-S. Yuan, Effect of coexisting ions on recovering lithium from high Mg^{2+}/Li^+ ratio brines by selective-electrodialysis, Sep. Purif. Technol. 207 (2018) 1–11.

[29] Y. Pan, B. Ji, W. Zhang, Charge transfer-driven enhanced lithium extraction using poly(acrylic) acid-modified layered double hydroxide, Chem. Eng. J. 494 (2024) 152939, https://doi.org/10.1016/j.cej.2024.152939.

[30] J. Chen, S. Lin, J. Yu, High-selective cyclic adsorption and magnetic recovery performance of magnetic lithium-aluminum layered double hydroxides (MLDHs) in extracting Li^+ from ultrahigh Mg/Li ratio brines, Sep. Purif. Technol. 255 (2021) 117710, https://doi.org/10.1016/j.seppur.2020.117710.

[31] J. Zhong, S. Lin, J. Yu, Lithium recovery from ultrahigh Mg^{2+}/Li^+ ratio brine using a novel granulated Li/Al-LDHs adsorbent, Sep. Purif. Technol. 256 (2021) 117780, https://doi.org/10.1016/j.seppur.2020.117780.

[32] Q. Luo, M. Dong, Q. Li, Z. Wu, Z. Liu, J. Li, Improve the durability of lithium adsorbent Li/Al-LDHs by Fe^{3+} substitution and nanocomposite of FeOOH, Miner. Eng. 185 (2022) 107717, https://doi.org/10.1016/j.mineng.2022.107717.

[33] A.M. D'altri, V. Sarhosis, G. Milani, J. Rots, S. Cattari, S. Lagomarsino, E. Sacco, A. Tralli, G. Castellazzi, S. De Miranda, Modeling strategies for the computational analysis of unreinforced masonry structures: review and classification, Archives of computational methods in engineering 27 (2020) 1153–1185.

[34] D. Luengo, L. Martino, M. Bugallo, V. Elvira, S. Särkkä, A survey of Monte Carlo methods for parameter estimation, EURASIP Journal on Advances in Signal Processing 25 (2020) 1–62.

[35] A.V. Brukhno, J. Grant, T.L. Underwood, K. Stratford, S.C. Parker, J.A. Purton, N. B. Wilding, DL_MONTE: a multipurpose code for Monte Carlo simulation, Mol. Simul. 47 (2–3) (2021) 131–151.

[36] D.S. Sholl, J.A. Steckel, Density Functional Theory: A Practical Introduction, John Wiley & Sons, 2022.

[37] H. Al-Mahayni, X. Wang, J.P. Harvey, G.S. Patience, A. Seifitokaldani, Experimental methods in chemical engineering: density functional theory, Can. J. Chem. Eng. 99 (9) (2021) 1885–1911.

[38] A. Jafari, P. Broumand, M. Vahab, N. Khalili, An eXtended finite element method implementation in COMSOL multiphysics: solid mechanics, Finite Elem. Anal. Des. 202 (2022) 103707.

[39] V.K. Selvaraj, J. Subramanian, A comparative study of smart polyurethane foam using RSM and COMSOL multiphysics for acoustical applications: from materials to component, J. Porous. Mater. 30 (2) (2023) 547–563.

[40] J. Tu, G.H. Yeoh, C. Liu, Y. Tao, Computational Fluid Dynamics: A Practical Approach, Elsevier, 2023.

[41] M.M. Bhatti, M. Marin, A. Zeeshan, S.I. Abdelsalam, Recent trends in computational fluid dynamics, Front. Phys. 8 (2020) 593111.

[42] H. Adloo, B. Abbasi, Some insights into the use of pore network simulations for predicting single-phase fluid flow in model porous media, Microfluid. Nanofluid. 25 (7) (2021) 61.

[43] S. Badillo, B. Banfai, F. Birzele, I.I. Davydov, L. Hutchinson, T. Kam-Thong, J. Siebourg-Polster, B. Steiert, J.D. Zhang, An introduction to machine learning, Clin. Pharmacol. Ther. (St. Louis, MO, U. S.) 107 (4) (2020) 871–885.

[44] M.M. Cencer, J.S. Moore, R.S. Assary, Machine learning for polymeric materials: an introduction, Polym. Int. 71 (5) (2022) 537–542.

[45] I. Tews, Quantum Monte Carlo methods for astrophysical applications, Front. Phys. 8 (2020) 153.

[46] M.J. Abraham, T. Murtola, R. Schulz, S. Páll, J.C. Smith, B. Hess, E. Lindahl, GROMACS: high performance molecular simulations through multi-level parallelism from laptops to supercomputers, SoftwareX 1 (2015) 19–25.

[47] D. Shen, Z. Liu, Z. Tu, S. Li, Understanding hydrogen adsorption performance of lithium-doped MIL-101 (Cr) by molecular simulations: effects of lithium distribution, Int. J. Hydrog. Energy 48 (48) (2023) 18366–18374.

[48] A.P. Thompson, H.M. Aktulga, R. Berger, D.S. Bolintineanu, W.M. Brown, P. S. Crozier, P.J. In't Veld, A. Kohlmeyer, S.G. Moore, T.D. Nguyen, LAMMPS-a flexible simulation tool for particle-based materials modeling at the atomic, meso, and continuum scales, Comput. Phys. Commun. 271 (2022) 108171.

[49] S. Thomas, S. Jana, B. Jun, C.H. Lee, S.U. Lee, Temperature-dependent lithium diffusion in phographene: insights from molecular dynamics simulation, J. Ind. Eng. Chem. 81 (2020) 287–293, https://doi.org/10.1016/j.jiec.2019.09.016.

[50] J.N. Glosli, M.R. Philpott, Molecular dynamics simulation of adsorption of ions from aqueous media onto charged electrodes, J. Chem. Phys. 96 (9) (1992) 6962–6969.

[51] C.J. Dickson, L. Rosso, R.M. Betz, R.C. Walker, I.R. Gould, GAFFlipid: a General Amber Force Field for the accurate molecular dynamics simulation of phospholipid, Soft Matter 8 (37) (2012) 9617–9627.

[52] L. Verlet, Computer" experiments" on classical fluids. I. Thermodynamical properties of Lennard-Jones molecules, Phys. Rev. 159 (1) (1967) 98.

[53] Z. Ding, A. Selloni, Electron trapping and ion leaching at the Li-modified quartz–water interface, J. Phys. Chem. C 124 (49) (2020) 26741–26747.
[54] T. Darden, D. York, L. Pedersen, Particle mesh Ewald: an N· log (N) method for Ewald sums in large systems, J. Chem. Phys. 98 (12) (1993) 10089–10092.
[55] G.R. Quezada, P.G. Toledo, Structure of the interface between lithium-rich spodumene and saltwater by density functional theory calculations and molecular dynamics simulations, J. Phys. Chem. C 124 (2) (2019) 1446–1457.
[56] Y. Ma, R. Wang, H. Zhou, A note on the equivalence of three major propagator algorithms for computational stability and efficiency, Earthq. Sci. 25 (2012) 55–64.
[57] P. Xiao, G. Henkelman, Kinetic Monte Carlo study of Li intercalation in $LiFePO_4$, ACS Nano 12 (1) (2018) 844–851.
[58] W.W. Wood, J.J. Erpenbeck, G.A. Baker Jr., J. Johnson, Molecular dynamics ensemble, equation of state, and ergodicity, Phys. Rev. E 63 (1) (2000) 011106.
[59] D. Nasr Esfahani, O. Leenaerts, H. Sahin, B. Partoens, F. Peeters, Structural transitions in monolayer MoS_2 by lithium adsorption, J. Phys. Chem. C 119 (19) (2015) 10602–10609.
[60] F. Fraternali, Restrained and unrestrained molecular dynamics simulations in the NVT ensemble of alamethicin, Biopolymers: Original Research on Biomolecules 30 (11–12) (1990) 1083–1099.
[61] J. Park, S.A. Fatima, Computational insight of lithium adsorption and intercalation in bilayer TiC3, Electrochim. Acta 477 (2024) 143763.
[62] S. Melchionna, G. Ciccotti, B. Lee Holian, Hoover NPT dynamics for systems varying in shape and size, Mol. Phys. 78 (3) (1993) 533–544.
[63] T. Ingebrigtsen, O.J. Heilmann, S. Toxvaerd, J.C. Dyre, Time reversible molecular dynamics algorithms with holonomic bond constraints in the NPH and NPT ensembles using molecular scaling, J. Chem. Phys. 132 (15) (2010) 154106.
[64] N. Li, M.-Z. Sun, S. Hwang, S. Li, H.-Y. Zhao, Y.-P. Du, B.-L. Huang, D. Su, Non-equilibrium insertion of lithium ions into graphite, J. Mater. Chem. A 9 (20) (2021) 12080–12086.
[65] N. Li, M. Sun, S. Hwang, S. Li, H. Zhao, Y. Du, B. Huang, D. Su, Non-equilibrium insertion of lithium ions into graphite, J. Mater. Chem. A 9 (20) (2021) 12080–12086.
[66] C.M. Shumeyko, E.B. Webb, G.J. Tucker, Effects of grain boundary structure on lithium transport in graphite, Mol. Simul. 42 (16) (2016) 1356–1363.
[67] C.Z. Mooney, Monte Carlo simulation, Sage 116 (1997) 1–112.
[68] Y. Hamoudi, Quantum Algorithms for the Monte Carlo Method, Ph. D. thesis,, Université de Paris, 2021.
[69] Y. Yan, D. Blume, Path integral Monte Carlo ground state approach: formalism, implementation, and applications, J. Phys. B Atomic Mol. Phys. 50 (22) (2017) 223001.
[70] J. Wei, A fast Monte Carlo method based on an acceptance-rejection scheme for particle coagulation, Aerosol Air Qual. Res. 13 (4) (2013) 1273–1281.
[71] R. Malik, First-principles Investigation of Li Intercalation Kinetics in Phospho-olivines, Massachusetts Institute of Technology, 2013.
[72] M. Dubecky, L. Mitas, P. Jurecka, Noncovalent interactions by quantum Monte Carlo, Chem. Rev. 116 (9) (2016) 5188–5215.
[73] R. Marthi, H. Asgar, G. Gadikota, Y.R. Smith, On the structure and lithium adsorption mechanism of layered H_2TiO_3, ACS Appl. Mater. Interfaces 13 (7) (2021) 8361–8369.
[74] J. Chen, S. Lin, J. Yu, Instant interlayer restoration strategy for lithium adsorption engineering enhancement in sulfate-type brines, ACS Appl. Mater. Interfaces 16 (27) (2024) 34850–34858.
[75] B. Song, J. Yang, J. Zhao, H. Fang, Intercalation and diffusion of lithium ions in a carbon nanotube bundle by ab initio molecular dynamics simulations, Energy Environ. Sci. 4 (4) (2011) 1379–1384.
[76] R. Jorn, L. Raguette, S. Peart, Investigating the mechanism of lithium transport at solid electrolyte interphases, J. Phys. Chem. C 124 (30) (2020) 16261–16270.
[77] A. Aggarwal, K. Gordiz, A. Baskin, D. Vivona, J. Halldin Stenlid, J.W. Lawson, J. C. Grossman, Y. Shao-Horn, Revealing the molecular origin of driving forces and thermodynamic barriers for Li^+ ion transport to electrode–electrolyte interfaces, J. Phys. Chem. C 128 (31) (2024) 12903–12915.
[78] J. Chen, J. Du, J. Yu, S. Lin, A one-step regeneration method in-situ for deactivated aluminum-based lithium adsorbent used in high Mg^{2+}/Li^+ brines, Desalination 554 (2023) 116491, https://doi.org/10.1016/j.desal.2023.116491.
[79] S.B. Olou'ou Guifo, J.E. Mueller, T. Markus, Molecular dynamics simulations of interfacial lithium–silicon interdiffusion in lithium-ion-battery anodes, J. Phys. Chem. C 128 (12) (2024) 4891–4904, https://doi.org/10.1021/acs.jpcc.3c08196.
[80] T. Zheng, Y. Zhang, N. Huang, H. Zhang, Electrolyte transport in lithium-ion battery systems with nanoporous polyethylene separators: insights from molecular dynamics simulations, Comput. Mater. Sci. 242 (2024) 113099, https://doi.org/10.1016/j.commatsci.2024.113099.
[81] J. Haruyama, S. Takagi, K. Shimoda, I. Watanabe, K. Sodeyama, T. Ikeshoji, M. Otani, Thermodynamic analysis of Li-intercalated graphite by first-principles calculations with vibrational and configurational contributions, J. Phys. Chem. C 125 (51) (2021) 27891–27900, https://doi.org/10.1021/acs.jpcc.1c08992.
[82] S.-Y. Sun, X.-Y. Nie, J. Huang, J.-G. Yu, Molecular simulation of diffusion behavior of counterions within polyelectrolyte membranes used in electrodialysis, J. Membr. Sci. 595 (2020) 117528, https://doi.org/10.1016/j.memsci.2019.117528.
[83] G.A. Tritsaris, E. Kaxiras, S. Meng, E. Wang, Adsorption and diffusion of lithium on layered silicon for Li-ion storage, Nano Lett. 13 (5) (2013) 2258–2263, https://doi.org/10.1021/nl400830u.
[84] B. Ghalami Choobar, H. Modarress, R. Halladj, S. Amjad-Iranagh, Electrodeposition of lithium metal on lithium anode surface, a simulation study by: kinetic Monte Carlo-embedded atom method, Comput. Mater. Sci. 192 (2021) 110343, https://doi.org/10.1016/j.commatsci.2021.110343.
[85] Y. Han, J. Ma, D. Liu, Y. Yang, T. Zhang, M. Wang, D. Liang, L. Wen, J. Ma, W. Wang, Microenvironment-modulating adsorption enables highly efficient lithium extraction under natural pH conditions, ACS Nano 18 (12) (2024) 9071–9081, https://doi.org/10.1021/acsnano.3c12978.
[86] M. Ge, C. Wei, T. Fang, X. Liu, Molecular insight into the separation mechanism of crown ether-based channels for lithium extraction, Sep. Purif. Technol. 338 (2024) 126415, https://doi.org/10.1016/j.seppur.2024.126415.
[87] Y. Chen, H. Zhan, Y. Qiao, Z. Qian, B. Lv, Z. Wu, Z. Liu, Facet dependent ion channel of iron phosphate for electrochemical lithium extraction, Chem. Eng. J. 477 (2023) 147136, https://doi.org/10.1016/j.cej.2023.147136.
[88] M. Wang, T. Zhang, Z. Meng, C. Wang, W. Dong, J. Liu, S. Yang, X. Hou, X. Cheng, W. Liu, Self-intercepting interference of hydrogen-bond induced flexible hybrid film to facilitate lithium extraction, Chem. Eng. J. 458 (2023) 141403.
[89] Q. Wang, M. Li, B. Zhao, B. Meng, W. Chen, Z. Jiang, X. He, B. Li, X.-Y. Li, L. Lin, Electricity facilitates the lithium sorption from salt-lake brine by $H_3LiTi_5O_{12}$ nanoparticles: kinetics, selectivity and mechanism, Chem. Eng. J. 471 (2023) 144532, https://doi.org/10.1016/j.cej.2023.144532.
[90] J. Zhang, W. Pan, Y. Zhou, C. Hai, Y. Xu, Y. Zhao, Y. Sun, S. Dong, X. He, Q. Xu, et al., Biochar-enhanced three-dimensional conductive network thick electrodes for efficient lithium extraction from salt lake brines with high magnesia-lithium ratios, Chemosphere 360 (2024) 142325, https://doi.org/10.1016/j.chemosphere.2024.142325.
[91] M. Zhao, J. Luan, C. Zhao, Y. Zhang, G. Pan, X. Zhang, Y. Liu, Highly selective granulation adsorbents for lithium recovery from gas field brine: selectivity, kinetics and mechanism, Desalination 583 (2024) 117699, https://doi.org/10.1016/j.desal.2024.117699.
[92] B. Zhao, Y. Qiao, Z. Qian, W. Wei, J. Li, Z. Wu, Z. Liu, Unraveling the Li^+ desorption behavior and mechanism of $Li_4Ti_5O_{12}$ with different facets to enhance lithium extraction, J. Mater. Chem. A 11 (13) (2023) 7094–7104, https://doi.org/10.1039/d2ta10016a.
[93] G. Luo, M. Zhou, Y. Chao, P. Cui, X. Li, L. Chen, G. Jiang, W. Zhu, Z. Liu, C. Xu, Augmented electrochemical extraction lithium performance via interface alloying modification, Sep. Purif. Technol. 354 (2025) 128683, https://doi.org/10.1016/j.seppur.2024.128683.
[94] Y. Qiao, X. Dai, B. Zhao, Z. Qian, Z. Wu, Z. Liu, Enhanced lithium extraction from aqueous solutions using multi-scale modified titanium adsorbent, Sep. Purif. Technol. 351 (2024) 128060, https://doi.org/10.1016/j.seppur.2024.128060.
[95] Y. Zhang, H. Xing, Q. Meng, Q. Liu, H. Liu, L. Yang, Facets regulation of $Li_{1.6}Mn_{1.6}O_4$ by B-doping to enable high stability and adsorption capacity for lithium extraction, Sep. Purif. Technol. 348 (2024) 127739, https://doi.org/10.1016/j.seppur.2024.127739.
[96] J. Hafner, Ab-initio simulations of materials using VASP: density-functional theory and beyond, J. Comput. Chem. 29 (13) (2008) 2044–2078.
[97] Y. Okamoto, Density functional theory calculations of lithium adsorption and insertion to defect-free and defective graphene, J. Phys. Chem. C 120 (26) (2016) 14009–14014.
[98] M. Bounbaâ, M. Khuili, N. Fazouan, E.H. Atmani, I. Allaoui, M. Houmad, Li adsorption and diffusion on the surfaces of molybdenum dichalcogenides MoX_2 (X= S, Se, Te) monolayers for lithium-ion batteries application: a DFT study, J. Mol. Model. 29 (12) (2023) 378.
[99] F. Hao, X. Chen, First-principles study of lithium adsorption and diffusion on graphene: the effects of strain, Materials Research Express 2 (10) (2015) 105016.
[100] M.V. Pajtler, I. Lukačević, V. Dušić, M. Mužević, Lithium adsorption on the interface of graphene/boron nitride nanoribbons, J. Mater. Sci. 58 (10) (2023) 4513–4524.
[101] E. Bosoni, L. Beal, M. Bercx, P. Blaha, S. Blügel, J. Bröder, M. Callsen, S. Cottenier, A. Degomme, V. Dikan, How to verify the precision of density-functional-theory implementations via reproducible and universal workflows, Nature Reviews Physics 6 (1) (2024) 45–58.
[102] A. Gao, Z. Sun, S. Li, X. Hou, H. Li, C. Wang, W. Wu, Self-assembled layered lithium manganese oxide shows ultra-large adsorption capacity and high selectivity for lithium, Chem. Eng. J. 471 (2023) 144287, https://doi.org/10.1016/j.cej.2023.144287.
[103] M.-M. Zhang, H.-Z. Wei, J.-J. Lu, A.E. Williams-Jones, C.J. Eastoe, W.-Q. Li, Z.-G. Xia, S.V. Hohl, J. Ma, Y. Cai, et al., Estimates of chlorine isotope fractionation factors using density functional theory: applications to ore-forming systems, Geochim. Cosmochim. Acta 367 (2024) 1–15, https://doi.org/10.1016/j.gca.2023.12.026.
[104] H. Chang, M.-S. Park, J.H. Kim, J. Moon, Defect mediated lithium adsorption on graphene-based silicon composite electrode for high capacity and high stability lithium-ion battery, J. Electroanal. Chem. 931 (2023) 117179, https://doi.org/10.1016/j.jelechem.2023.117179.
[105] A. Gao, X. Hou, Z. Sun, S. Li, H. Li, J. Zhang, Lithium-desorption mechanism in $LiMn_2O_4$, $Li_{1.33}Mn_{1.67}O_4$, and $Li_{1.6}Mn_{1.6}O_4$ according to precisely controlled acid treatment and density functional theory calculations, J. Mater. Chem. A 7 (36) (2019) 20878–20890, https://doi.org/10.1039/c9ta06080d.
[106] L. Zhang, T. Zhang, Y. Zhao, G. Dong, S. Lv, S. Ma, S. Song, M. Quintana, Doping engineering of lithium-aluminum layered double hydroxides for high-efficiency lithium extraction from salt lake brines, Nano Res. 17 (3) (2023) 1646–1654, https://doi.org/10.1007/s12274-023-5950-1.
[107] Y. Zhao, H. Xing, M. Rong, Z. Li, X. Wei, C. Chen, H. Liu, L. Yang, Quantum chemical calculation assisted efficient lithium extraction from unconventional oil and gas field brine by β-diketone synergic system, Desalination 565 (2023) 116890, https://doi.org/10.1016/j.desal.2023.116890.

[108] A. Jalbout, F. Nazari, L. Turker, Gaussian-based computations in molecular science, J. Mol. Struct. (THEOCHEM) 671 (1–3) (2004) 1–21.

[109] R. Coterillo Ruisánchez, L.E. Gallart Tauler, E. Fernández-Escalante Barquín, F. J. Junquera Quintana, I. Ortiz Uribe, R. Ibáñez Mendizábal, San Román San Emeterio, M. F., Selective extraction of lithium from seawater desalination concentrates: study of thermodynamic and equilibrium properties using Density Functional Theory (DFT), Desalination 532 (2022) 115704, https://doi.org/10.1016/j.desal.2022.115704.

[110] Q. Sun, H. Chen, J. Yu, A density functional theory insight into the extraction mechanism of lithium recovery from alkaline brine by β-diketones, AICHE J. 69 (7) (2023) e18094.

[111] M.V. Malyshkina, A.S. Novikov, Modern software for computer modeling in quantum chemistry and molecular dynamics, Compounds 1 (3) (2021) 134–144.

[112] J. Hua, F. Yang, J. He, J. Du, B. Dong, X. Ma, J. Li, A highly efficient ternary extraction system with tributyl phosphate/crown ether/$NaNTf_2$ for the recovery of Li^+ from low-grade salt lakes, Desalination 583 (2024) 117702, https://doi.org/10.1016/j.desal.2024.117702.

[113] W. Qu, Y. Fu, Y. Zhang, W. Wang, C. Xu, C. Liu, Y. Zhang, Q. Wang, B. Liu, Structural/surficial dual regulated granular H_2TiO_3 lithium-ion sieves for lithium extraction from salt lake brine, J. Clean. Prod. 449 (2024) 141789, https://doi.org/10.1016/j.jclepro.2024.141789.

[114] J. Hua, J. He, H. Pei, J. Du, X. Ma, J. Li, A remarkable improved Li^+/Mg^{2+} selectivity and Li+ recovery simultaneously by adding crown ether to tributyl phosphate-ionic liquid extraction system as co-extractant, Sep. Purif. Technol. 335 (2024) 126162, https://doi.org/10.1016/j.seppur.2023.126162.

[115] S. Lv, Y. Zhao, L. Zhang, T. Zhang, G. Dong, D. Li, S. Cheng, S. Ma, S. Song, M. Quintana, Anion regulation strategy of lithium-aluminum layered double hydroxides for strengthening resistance to deactivation in lithium recovery from brines, Chem. Eng. J. 472 (2023) 145026, https://doi.org/10.1016/j.cej.2023.145026.

[116] X. An, Z. Du, B. Qiao, S. Wang, P. Wang, X. Ma, Y. Li, X. Du, X. Hao, G. Guan, Co-doping induced Mn-vacancy $LiMn_2O_4$ based membrane electrode for lithium extraction by electrochemically switched ion permselective process, Desalination 591 (2024) 118016, https://doi.org/10.1016/j.desal.2024.118016.

[117] J.P. Perdew, K. Burke, M. Ernzerhof, Generalized gradient approximation made simple, Phys. Rev. Lett. 77 (18) (1996) 3865–3868, https://doi.org/10.1103/PhysRevLett.77.3865.

[118] Z. He, W. Que, Molybdenum disulfide nanomaterials: structures, properties, synthesis and recent progress on hydrogen evolution reaction, Appl. Mater. Today 3 (2016) 23–56.

[119] T. Maihom, J. Sittiwong, M. Probst, J. Limtrakul, Understanding the interactions between lithium polysulfides and anchoring materials in advanced lithium–sulfur batteries using density functional theory, Phys. Chem. Chem. Phys. 24 (15) (2022) 8604–8623.

[120] Y. Hu, H. Su, Z. Zhu, M. Zhou, T. Qi, Mechanisms for the separation of Li^+ and Mg^{2+} from salt lake brines using TBP and TOP systems, Desalination 583 (2024) 117698, https://doi.org/10.1016/j.desal.2024.117698.

[121] H. Zhang, X. Du, S. Ding, Q. Wang, L. Chang, X. Ma, X. Hao, C. Pen, DFT calculations of the synergistic effect of λ-MnO_2/graphene composites for electrochemical adsorption of lithium ions, Phys. Chem. Chem. Phys. 21 (15) (2019) 8133–8140.

[122] Y. Xin, Y.-X. Yu, Adsorption and mobility of lithium on pristine and Stone-Thrower-Wales defective silicenes, in: International Conference on Materials Chemistry and Environmental Protection 2015, Atlantis Press, 2016, pp. 50–54.

[123] W. Chen, Y. Tian, C. Hu, Z. Zhao, L. Xu, B. Tong, Theoretical and extraction studies on the selectivity of lithium with $14C_4$ derivatives, New J. Chem. 44 (46) (2020) 20341–20350.

[124] Y. Chen, H. Tao, J. Cheng, S. Lin, C. Lian, H. Liu, A molecular model for understanding the membrane separation of Li^+/Mg^{2+}, Ind. Eng. Chem. Res. 62 (21) (2023) 8433–8443, https://doi.org/10.1021/acs.iecr.3c00136.

[125] S. Sun, L. Chen, H. Sun, T.-Y. Zhang, Adsorption and charge transfer of lithium at electrified graphene/electrolyte interface, Electrochim. Acta 259 (2018) 1089–1094.

[126] H. Wang, Z. Jing, H. Liu, X. Feng, G. Meng, K. Wu, Y. Cheng, B. Xiao, A high-throughput assessment of the adsorption capacity and Li-ion diffusion dynamics in Mo-based ordered double-transition-metal MXenes as anode materials for fast-charging LIBs, Nanoscale 12 (48) (2020) 24510–24526.

[127] T. Ding, M. Zheng, Y. Lin, Adsorption of Li(I) ions through new high-performance electrospun PAN/kaolin nanofibers: a combined experimental and theoretical calculation, ACS Omega 7 (13) (2022) 11430–11439, https://doi.org/10.1021/acsomega.2c00658.

[128] J. Chen, K. Huang, J. Du, C. Lian, J. Yu, S. Lin, Why is aluminum-based lithium adsorbent ineffective in Li^+ extraction from sulfate-type brines, AICHE J. 69 (10) (2023), https://doi.org/10.1002/aic.18176.

[129] X. Liu, N. Liu, C. Zhao, Q. Liu, Y. Liu, Z. Liu, A. Ying, Hard carbon with an "adsorption-intercalation/filling" behavior for selective deionization of lithium ions, Desalination 544 (2022) 116124, https://doi.org/10.1016/j.desal.2022.116124.

[130] Z.-C. Xiong, Y. Xie, T.-F. Yi, H.-T. Yu, Y.-R. Zhu, Y.-Y. Zeng, Effect of lithium extraction on the stabilities, electrochemical properties, and bonding characteristics of $LiFePO_4$ cathode materials: a first-principles investigation, Ceram. Int. 40 (2) (2014) 2655–2661, https://doi.org/10.1016/j.ceramint.2013.10.059.

[131] K.K. Surthi, M. Thak, K.K. Kar, Charge–discharge mechanism, lithium-ion diffusion in Al, Ca, and Cu doped lithium metatitanate based anodes for Li-ion batteries: first principles study, J. Mater. Chem. A 12 (20) (2024) 12098–12111.

[132] F. Qian, B. Zhao, M. Guo, Z. Qian, Z. Wu, Z. Liu, Trace doping by fluoride and sulfur to enhance adsorption capacity of manganese oxides for lithium recovery, Mater. Des. 194 (2020) 108867, https://doi.org/10.1016/j.matdes.2020.108867.

[133] P. Zhang, M. Yang, C. Xu, Q. Wang, C. He, C. Liu, B. Lai, Insight into the synergistic mechanism of Co and N doped titanium-based adsorbents for liquid lithium extraction, Chem. Eng. J. 480 (2024) 147631, https://doi.org/10.1016/j.cej.2023.147631.

[134] Q. Wu, Z. Wang, Q. Hu, Y. Ji, D. Li, J. Wang, Q. Xia, L. Wang, A. Zhou, Lithium storage performance enhanced by lithiation-induced structural phase transitions of fluorinated MXenes, Phys. Chem. Chem. Phys. 25 (20) (2023) 14406–14416.

[135] A. Erraji, R. Masrour, L. Xu, Investigation of electrochemical, structural, electronic, thermodynamic, and optical properties of $LiTi_2O_4$ cathode material for Li-ion battery: an ab initio calculations, Ionics 30 (2024) 5979–5987.

[136] J. Halldin Stenlid, P. Žguns, D. Vivona, A. Aggarwal, K. Gordiz, Y. Zhang, S. Pathak, M.Z. Bazant, Y. Shao-Horn, A. Baskin, Computational insights into electrolyte-dependent Li-ion charge-transfer kinetics at the Li_xCoO_2 interface, ACS Energy Lett. 9 (7) (2024) 3608–3617.

[137] Z. Zhou, H.D. Luong, B. Gao, T. Momma, Y. Tateyama, $LiNbO_3$ and $LiTaO_3$ coating effects on the interface of the $LiCoO_2$ cathode: a DFT study of Li-ion transport, ACS Appl. Mater. Interfaces 16 (32) (2024) 42093–42099.

[138] X. Qin, A. Bhowmik, T. Vegge, I.E. Castelli, Computational investigation of LiF formation at graphite–electrolyte interfaces, ACS Appl. Mater. Interfaces 16 (22) (2024) 29347–29354, https://doi.org/10.1021/acsami.4c01719.

[139] Y. Yuan, R. Li, X. Bi, M. Yan, J. Cheng, J. Gu, Review on numerical simulation of ultrasonic impact treatment (UIT): present situation and prospect, J. Mater. Res. Technol. 30 (2024) 1319–1340.

[140] Akshya, S.; Juliet, A. V. Study of toxic gas adsorption on silicon substrate integrated with piezoelectric material for sensing application using COMSOL Multiphysics. In IOP Conference Series: Materials Science and Engineering, 2021; IOP Publishing: Vol. 1070, p 012003.

[141] M.M. Hathal, B.O. Hasan, Studying the effect of operating parameters on the removal of nickel ion from an adsorber by using COMSOL multiphysics simulation, Al-Nahrain Journal for Engineering Sciences 23 (4) (2020) 357–364.

[142] S.E. Pour, A.H. Mamaghani, Z. Hashisho, Modeling of adsorption process on monolith adsorbents: a mini-review, Sep. Purif. Technol. 354 (2025) 128846.

[143] X. Zhang, Z. Li, J. Liu, F. Xu, L. Zheng, S. De Wolf, Z. Lai, X. Lu, Solar-driven ultrafast lithium extraction from low-grade brine using microfluidics-mediated vortex in scalable electrochemical reactors, Chem. Eng. J. 454 (2023) 140074, https://doi.org/10.1016/j.cej.2022.140074.

[144] O. Abushammala, R. Hreiz, C. Lemaître, E. Favre, Optimal design of helical heat/mass exchangers under laminar flow: CFD investigation and correlations for maximal transfer efficiency and process intensification performances, Int. J. Heat Mass Transf. 153 (2020) 119610.

[145] Z. Li, Y. Yang, J. Yu, Modeling and application of continuous ion exchanges process for lithium recovery from salt lake brine, Sep. Purif. Technol. 326 (2023) 124841.

[146] X. Guo, Y. Liu, J. Wang, Equilibrium, kinetics and molecular dynamic modeling of Sr^{2+} sorption onto microplastics, J. Hazard. Mater. 400 (2020) 123324.

[147] O.A. Simonov, Y.Y. Erina, A.A. Ponomarev, Review of modern models of porous media for numerical simulation of fluid flows, Heliyon 9 (12) (2023).

[148] K.V. Kumar, K. Porkodi, R.A. Rondon, F. Rocha, Neural network modeling and simulation of the solid/liquid activated carbon adsorption process, Ind. Eng. Chem. Res. 47 (2) (2008) 486–490.

[149] M. Molashahi, H. Hashemipour, Experimental study and artificial neural network simulation of methane adsorption on activated carbon, Korean J. Chem. Eng. 29 (2012) 601–605.

[150] J. Moleón, A. Moya, Transient electrical response of ion-exchange membranes with fixed-charge due to ion adsorption. A network simulation approach, J. Electroanal. Chem. 633 (2) (2009) 306–313.

[151] W.R. Vieth, K. Sladek, A model for diffusion in a glassy polymer, J. Colloid Sci. 20 (9) (1965) 1014–1033.

[152] Z. Wang, M. Gao, Numerical simulations of oscillating laser welding: a review, J. Manuf. Process. 119 (2024) 744–757.

[153] D.E. Wiley, D.F. Fletcher, Techniques for computational fluid dynamics modelling of flow in membrane channels, J. Membr. Sci. 211 (1) (2003) 127–137.

[154] Z. Khan, X. Long, E. Casey, D. Dowling, S. Ferguson, Development of continuous spatially distributed diafiltration unit operations, React. Chem. Eng. 8 (7) (2023) 1785–1798.

[155] S. Yang, W. Shang, H. Shi, F. Sun, H. Zeng, Development of an automatic and object-oriented method for spacer design in the spiral wound nanofiltration modules to comprehensively enhance filtration performance, Desalination 566 (2023) 116945.

[156] Y. Liu, J. Ran, Q. Guo, L. Gao, S. Yin, S. Li, X. Jiang, N. Zhang, G. Zhou, Advancements in nanofiltration fouling phenomenon: from water treatment to salt lakes environments, Desalination 583 (2024) 117649.

[157] Y. Liu, T. Li, Q. Guo, L. Gao, S. Yin, S. Li, Simulation of nanofiltration mass transfer for magnesium and lithium separation in salt lakes, ACS Omega 9 (10) (2024) 12219–12227.

[158] A.S. Berman, Laminar Flow in Channels with Porous Walls, Carbide and Carbon Chemicals Company, K-25 Plant, 1952.

[159] J. Yu, J. Zhu, Z. Han, P. Cui, H. Mi, A. Zhang, L. Chen, X. Li, P. Wu, Y. Chao, 3D-printed devices for continuous-flow lithium recovery of brines, Desalination 586 (2024) 117748.

[160] Y.S. Jeon, S.I. Cheong, J.W. Rhim, Design shape of CDI cell applied with APSf and SPEEK and performance in MCDI, Macromol. Res. 25 (2017) 712–721.

[161] M.S. Gaikwad, C. Balomajumder, A.K. Tiwari, Acid treated RHWBAC electrode performance for Cr (VI) removal by capacitive deionization and CFD analysis study, Chemosphere 254 (2020) 126781.
[162] X. Liu, J. Wang, Electro-adsorption characteristics and mechanism of Sr^{2+} ions by capacitive deionization and CFD analysis study, Prog. Nucl. Energy 133 (2021) 103628.
[163] D. Zhang, X. Zhang, L. Xing, Z. Li, Numerical simulation of continuous extraction of Li^+ from high Mg^{2+}/Li^+ ratio brines based on free flow ion concentration polarization microfluidic system, Membranes 11 (9) (2021) 697.
[164] H. Joo, S.Y. Jung, S. Kim, K.H. Ahn, W.S. Ryoo, J. Yoon, Application of a flow-type electrochemical lithium recovery system with λ-$MnO_2/LiMn_2O_4$: experiment and simulation, ACS Sustain. Chem. Eng. 8 (26) (2020) 9622–9631.
[165] S. Wang, X. Yu, X. Hu, Electrochemical lithium extraction with gas flushing of porous electrodes, Nanomaterials 13 (9) (2023) 1471.
[166] M. Lu, A. Ozcelik, C.L. Grigsby, Y. Zhao, F. Guo, K.W. Leong, T.J. Huang, Microfluidic hydrodynamic focusing for synthesis of nanomaterials, Nano Today 11 (6) (2016) 778–792.
[167] M. Spiga, G. Morino, A symmetric solution for velocity profile in laminar flow through rectangular ducts, International communications in heat and mass transfer 21 (4) (1994) 469–475.
[168] Z. Li, Y. Chen, Y. Nie, F. Yang, X. Liu, Y. Gao, B. Shan, R. Chen, Multiscale computational fluid dynamics modelling of spatial ALD on porous li-ion battery electrodes, Chem. Eng. J. 479 (2024) 147486.
[169] Y. Jiang, K. Li, S.I. Alhassan, Y. Cao, H. Deng, S. Tan, H. Wang, C. Tang, L. Chai, Spinel $LiMn_2O_4$ as a capacitive deionization electrode material with high desalination capacity: experiment and simulation, Int. J. Environ. Res. Public Health 20 (1) (2022) 517.
[170] F.S. Wanyonyi, T.T. Fidelis, H. Louis, G.K. Mutua, F. Orata, L. Rhyman, P. Ramasami, A.M. Pembere, Simulation guided prediction of zeolites for the sorption of selected anions from water: machine learning predictors for enhanced loading, J. Mol. Liq. 355 (2022) 118913.
[171] Z. Fu, W. Liu, C. Huang, T. Mei, A review of performance prediction based on machine learning in materials science, Nanomaterials 12 (17) (2022) 2957.
[172] C. Wang, K. Aoyagi, P. Wisesa, T. Mueller, Lithium ion conduction in cathode coating materials from on-the-fly machine learning, Chem. Mater. 32 (9) (2020) 3741–3752.
[173] S.M. Moosavi, K.M. Jablonka, B. Smit, The role of machine learning in the understanding and design of materials, J. Am. Chem. Soc. 142 (48) (2020) 20273–20287.
[174] D.S. Franco, F.A. Duarte, N.P.G. Salau, G.L. Dotto, Analysis of indium (III) adsorption from leachates of LCD screens using artificial neural networks (ANN) and adaptive neuro-fuzzy inference systems (ANIFS), J. Hazard. Mater. 384 (2020) 121137.
[175] S. Lee, B. Kim, J. Kim, Predicting performance limits of methane gas storage in zeolites with an artificial neural network, J. Mater. Chem. A 7 (6) (2019) 2709–2716.
[176] S.H. Guan, C. Shang, Z.P. Liu, Structure and dynamics of energy materials from machine learning simulations: a topical review, Chin. J. Chem. 39 (11) (2021) 3144–3154.
[177] M. Hussain, F. Uddin, N. Raza, W. Aleem, S. Hussain, A. Idris, S. Qadir, Optimization of lithium adsorption from seawater via aluminum chloride as adsorbent using response surface methodology, Energy Sources, Part A 46 (1) (2024) 2907–2921, https://doi.org/10.1080/15567036.2024.2310742.
[178] L. Zheng, J. Chen, J. Sun, M. Liu, Y. Gao, Z. Guo, Highly selective lanthanide-doped ion sieves for lithium recovery from aqueous solutions, J. Chem. Res. 47 (2) (2023) 17475198231159051, https://doi.org/10.1177/17475198231159051.
[179] Z. Wang, D. Wang, Z. Zou, T. Song, D. Ni, Z. Li, X. Shao, W. Yin, Y. Wang, W. Luo, et al., Efficient potential-tuning strategy through p-type doping for designing cathodes with ultrahigh energy density, Natl. Sci. Rev. 7 (11) (2020) 1768–1775, https://doi.org/10.1093/nsr/nwaa174.
[180] K. Horn, A. Hohlfeld, J. Somers, T. Lindner, P. Hollins, A.M. Bradshaw, Identification of the s-derived valence-electron level in photoemission from alkali-metal adlayers on aluminum, Phys. Rev. Lett. 61 (21) (1988) 2488–2491, https://doi.org/10.1103/PhysRevLett.61.2488.
[181] M. Belgiu, L. Drăguţ, Random forest in remote sensing: a review of applications and future directions, ISPRS J. Photogramm. Remote Sens. 114 (2016) 24–31, https://doi.org/10.1016/j.isprsjprs.2016.01.011.
[182] A. Malloum, K.A. Adegoke, J.O. Ighalo, J. Conradie, C.R. Ohoro, J.F. Amaku, K. O. Oyedotun, N.W. Maxakato, K.G. Akpomie, E.S. Okeke, et al., Computational methods for adsorption study in wastewater treatment, J. Mol. Liq. 390 (2023) 123008, https://doi.org/10.1016/j.molliq.2023.123008.
[183] V. Nourani, H. Gökçekuş, I.K. Umar, H. Najafi, An emotional artificial neural network for prediction of vehicular traffic noise, Sci. Total Environ. 707 (2020) 136134, https://doi.org/10.1016/j.scitotenv.2019.136134.
[184] V.L. Deringer, A.P. Bartók, N. Bernstein, D.M. Wilkins, M. Ceriotti, G. Csányi, Gaussian process regression for materials and molecules, Chem. Rev. 121 (16) (2021) 10073–10141, https://doi.org/10.1021/acs.chemrev.1c00022.
[185] G. Chirici, M. Mura, D. McInerney, N. Py, E.O. Tomppo, L.T. Waser, D. Travaglini, R.E. McRoberts, A meta-analysis and review of the literature on the k-nearest neighbors technique for forestry applications that use remotely sensed data, Remote Sens. Environ. 176 (2016) 282–294, https://doi.org/10.1016/j.rse.2016.02.001.
[186] J.A. Keith, V. Vassilev-Galindo, B. Cheng, S. Chmiela, M. Gastegger, K.-R. Müller, A. Tkatchenko, Combining machine learning and computational chemistry for predictive insights into chemical systems, Chem. Rev. 121 (16) (2021) 9816–9872, https://doi.org/10.1021/acs.chemrev.1c00107.
[187] N.C. Frey, D. Akinwande, D. Jariwala, V.B. Shenoy, Machine learning-enabled design of point defects in 2D materials for quantum and neuromorphic information processing, ACS Nano 14 (10) (2020) 13406–13417, https://doi.org/10.1021/acsnano.0c05267.
[188] S. Gong, S. Wang, T. Zhu, X. Chen, Z. Yang, M.J. Buehler, Y. Shao-Horn, J. C. Grossman, Screening and understanding Li adsorption on two-dimensional metallic materials by learning physics and physics-simplified learning, JACS Au 1 (11) (2021) 1904–1914, https://doi.org/10.1021/jacsau.1c00260.
[189] M. Dou, M. Fyta, Lithium adsorption on 2D transition metal dichalcogenides: towards a descriptor for machine learned materials design, J. Mater. Chem. A 8 (44) (2020) 23511–23518, https://doi.org/10.1039/D0TA04834H.
[190] G. Chaney, A. Ibrahim, F. Ersan, D. Çakır, C. Ataca, Comprehensive study of Lithium adsorption and diffusion on Janus Mo/WXY (X, Y = S, Se, Te) using first-principles and machine learning approaches, ACS Appl. Mater. Interfaces 13 (30) (2021) 36388–36406, https://doi.org/10.1021/acsami.1c05508.
[191] S.I. Abba, J. Usman, I. Abdulazeez, L.T. Yogarathinam, A.G. Usman, D. Lawal, B. Salhi, N. Baig, I.H. Aljundi, Enhancing Li^+ recovery in brine mining: integrating next-gen emotional AI and explainable ML to predict adsorption energy in crown ether-based hierarchical nanomaterials, RSC Adv. 14 (21) (2024) 15129–15142, https://doi.org/10.1039/D4RA02385D.
[192] I. Abdulazeez, S.I. Abba, J. Usman, A.G. Usman, I.H. Aljundi, Recovery of brine resources through crown-passivated graphene, silicene, and boron nitride nanosheets based on machine-learning structural predictions, ACS Applied Nano Materials 6 (24) (2023) 23207–23221, https://doi.org/10.1021/acsanm.3c04421.
[193] N. Kireeva, V.E. Baulin, A.Y. Tsivadze, A machine learning-based study of Li^+ and Na^+ metal complexation with phosphoryl-containing ligands for the selective extraction of Li^+ from brine, ChemEngineering 7 (3) (2023) 41.
[194] A.D. Powell, G.-J. Kroes, K. Doblhoff-Dier, Quantum Monte Carlo calculations on dissociative chemisorption of H_2 + Al(110): minimum barrier heights and their comparison to DFT values, J. Chem. Phys. 153 (22) (2020), https://doi.org/10.1063/5.0022919.
[195] Z. Gao, X. Cheng, M. Zhao, Ab initio diffusion quantum Monte Carlo study of the structural and electronic properties of small lithium-chloride $Li_nCl^{(0,1+)}$ (n = 1–7) clusters, Computational and Theoretical Chemistry 1214 (2022) 113781, https://doi.org/10.1016/j.comptc.2022.113781.
[196] P. Ganesh, J. Kim, C. Park, M. Yoon, F.A. Reboredo, P.R.C. Kent, Binding and diffusion of lithium in graphite: quantum Monte Carlo benchmarks and validation of van der Waals density functional methods, J. Chem. Theory Comput. 10 (12) (2014) 5318–5323, https://doi.org/10.1021/ct500617z.
[197] G.I. Prayogo, H. Shin, A. Benali, R. Maezono, K. Hongo, Importance of Van der Waals interactions in hydrogen adsorption on a silicon-carbide nanotube revisited with vdW-DFT and quantum Monte Carlo, ACS Omega 6 (38) (2021) 24630–24636, https://doi.org/10.1021/acsomega.1c03318.